ผลของกรดลิวอิสต่อความว่องไวของตัวเร่งปฏิกิริยาซีเกลอร์-แนตตาและสมบัติต่างๆ ของพอลิเอททีลีน

นางสาววรรณา ผิวเกลี้ยง

วิทยานิพนธ์นี้เป็นส่วนหนึ่งของการศึกษาตามหลักสูตรปริญญาวิศวกรรมศาสตรดุษฎีบัณฑิต
สาขาวิชาวิศวกรรมเคมี ภาควิชาวิศวกรรมเคมี
คณะวิศวกรรมศาสตร์ จุฬาลงกรณ์มหาวิทยาลัย
ปีการศึกษา 2556

EFFECT OF LEWIS ACID ON THE ACTIVITY OF ZIEGLER-NATTA CATALYST AND THE PROPERTIES OF POLYETHYLENE

Miss Wanna Phiwkliang

A Dissertation Submitted in Partial Fulfillment of the Requirements
for the Degree of Doctor of Engineering Program in Chemical Engineering
Department of Chemical Engineering
Faculty of Engineering
Chulalongkorn University
Academic Year 2013

Thesis Title	EFFECT OF LEWIS ACID ON THE ACTIVITY OF ZIEGLER-NATTA CATALYST AND THE PROPERTIES OF POLYETHYLENE
By	Miss Wanna Phiwkliang
Field of Study	Chemical Engineering
Thesis Advisor	Professor Piyasan Praserthdam, Dr.Ing.
Thesis Co-advisor	Professor Minoru Terano, D.Eng. Sumate Charoenchaidet, Ph.D.

Accepted by the Faculty of Engineering, Chulalongkorn University in Partial Fulfillment of the Requirements for the Doctoral Degree

.....Dean of the Faculty of Engineering
(Associate Professor Boonsom Lerdhirunwong, Dr.Ing.)

THESIS COMMITTEE

.....Chairman
(Assistant Professor Anongnat Somwangthanaroj, Ph.D.)

.....Thesis Advisor
(Professor Piyasan Preserthdam, Dr.Ing.)

.....Thesis Co-advisor
(Professor Minoru Terano, D.Eng.)

.....Thesis Co-advisor
(Sumate Charoenchaidet, Ph.D.)

.....Examiner
(Associate Professor ML. Supakanok Thongyai, Ph.D.)

.....Examiner
(Associate Professor Bunjerd Jongsomjit, Ph.D.)

.....External Examiner
(Sirachaya Kunjara Na Ayudhya, D.Eng.)

วรรณา ผิวเกลี้ยง : ผลของกรดลิวอิสต่อความว่องไวของตัวเร่งปฏิกิริยาซีเกลอร์-แนตตาและสมบัติต่างๆของพอลิเอททีลีน (EFFECT OF LEWIS ACID ON THE ACTIVITY OF ZIEGLER-NATTA CATALYST AND THE PROPERTIES OF POLYETHYLENE) อ. ที่ปรึกษาวิทยานิพนธ์หลัก: ศ.ดร.ปิยะสาร ประเสริฐธรรม, อ. ที่ปรึกษาวิทยานิพนธ์ร่วม: ศ.ดร.มิโนรุ เทอราโน, ดร. สุเมธ เจริญชัยเดช, 151 หน้า.

วิทยานิพนธ์ฉบับนี้ศึกษาผลของสารประกอบกรดลิวอิสในเอททีลีนพอลิเมอร์ไรเซชันโดยใช้ตัวเร่งปฏิกิริยาซีเกลอร์-แนตตา ที่มีแมกนีเซียมคลอไรด์เป็นตัวรองรับ ซึ่งในการศึกษาครั้งนี้สามารถแบ่งงานวิจัยออกเป็น 3 ส่วน ในส่วนแรก การปรับปรุงแมกนีเซียมอัลค็อกไซด์ในระบบตัวเร่งปฏิกิริยาซีเกลอร์-แนตตาด้วยโลหะคลอไรด์ต่างๆ เพื่อใช้ในการศึกษาในเอททีลีนโฮโมพอลิเมอร์ไรเซชันและเอททีลีนโคพอลิเมอร์ไรเซชันกับ 1-เฮกซีน โลหะคลอไรด์ที่เลือกมาใช้ [ไอร์ออน (II) คลอไรด์ แมกนีเซียมคลอไรด์ และซิงค์คลอไรด์] ร่วมกับซิลิกอนเตตระคลอไรด์ ในขั้นตอนการเปลี่ยนแมกนีเซียมอัลค็อกไซด์เป็นแมกนีเซียมคลอไรด์ (Chlorination stage) ผลการทดลองในเรื่องโลหะต่างๆ พบว่า ไอร์ออน (II) คลอไรด์ สามารถเพิ่มพื้นที่ผิวและอัตราส่วนของไทเทเนียมต่อแมกนีเซียมโดยอะตอมบนพื้นผิวของตัวเร่งปฏิกิริยา นำไปสู่ความว่องไวสูงที่สุดทั้งใน เอททีลีนโฮโมและโคพอลิเมอร์ไรเซชัน เนื่องด้วยไทเทเนียมอะตอมที่อยู่บนพื้นผิวภายนอก ซึ่งง่ายต่อปรากฏการณ์ถ่ายเทมวล นำไปสู่การปรับปรุงประสิทธิภาพของตัวเร่งปฏิกิริยานี้ ในส่วนที่สองได้ศึกษาการเตรียมตัวเร่งปฏิกิริยาที่แตกต่างกัน 2 วิธี ที่ถูกปรับปรุงด้วยไอร์ออน (II) คลอไรด์ประกอบด้วย การเตรียมตัวเร่งปฏิกิริยาในสารละลายเตตระไฮโดรฟูแรน และการเตรียมตัวเร่งปฏิกิริยาโดยการตกผลึกซ้ำด้วยเอทานอล ซึ่งจากการทดลองพบว่า ตัวเร่งปฏิกิริยาที่ผ่านการปรับปรุงด้วยไอร์ออน (II) คลอไรด์ทั้งสองระบบสามารถเพิ่มความว่องไวของตัวเร่งปฏิกิริยานี้ นอกจากนี้พบว่าไอร์ออน (II) คลอไรด์ในระบบของสารละลายเตตระไฮโดรฟูแรน แสดงความว่องไวสูงกว่าในระบบเอทานอล เนื่องจากแรงระหว่างไทเทเนียม (IV) คลอไรด์และแมกนีเซียมคลอไรด์ที่เหมาะสมและไทเทเนียมอะตอมส่วนใหญ่อยู่บนพื้นผิว ซึ่งถูกวิเคราะห์โดย TGA และ EDX ตามลำดับ ส่วนสุดท้ายของงานวิจัยนี้เป็นการศึกษาผลของการผสมซิงค์คลอไรด์กับซิลิกอนคลอไรด์ร่วมกัน ลงไปในตัวเร่งปฏิกิริยาซีเกลอร์-แนตตา ที่มีแมกนีเซียมคลอไรด์เป็นตัวรองรับในสารละลายเตตระไฮโดรฟูแรน สำหรับเอททีลีนโฮโมพอลิเมอร์ไรเซชันและเอททีลีนโคพอลิเมอร์ไรเซชันกับ 1-เฮกซีน หรือเอททีลีนโคพอลิเมอร์ไรเซชันกับ 1-ออกทีน ซึ่งผลการทดลองพบว่าตัวเร่งปฏิกิริยา ที่ผ่านการปรับปรุงด้วยซิงค์คลอไรด์กับซิลิกอนคลอไรด์ร่วมกัน แสดงความว่องไวสูงที่สุดทั้งระบบเอททีลีนโฮโมและโคพอลิเมอร์ไรเซชัน นอกจากนี้พอลิเมอร์ที่ได้ยังมีค่าน้ำหนักโมเลกุลที่สูงอีกด้วย

ภาควิชา	วิศวกรรมเคมี	ลายมือชื่อนิสิต	.....
สาขาวิชา	วิศวกรรมเคมี	ลายมือชื่อ อ.ที่ปรึกษาวิทยานิพนธ์หลัก	.....
ปีการศึกษา	2556	ลายมือชื่อ อ.ที่ปรึกษาวิทยานิพนธ์ร่วม	.....
		ลายมือชื่อ อ.ที่ปรึกษาวิทยานิพนธ์ร่วม	.....

5171855421 : MAJOR CHEMICAL ENGINEERING
KEYWORDS : ZIEGLER-NATTA / ETHYLENE POLYMERIZATION / LEWIS ACID / MAGNESIUM CHLORIDE / COPOLYMERIZATION

WANNA PHIWKLIANG : EFFECT OF LEWIS ACID ON THE ACTIVITY OF ZIEGLER-NATTA CATALYST AND THE PROPERTIES OF POLYETHYLENE. ADVISOR : PROF. PIYASAN PRASERTHDAM, Dr.Ing., CO-ADVISOR : PROF. MINORU TERANO, D.Eng., SUMATE CHAROENCHAIDET, Ph.D., 151 pp.

This dissertation investigated the effects of Lewis acid compounds on ethylene polymerization with $MgCl_2$-supported Ziegler-Natta catalysts. The study could be divided into three parts. Firstly, the modification of $Mg(OEt)_2$-based Ziegler-Natta catalysts with various metal chlorides were examined on ethylene homopolymerization and ethylene copolymerization with 1-hexene. One of selected metal chlorides ($FeCl_2$, $MnCl_2$, and $ZnCl_2$), was added together with $SiCl_4$ in the chlorination stage of $Mg(OEt)_2$. The result showed that among various metal chlorides, the addition of $FeCl_2$ could enhance both BET specific surface area and the surface atomic ratio of Ti/Mg, leading to the highest activity in both ethylene homo- and copolymerization. The exposure of Ti species on outer surfaces could be thought as a sign of easier mass transfer phenomena leading to the improvement of catalyst performances. Secondly, two methods of catalyst preparations modified with $FeCl_2$ including $TiCl_4/MgCl_2$ complexes in tetrahydrofuran (THF) soluble and recrystallization method by ethanol (EtOH), were examined. It was found that $FeCl_2$ modification with both two methods could improve the activity. However, Fe-THF catalyst exhibited higher activity than Fe-EtOH catalyst because of a suitable of interaction between $TiCl_4$ and $MgCl_2$ and the proper location of Ti atoms on the surface as proven by thermogravimetric analysis (TGA) and energy dispersive X-spectroscopy (EDX), respectively. Finally, the effect of the $ZnCl_2$-$SiCl_4$ doped $TiCl_4/MgCl_2$/THF catalyst for ethylene homopolymerization and ethylene/1-hexene or ethylene/1-octene copolymerization was also studied. It indicated that the $ZnCl_2$-$SiCl_4$ modified catalyst exhibited very high activities in ethylene homo-and copolymerization and high the viscosity average molecular weight (M_v) of polymer obtained.

Department : Chemical Engineering Student's Signature.....

Field of Study : Chemical Engineering Advisor's Signature.....

Academic Year : 2013 Co-advisor's Signature.....

Co-advisor's Signature.....

ACKNOWLEDGEMENTS

First of all, I would like to express my heartfelt thanks to all those individuals whose wisdom, support, and encouragement made my journey possible. Special thanks extended to Professor Piyasan Praserthdam, my advisor and Associate Professor Bunjerd Jongsomjit, who guided me through hurdles, and provided constant support that made my journey completed lot easier than it would have been. Despite their busy schedules, they would always find the time to discuss anything from intriguing experimental to an issue of surviving in the scientific world. As the publication requirement, I would like to thank Dr. Sumate Charoenchaidet, Associate Professor ML. Supakanok Thongyai, and Dr. Sirachaya Kunjara Na Ayudhya for their helps. Moreover, I also would like to thank to Assistant Professor Anongnat Somwangthanaroj, who has been the chairman of the committee.

I wish to express my warmest thanks to Professor Minoru Terano for a great opportunity and experience to carry out research work at Japan Advanced Institute of Science and Technology (JAIST). I cannot miss to thanks Associate Professor Toshiaki Taniike for his kind advice in this project and valuable guidance of this study in JAIST. I owe special thanks to the whole students of Terano laboratory for the warm welcome, supports and wonderful times we have had during my stay.

Many thanks for kind suggestions and useful help to Mr. Watcharapong Khaodee and many friends in the Center of Excellence on Catalysis and Catalytic Reaction Engineering (CECC) from Chulalongkorn University who always provided the encouragement and co-operate along the thesis study.

Sincere thanks given to the Dusadeepipat scholarship (Chulalongkorn University Fund) and the Thailand Research Fund (TRF) for the financial support.

Most of all, I would like to express my greatest gratitude to my parents and my sister who always gave me suggestions, support, and encouragement.

CONTENTS

PAGE

PAGE

PAGE

LIST OF TABLES

PAGE

PAGE

LIST OF FIGURES

PAGE

PAGE

PAGE

CHAPTER I
INTRODUCTION

Nowadays, polyolefins are indispensable plastics in our daily life, covering a wide range of applications such as garbage containers, films, sheets, automobile parts, kitchen helpers, water pipes, bottle plastic bags, agricultural materials, electronic parts, and so on [1]. Especially, polyethylene (PE) is one of the promising polymers, having a lot of advantages including good chemical resistance, high impact strength, and stiffness even at low temperatures [2]. There are three main types of ethylene polymerization catalysts: Ziegler-Natta (ZN), Phillips and metallocene catalysts. In particular, ZN catalysts have been mainly employed in the production of high-density and linear low-density PE due to their outstanding features such as high productivities [1, 2], broad molecular weight distribution (MWD) [3, 4], and good morphology controls [5, 6].

A general ZN catalytic system comprises titanium tetrachloride supported on a magnesium chloride ($TiCl_4/MgCl_2$), which is activated by alkylaluminium. Several researchers have been devoted in academic and industrial fields not only for better understanding of the catalytic mechanisms, but also for the specific targets including higher activity [1, 2], better morphology control (shape, size, distribution, bulk, and density, etc.) [7-9], higher hydrogen response [3, 9, 10], adjustments in molecular weight (MW) and molecular weight distribution (MWD) [2, 3, 7, 10-17], enhanced comonomer incorporation efficiency, and more uniform chemical composition distribution (CCD) [18, 19]. In order to achieve these targets, the choice of starting materials to obtain $MgCl_2$ carrier is one of the most substantial parameters [20]. For the catalyst preparation, it can be roughly divided into two kinds classifying by the method of $MgCl_2$ addition into a carrier. Considering the first method, it can be synthesized from the commercial anhydrous $MgCl_2$ as a starting material. The main difficulty in the preparation of this catalyst is to make $MgCl_2$ soluble in organic solvent. For another method, the $MgCl_2$ used can be gained from the reactions

occurred during the catalyst preparation. Practically, the sources of magnesium are the organomagnesium compounds such as $Mg(OR)_2$, MgR_2, the mixtures of MgR_2 and AlR_3, or Grignard reagents. In general, this system is neccessary to use the chloride-containing sources ($TiCl_4$, HCl, $SiCl_4$, or chloro-organic compound) for converting the organomagnesium compounds to $MgCl_2$ [21].

Currently, several investigations are devoted to develop the catalyst performances. Nonetheless, most studies have involved the investigation of effect of electron donor (Lewis base) on catalyst performances due to their commercial interest. Consequently, the electron donor is considered to be a crucial component, which can efficiently improve the stereospecificity, especially MWD. The electron donor has several functions, such as making a complex or reacting with $MgCl_2$, $TiCl_4$ and cocatalyst, stabilizing $MgCl_2$ crystals, and deactivating astereospecific polymerization sites or converting astereospecific sites to stereospecific ones, thus increasing the isotactic index [22, 23]. As reported by Chen *et al*. [24], the MWD could be modified by adding the electron donor during the polymerization, but the reduction in the catalytic activity was then occurred. On the other hand, only a few published papers have reported the modification of ZN catalysts by doping the Lewis acid compounds in the support in order to improve the catalyst performances [24-26]. However, Lewis acid halide additives have been used as a promising alternative to improve the activity of catalyst because Lewis acid halides introduced into $MgCl_2$ support have the ability to change the surface properties of $MgCl_2$ crystalline, resulting in the modification of active center distribution (ACD) of catalysts. It consequently causes the improvement in catalytic performances and polymer properties [11]. Some researchers claimed that the addition of $AlCl_3$, $MnCl_2$, and $ZnCl_2$ could make the defect on the $MgCl_2$ support which finally contributed to the improvement of the catalytic activities and polymer properties in Ziegler-Natta catalyst system [11, 25, 26]. In addition, the modification with Lewis acid halide could effectively eliminate alcohol from $MgCl_2$•*n*ROH adduct. For example, the addition of $SiCl_4$ additive during the preparation of catalysts exhibited the highest activity for both homo- and copolymerization of ethylene [27]. Moreover, regarding to ethylene/1-hexene copolymerization, it was further revealed that $AlCl_3$ doped in the

support of the $TiCl_4/MgCl_2$ catalyst markedly increased 1-hexene incorporation leading to high activity because doping $AlCl_3$ in the catalyst could change the active center distribution, eventually resulting in the formation of more active centers with high ability of copolymerization [28].

According to many reasons as mentioned above, this thesis focuses on the effects of Lewis acid modifications on Ziegler-Natta catalytic systems for ethylene homo- and copolymerization in terms of catalytic activities and polymer properties.

1.1 Objectives

In order to propose an alternative way for improving of a highly efficient Ziegler-Natta catalysts for ethylene homopolymerization and ethylene/1-olefins copolymerization, the Lewis acid halides are selected to study in this research. Therefore, the objectives of this work are summarized as follows:

1. To elucidate the effects of metal chloride compounds on the activity of $Mg(OEt)_2$-based Ziegler-Natta catalyst for ethylene homo- and copolymerization.

2. To study the effects of $FeCl_2$ doping on the characteristics and the catalytic properties of Ziegler-Natta catalyst prepared by different methods.

3. To investigate the synergistic effects of the $ZnCl_2$-$SiCl_4$ modified $TiCl_4/MgCl_2/THF$ catalytic system on the ethylene homo- and copolymerization.

1.2 Scope of Work

To achieve the objectives of this research, the scopes of these investigations are listed below.

1. Preparation of $Mg(OEt)_2$-based $TiCl_4/MgCl_2$ catalyst system with different types of Lewis acid halide, including $FeCl_2$, $MnCl_2$, $ZnCl_2$, and $SiCl_4$.

2. Characterization of this catalyst system by titration method, N_2 physisorption, X-ray photoelectron spectroscopy (XPS), and scanning electron microscopy (SEM).

3. Preparation of $FeCl_2$ modified $TiCl_4/MgCl_2$ catalyst systems with two preparation methods i.e., $TiCl_4/MgCl_2$ complexes in THF ($TiCl_4/MgCl_2$/THF) and recrystallization method with ethanol.

4. Characterization of both catalyst systems by means of inductively coupled plasma (ICP), scanning electron microscopy and energy dispersive X-ray spectroscopy (SEM/EDX), X-ray diffraction (XRD), fourier transforms infrared spectroscopy (FT-IR), and thermogravimetric analysis (TGA).

5. Preparation of $TiCl_4/MgCl_2$/THF catalytic system modified with Lewis acid compounds such as $ZnCl_2$, $SiCl_4$, and $ZnCl_2$-$SiCl_4$ mixtures.

6. Characterization of the obtained catalysts by means of inductively coupled plasma (ICP), scanning electron microscopy and energy dispersive X-ray spectroscopy (SEM/EDX), X-ray diffraction (XRD), fourier transforms infrared spectroscopy (FT-IR), and gas chromatography (GC).

7. Studying the effects of metal chloride compounds on $Mg(OEt)_2$-based Ziegler-Natta catalyst for homopolymerization of ethylene and copolymerization of ethylene with 1-hexene by characterizing the polymer properties via ^{13}C nuclear magnetic resonance (^{13}C NMR) and differential scanning calorimeter (DSC).

8. Studying the effects of $FeCl_2$ modified $TiCl_4/MgCl_2$ catalyst systems with different catalyst preparation methods on the ethylene homopolymerization

behavior by characterizing the polymer properties via differential scanning calorimeter (DSC) and scanning electron microscopy (SEM).

9. Studying the effects of $TiCl_4/MgCl_2/THF$ catalytic system modified with Lewis acid compounds on homopolymerization of ethylene and copolymerization of ethylene with 1-hexene or 1-octene via differential scanning calorimeter (DSC), scanning electron microscopy (SEM), ^{13}C nuclear magnetic resonance (^{13}C NMR), and the viscosity method.

1.3 Overview

This dissertation focuses on the effects of Lewis acid halides in order to improve the catalytic activity of Ziegler-Natta catalyst for ethylene homo- and copolymerization. The dissertation consists of five chapters to achieve the overall purposes. The first chapter involves the general introduction of this research and an overview of the use of Ziegler-Natta catalyst for producing the polyethylene. Chapter II provides an introduction of Ziegler-Natta catalyst with a brief review on the catalytic history and development. The basic chemical principles on both catalysis and polymerization are also addressed. The chemical used, catalyst preparation, polymerization procedure, and characterization techniques are explained in Chapter III. Chapter IV gathers the results of the ethylene and ethylene/α-olefins polymerizations from three parts of investigations as mentioned above and the discussion is then performed. Lastly, the conclusions of this research and the necessary recommendations for future work are presented in Chapter V.

CHAPTER II
THEORY AND LITERATURE REVIEW

In this chapter, including theory and literature review can be divided into five parts. The first part describes common structures as well as properties and applications of polyethylene. The second part present the structure and chemistry of catalyst system. The third part represent the mechanism of ethylene polymerization. The catalyst particle morphology and particle growth mechanism are provided in the fourth and fifth parts, respectively.

2.1 Polyethylene

Polyethylene is a thermoplastic material, which has the highest production volumes of all synthetic polymers [29]. It has excellent chemical resistance and can be processed in a variety of ways (blown film, pipe extrusion, blow molding, injection molding, etc.) into myriad shapes and devices [29]. There are three main types of polyethylene depending on the production process and the catalysts used; high density polyethylene (HDPE), low density polyethylene (LDPE), and linear low density polyethylene (LLDPE) as seen in Table 2.1.

As observed in Table 2.1, it can be summarized that the physical characteristics of polyethylene vary widely as a function of their density. Therefore, the difference in structure of polymer affects to the physical properties of polymer and the application of polymer. Due to the low level of branching, there is little to hinder the crystallization of HDPE [30]. Microstructure HDPE has crystallinity levels in excess of 60%, which translate into densities ranging from approximately 0.94 to 0.97 g/cm^3. HDPE has a wide variety of applications such as plastic bags, fuel tanks and water pipes. Moreover, the industrial interest in HDPE due to the economics allowed by the low pressure production processes as to its suitability in field where it can be replaced conventional LDPE.

Table 2.1 Structure and properties of polyethylene [30].

Lists	Low-density polyethylene (LDPE)	High-density polyethylene (HDPE)	Linear low-density polyethylene (LLDPE)
Preparation	-Operated at very high pressure -Free radical initiator: O_2 (air), an azo-compound, a peroxide or a peroxyester	-Operated under normal pressure or high pressure - Catalyst used : Phillips catalyst, Ziegler-Natta catalyst, and Metallocene catalyst	-Operated at low pressure - high pressure - Catalyst used : Ziegler-Natta catalyst and Metallocene catalyst -Comonomers such as 1-butene, 1-hexene, and 1-octene etc.
Molecular structure			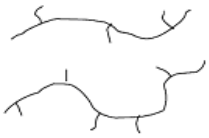
Density (g/cm^3)	0.86-0.91	0.94-0.97	0.91-0.94
Types of processing and application.	-Using in processes involving extrusion (film, extruded products, extrusion coating). -Typical applications: high-clarity film, flexible food packaging, and heavy duty films	-Showing significant levels in blow molding, injection molding, and film. - Typical applications: detergent bottles, milk bottles, pails, thin-wall containers, drink cups, cases and crates, and grocery bags	- Going into film applications. -Other typical applications: heavy-duty shipping sacks, industrial packaging, flexible food packaging, storage boxes, and thin-wall lids.

LDPE is produced only by a free radical polymerization of ethylene initiated by organic peroxides or other regents that readily decompose into free radicals. The production of LDPE is employed under high-temperature and high-pressure polymerization. The high levels of branching found in low density polyethylene disrupts its ability to crystallize, which limits its density in the solid state to approximately 0.86 to 0.91 g/cm^3 [30]. The highly branched nature of low density polyethylene and its broad molecular weight distribution give it high melt strength and good shear thinning properties, which are desirable processing characteristics. The characteristics determining the advantages of LDPE for some particular use are excellent processability at relatively low temperatures, excellent optical characteristics, impact as well as tearing resistance, and flexibity. These are the properties which lead to the utilization of LDPE in commercial packaging films [31].

LLDPE products have similar degrees of crystallinity and stiffness compared to their LLDPE. Transparency, flexibility, and resilience increase as density decrease. LLDPE is mainly made by copolymerization of ethylene with α-olefins, including propylene, 1-butene, 1-hexene, 1-occtene and so on. The properties of LLDPE such as, thermal, physical, and mechanical properties depend on the distribution of short chain in the copolymer and polymer microstructure (triad and dyad distributions). Thus, the several LLDPE grades are classified by microstructure of polymer. Typically, comonomer content is between about 2% and 8 mole% [30]. LLDPE seems to fit these requirements as a polymer suitable for several fields [32].

In this study, we focused on the synthesis of polyethylene such as HDPE and LLDPE. Generally, the catalyst systems for the synthesis of polyethylene can be divided into three main types: Ziegler-Natta, Phillips, and metallocene catalysts. In particular, ZN catalysts are most widely used for industrial polyolefin production. The development of ZN catalysts have a long history with the industrial demands due to their distinct features such as high productivity [1, 2], broad MWD and CCD [3, 4], and good morphology control [5, 6].

2.2. Structure and Chemistry of Catalyst System

Titanium-based Ziegler–Natta catalytic systems for olefin polymerization have been widely utilized for over 60 years. Up to the present time, several researchers have devoted to improve the catalytic activities and polymer properties in both areas of academic and industrial researches. For the commercialize process at industrial scale production, more than 50% of polyethylene (HDPE) and 90% of polypropylene (PP) have been produced by using Ziegler-Natta catalysts owing to their good catalytic activities and different polymer properties. The chemistry and the roles of each component are mentioned as follows:

2.2.1 Structure of the Carrier: $MgCl_2$

Kashiwa [33] and Galli *et al*. [34] found that $MgCl_2$ indicated the highest activity for ethylene polymerization among various solid carries due to the similarities in the crystal structures and ionic radii of $MgCl_2$ (Mg^{2+} = 0.066 nm) and $TiCl_4$ (Ti^{4+} = 0.068 nm) as shown in Table 2.2. Such a dramatic increase in activity was revealed to be caused by marked increases in the propagation rate constant (k_p) as well as the number of active species [C*] [35]. The latter effect is easily understood in terms of a high dispersion of the active titanium species on the large surface of $MgCl_2$. Moreover, the major advantage of this catalyst is its high activity, which leads to low concentration of the catalyst. However, catalyst residues can remain in the polymer [36].

Table 2.2 Crystallographic data for δ-$MgCl_2$ and δ-$TiCl_3$ [35]

δ-$MgCl_2$	δ-$TiCl_3$
hexagonal close packing of the Cl ions	
a = b = 3.63Å	a = b = 3.54Å
c = 5.93Å	c = 5.86Å
Cation coordination: octahedral	
Mg–Cl = 1.23Å	Ti–Cl = 1.25Å
Mg^{2+} = 0.65Å	Ti^{4+} = 0.68Å
	Ti^{3+} = 0.76Å

It is generally accepted that $MgCl_2$ is the best support for Ziegler-Natta catalytic system. As reported by many researchers, two crystalline modifications, including the commercial α-form and the less stable β-form, are known for $MgCl_2$. Similar to the γ-$TiCl_3$, the α-from has a layer of $CdCl_2$ type and shows a cubic close-packed stacking (ABC…ABC…) of double chloride layers with interstitial Mg^{2+} ions in sixfold coordination [37]. The structure of α-$MgCl_2$ display an X-ray diffraction spectrum with a strong reflex (104) for d = 2.56 Å, because of the cubic packing of the Cl atoms (Figure 2.1). The less known β-form of $MgCl_2$ because it is thermodynamically less stable. It has hexagonal close packed structure and its structure displays an X-ray diffraction spectrum at d = 2.78Å (Figure 2.1).

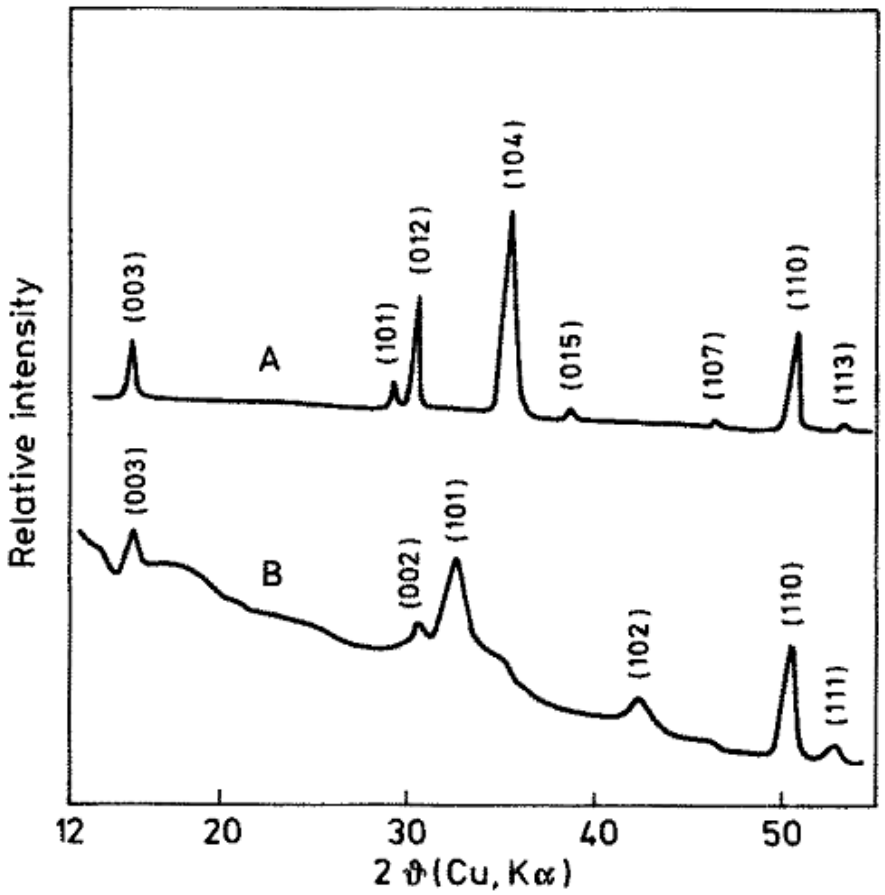

Figure 2.1 XRD patterns of α-$MgCl_2$ (A) and β-$MgCl_2$ (B) [37].

With regard to the highly activated form of $MgCl_2$ (namely δ-$MgCl_2$), it can be obtained from the transformation of α-$MgCl_2$ into the active δ form of $MgCl_2$. It shows a disordered structure arising from the translation and rotation of the layers [37]. The dominant lateral terminations in $MgCl_2$ supports are the (104) and the (110) surfaces, with 5-and 4-coordinate Mg cations, respectively. The X-ray diffraction of $MgCl_2$ pattern is characterized by a peak at $2\theta = 15^o$ corresponding to the separation of successive Cl-Mg-Cl triple-layers and by reflections at $2\theta = 32\text{-}35^o$ and $2\theta = 50^o$ representing the (104) and (110) peaks, respectively. Comparison to α-$MgCl_2$, the δ-forms of $MgCl_2$ are characterized by the replacement of the (104) peak by a broad halo. In highly activated $MgCl_2$, the diffraction peak at $2\theta = 15^o$ may be totally absent, indicating that the support comprises single Cl-Mg-Cl structural layers (monolayers) [38]. However, The XRD spectrum of δ-$MgCl_2$ was reported by Noto and Bresadola as seen in Figure 2.2 [39].

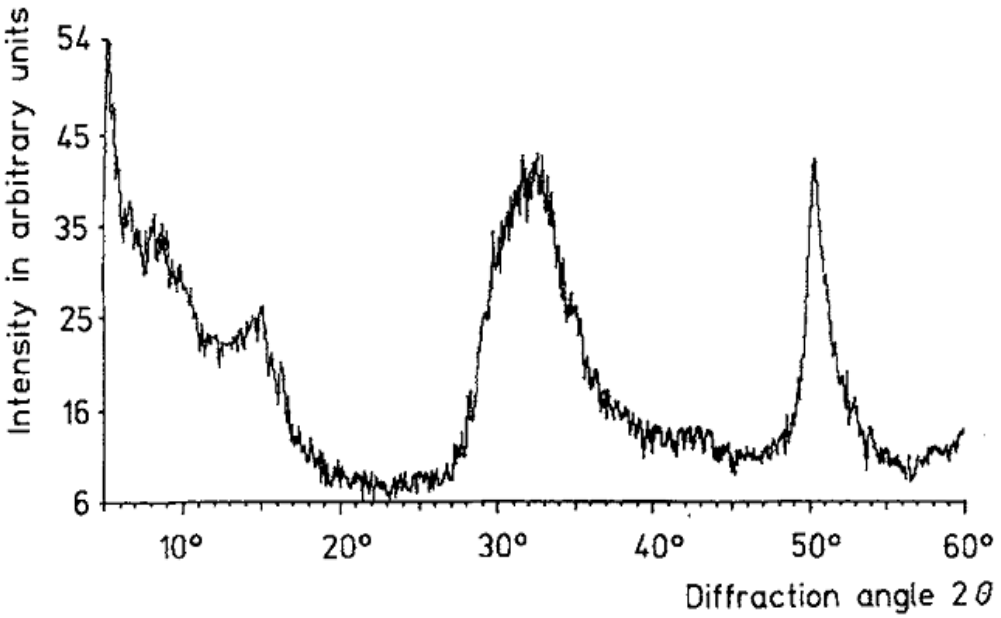

Figure 2.2 XRD patterns of δ-$MgCl_2$ [39].

Moreover, active $MgCl_2$ can also be obtained by contacting $MgCl_2$ with Lewis base. Noto *et al* [40] investigated the internal donor (LB) modification in $TiCl_4$/ $MgCl_2$ catalytic system. Figure 2.3A illustrate the XRD patterns of general formula $[MgCl_2(C_2H_5COOC_2H_5)_x]_n$ supports where x is between 0 and 0.89. It could be seen that the adducts were determined form higher x value of some XRD peaks at $2\theta < 10^o$. In case of the removal of coordinated internal donor (x value decreasing), the chang of XRD pattern was described as follows.

(i) For x value decreasing, the intensity peaking at $2\theta \approx 9^o$, which correlated to the ID content, disappears and the diffraction peaks around $2\theta \approx 15^o$, 32°, and 50.5^o gradually became more visible;

(ii) Decreasing ID content in the supports, the full width at half maximum (FWHM) of these peaks seem more and more broaded;

(iii) According to $x > 0$, new peaks were seen at $2\theta < 15^o$ could be related to the structural changes of the covalent $MgCl_2$ double chlorine-bridged chains of the supports [40].

In addition to the peaks around 2θ ≈ 9º, whose intensity decreased with decreasing the base content. It exhibited the close packing of the $MgCl_2(ID)_x$ complexes. The completed removal of ID left a support whose XRD pattern associated to that showed by the structurally disordered δ-$MgCl_2$ forms

Moreover, they had also reported that the XRD pattern of procatalyst obtained by treating supported with $TiCl_4$, exhibited a decrease in the base content. The formation of soluble of $[TiCl_4(EP)]_2$ complexes caused the coordinated ID loss from the supports by treating with $TiCl_4$. From the comparison between the XRD pattern of Figure 2.3A and Figure 2.3B showed that both the supports and the titanated derivatives with low ethyl propionate (EP) content were similar in structural features.

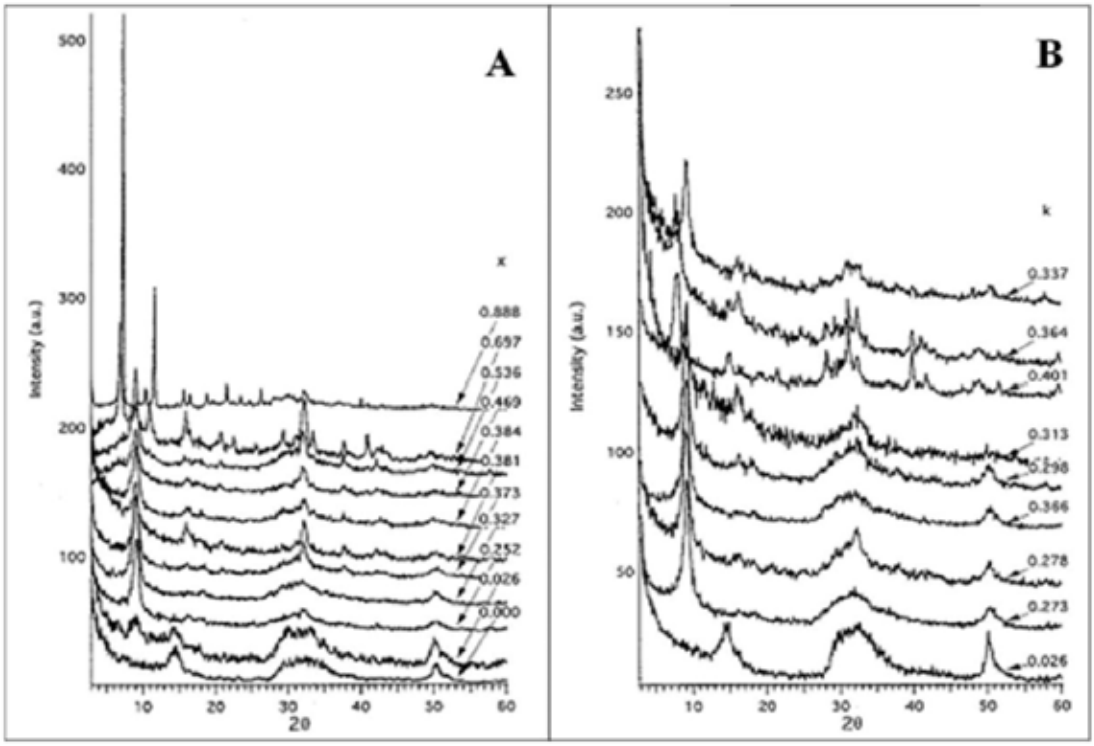

Figure 2.3 (A) XRD patterns of $[MgCl_2(EP)_x]_n$ adducts, where $0 \leq x < 0.89$; (B) XRD patterns of procatalysts $[MgCl_2(EP)_k(TiCl_4)_m]_n$. The sequence of the spectra according to that of the parent supports of Figure 2.3A [40].

The nature of the active forms of $MgCl_2$ was investigated by Auriemma and Rosa [41]. Figure 2.4B shows the high degree of supported catalyst porosity obtained from $MgCl_2$•*n*Lewis base complexes with *n* = 2-3. This brought the high activity for ZN catalyst due to structural transformations, which created amorphous or highly disordered crystalline $MgCl_2$ polynuclear species. They suggested that these amorphous structures play a key role in the crystallization of δ-$MgCl_2$ form. The active sites could be located at the edge of thin δ-$MgCl_2$ lamillae Therefore, a high degree of nanoporous enhanced contour length of the lateral faces of $MgCl_2$ crystals available for the epitactic coordination of Ti species and of internal and external donors (Figure 2.4A). Hence, the suitable stochiometry of $MgCl_2$•*n*Lewis base complexes plays a key role in the formation of nanoporous of δ-$MgCl_2$ crystals. This could be concluded that the most important parameter is affected by the processing conditions of ZN catalysts. This was the concentration of Mg sites available for the coordination of active centers, which was dependant on the size, concentration, and distribution of nanoporous. Their analysis suggested that a deep understanding of the structural transformations that occur during the late stages of the catalysts preparation may be highly beneficial not only in fundamental studies of the Ziegler–Natta stereospecific polymerization of olefins but also in practical application because it allows for a better optimization of the processing conditions for obtainment of nanoporous δ-$MgCl_2$ crystals.

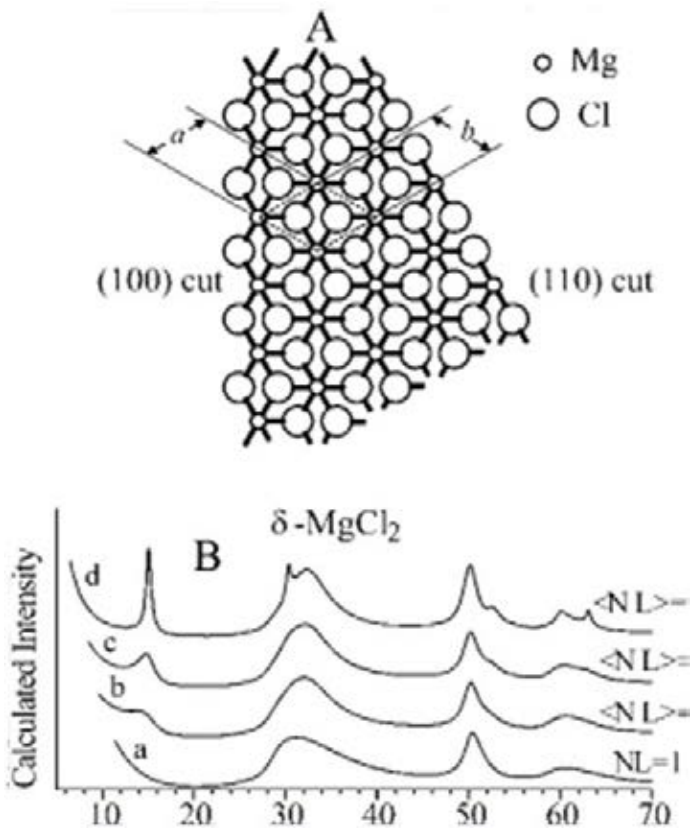

Figure 2.4 (A) Model of Cl-Mg-Cl structural layer in $MgCl_2$ layer compounds indicating the (100) and (110) cuts. (B) XRD patterns of the δ-$MgCl_2$, according to the indicited numbers of structure layers piled along the c-axis (NL) [41].

A border-line case is shown in Figure 2.5 which exhibited the spectrum of active $MgCl_2$ obtained by chlorination of a Grignard compound. In this manner it is possible to obtain highly disordered crystalline forms and clearly more disordered than those obtained by even prolonged mechanical treatments [37].

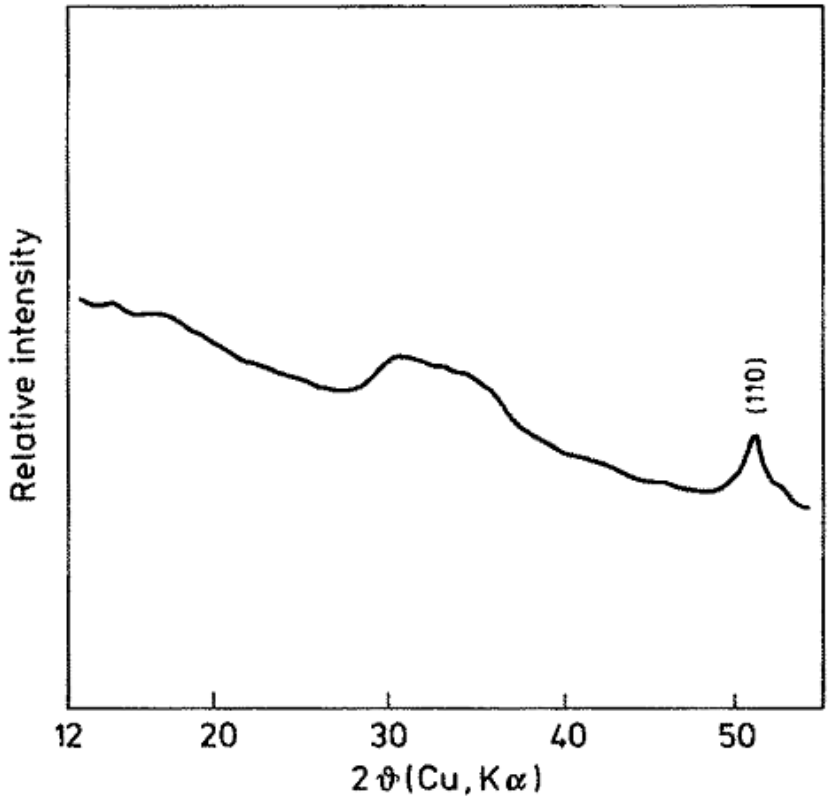

Figure 2.5 XRD patterns of $MgCl_2$ prepared by chlorination of a Grignard compound [37] .

According to $TiCl_4/MgCl_2$/THF catalytic system, Chang and co-workers [42] studied the influences of THF removal from $TiCl_3$(AA)/3$MgCl_2$/THF catalyst by diethylaluminium chloride (DEAC) addition. From XRD patterns, it was exhibited the XRD peaks of anhydrous $MgCl_2$ (ME) and $TiCl_3$(AA) (T3M) precursors were different from those of their precursors. This indicated that anhydrous $MgCl_2$ and $TiCl_3$(AA) underwent structural transformation through the interactions with THF. $TiCl_3$(AA)/3$MgCl_2$/THF (T3ME) catalyst exhibited the mixture of XRD pattern of ME and T3E as seen in Figure 2.6. The characteristic peaks of ME were presented at 2θ = 9.75, 20.38, and 32.38º. Regarding the XRD patterns of T3ME, T3MED2, T3MED4, T3MED8, and T3MED12, it was found that the removal of THF led to the change in structural through interaction with DEAC. Additionally, the characteristics of $MgCl_2$/THF (ME) structure had been maintained in T3MED2 and T3MED4 but lost in T3MED8 and T3MED12. This results indicated that a small amount of DEAC

does not break the ME structure; however, that a lot of DEAC amounts can break the ME structure.

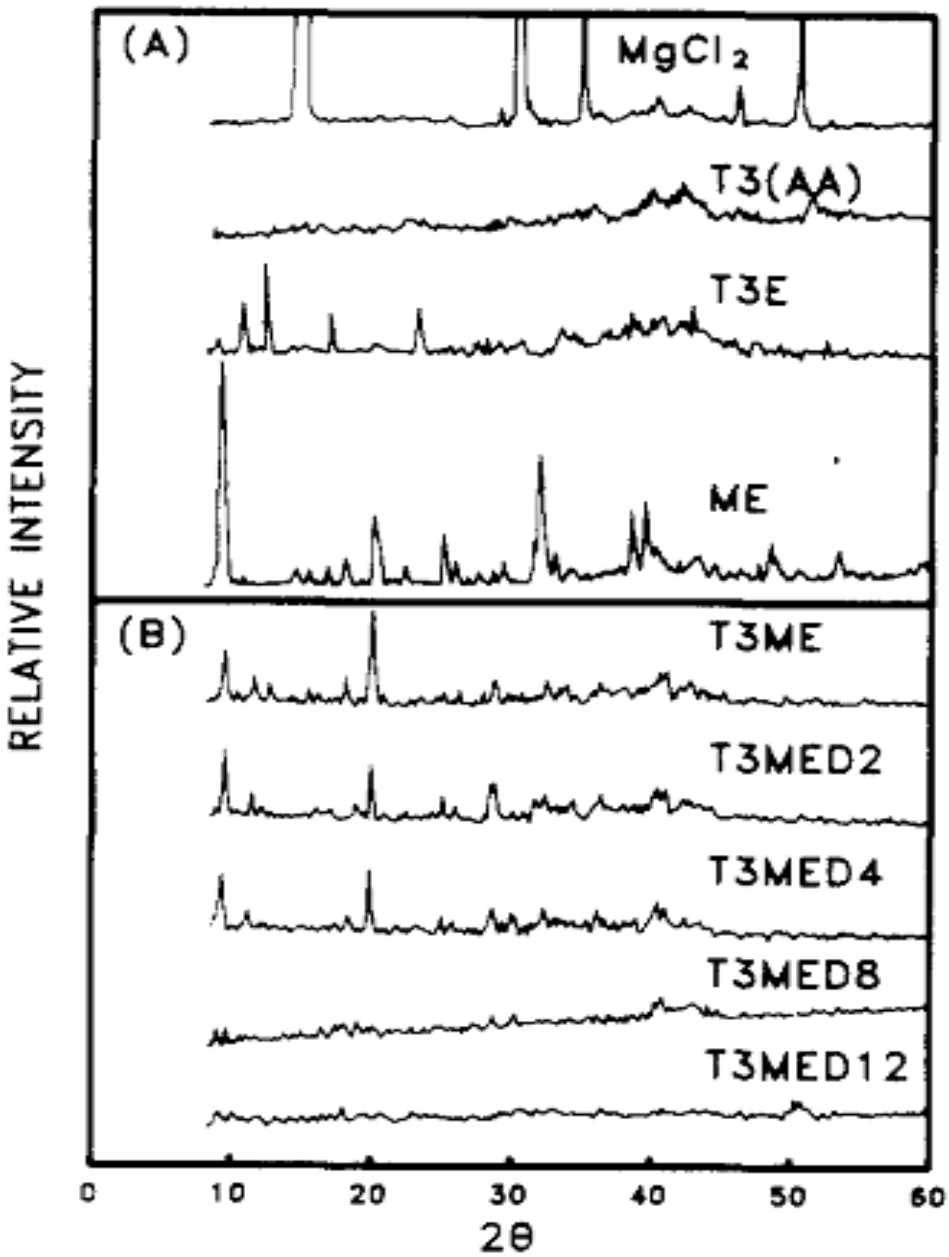

Figure 2.6 XRD patterns of (A) anhydrous $MgCl_2$, $TiCl_3$(AA) (T3(AA)), $TiCl_3$(AA)/THF (T3E), and $MgCl_2$/THF (ME) and (B) $TiCl_3$(AA)/3$MgCl_2$/THF (T3ME and T3MEDX, X = 2, 4, 8, 12) catalytic system [42].

Chu *et al*. [43] also studied the effects of DEAC addition over $TiCl_3$/2.5$MgCl_2$(0.5$MgEt_2$)/THF catalyst. The effect of DEAC addition on the

structure of catalysts was investigated using FT-IR and XRD measurements. According to FT-IR analysis was used to characterize the interaction of $MgCl_2$ with $TiCl_4$ or $TiCl_3$ in the presence of THF. Table 2.3 and Figure 2.7 represent the FT-IR spectra of different kinds of complexes. According to pure THF had an asymmetrical and a symmetrical C-O-C stretching bands at 912 cm^{-1} and 1071 cm^{-1}, respectively. For the synthesize of T3ME catalyst, $TiCl_3$(AA) was used to form a complex with $MgCl_2$ in THF. Concerning the transformation to acid-base property of $MgCl_2$ compounds, the reaction between $MgCl_2$ and $AlCl_3$ contained in the $TiCl_3$(AA) compound resulted in the formation of Al-Mg-THF (AME) complex. The AME complex was related to the ability of the aluminium compound which abstracted a halide anion from $MgCl_2$ [44]. The infrared spectrum of the R catalyst might be because of the existence of $MgEt_2$ (Mg of $MgEt_2$ is more basic than that of $MgCl_2$) in the support matrix. With regard to the addition to DEAC in the R catalyst, the characteristic peaks of C-O-C were shifted to the lower frequencies since Mg of AME was also more basic than that of $MgCl_2$. In the case of R12, the characteristic peaks disappeared because of the reduction of titanium (III) to titanium (II) [45]. The reduction of titanium (III) transformed the acidity of titanium and broke the complex structure. Figure 2.8 represents XRD patterns of the R catalysts. As observed in this Figure, it was found that the characteristics of the ME structure had been kept in R, R2, R4, and R8 but lost in R12. This exhibited that a small amount of DEAC does not break the ME structure but a lot of DEAC amounts can break the ME structure.

Table 2.3 FT-IR bands of different kinds of complexes [43]

Catalyst Abbreviation	Components	Characteristic absorbance (cm^{-1})	
THF		1071	912
T4ME	$TiCl_4/3MgCl_2/THF$	1027	876
ME	$MgCl_2/THF$	1036	891
T3E	$TiCl_3(AA)/THF$	1010	854
Mixture of ME and T3E		1036/1010	891/854
T3ME	$TiCl_3(AA)/3MgCl_2/THF$	1027	876
R	$TiCl_3/2.5MgCl_2(0.5MgEt)/THF$	1035	885
R2	$TiCl_3/2.5MgCl_2(0.5MgEt)/THF(0.2)$	1032	880
R4	$TiCl_3/2.5MgCl_2(0.5MgEt)/THF(0.4)$	1028	878
R8	$TiCl_3/2.5MgCl_2(0.5MgEt)/THF(0.8)$	1027	876
R12	$TiCl_3/2.5MgCl_2(0.5MgEt)/THF(1.2)$	1022/997	876

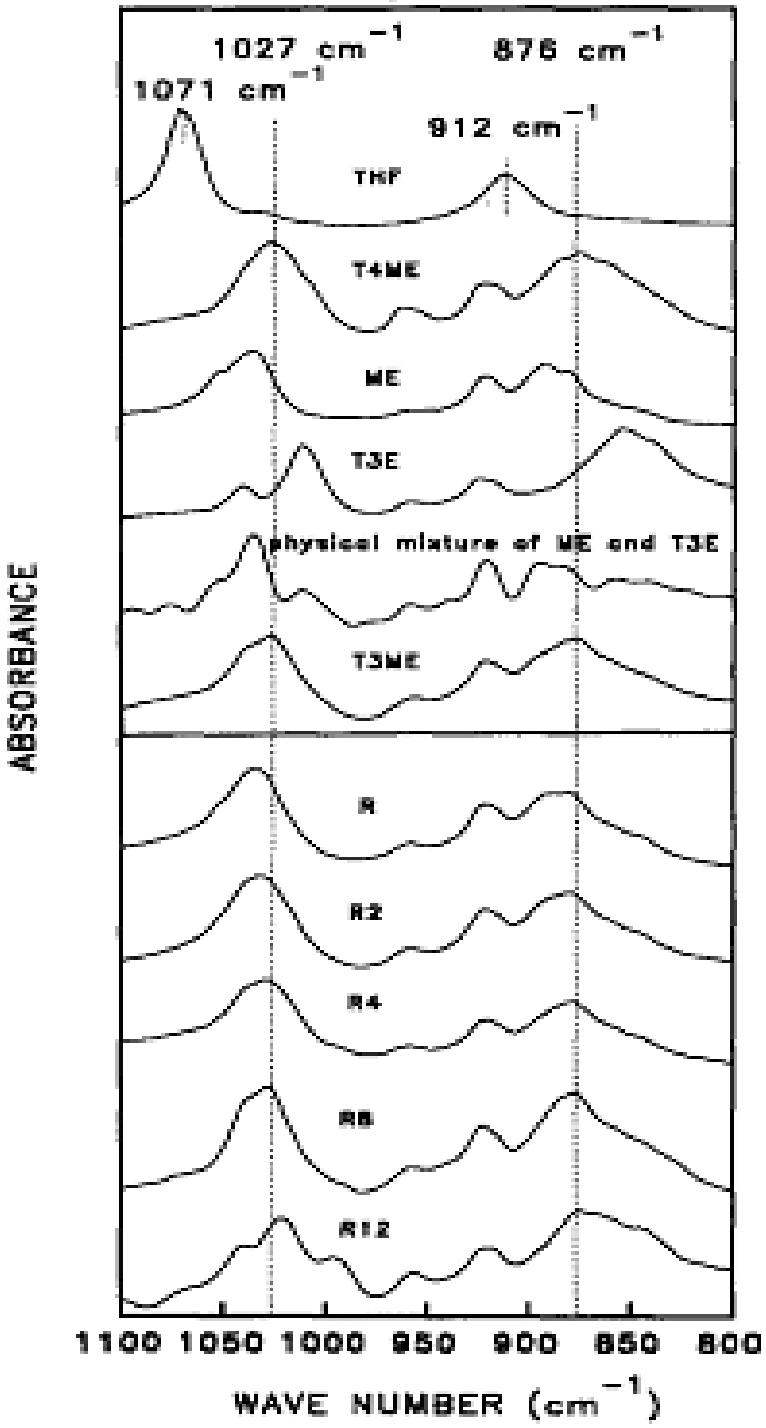

Figure 2.7 FT-IR spectra of tetrahydrofuran (THF), T4ME, ME, T3E, the physical mixture of ME and T3E, R, R2, R4, R8, and R12 respectively [43].

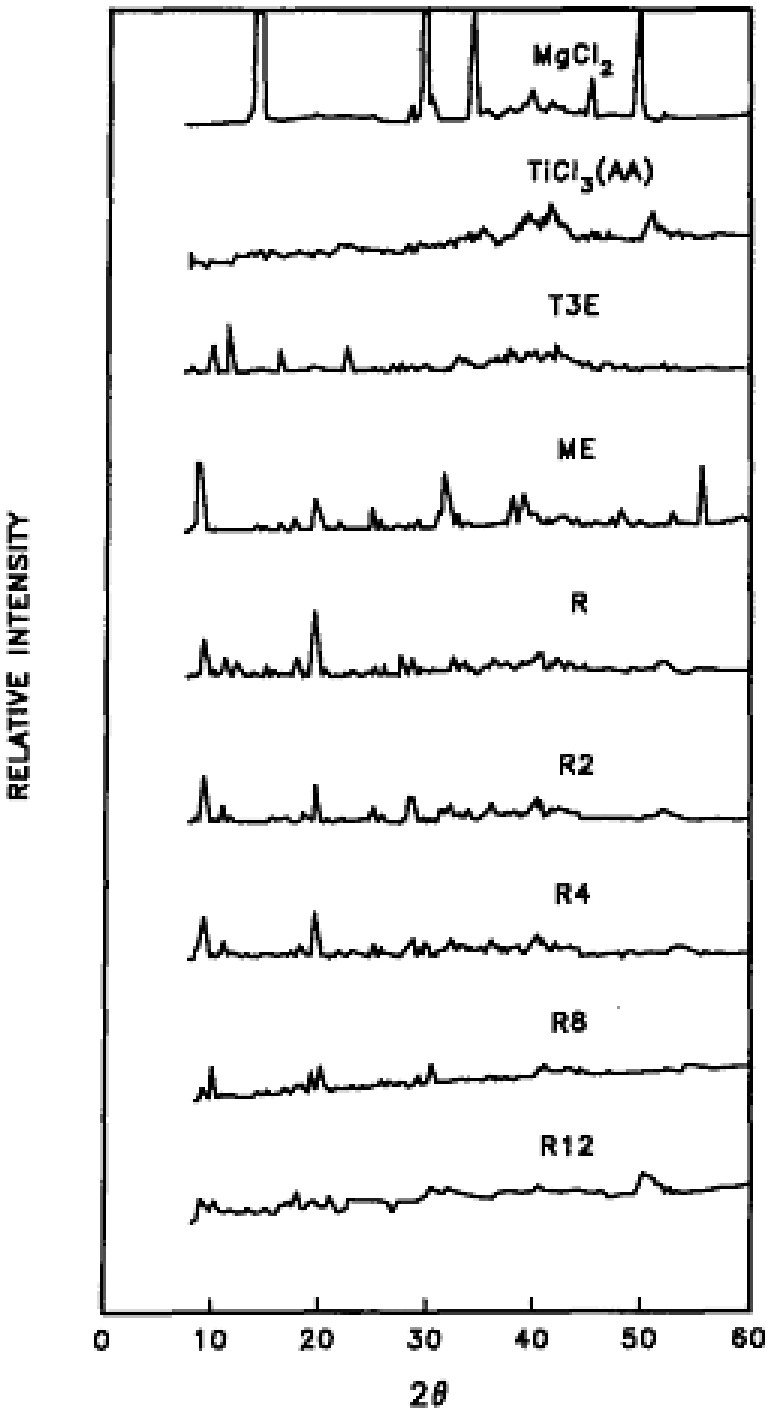

Figure 2.8 XRD patterns of $MgCl_2$, $TiCl_3$(AA), T3E, ME, R, R2, R4, R8, and R12 respectively [43].

2.2.2 Preparation Methods

All procedure of catalyst preparation can be divided into two types depending on the method in which $MgCl_2$ is introduced into a carrier:

(i) Catalysts are synthesized by used directly from anhydrous $MgCl_2$ as starting material. The main difficulty in preparation of these catalysts is to make $MgCl_2$ soluble in organic solvents such as THF and EtOH.

(ii) Catalysts in which $MgCl_2$ are synthesized during catalyst preparation. The sources of magnesium are organomagnesium compounds such as $Mg(OR)_2$, MgR_2, mixtures of MgR_2 and AlR_3, or Grignard reagents. The chlorinating agents needed to convert the organomagnesium compounds to $MgCl_2$ are $SiCl_4$, $TiCl_4$, and CCl_4 [21].

2.2.2.1 Catalysts Produced from Soluble $MgCl_2$ Complexes

Catalyst produced from soluble $MgCl_2$ complexes can be subdivided into two classes:

- Catalyst recipes based on $TiCl_4$ ($TiCl_3$), $MgCl_2$, and THF

By dissolving $MgCl_2$ and $TiCl_3$ together in THF, a complexation system was formed *in situ*:

$$3.14MgCl_2 + TiCl_4 + THF(Sol.) \rightarrow (TiCl_4)(MgCl_2)_{3.14}(THF)_x \quad (2.1)$$

$$3.14MgCl_2 + TiCl_3 \cdot 1/3AlCl_3 + THF(Sol.) \rightarrow TiCl_3)(AlCl_3)_{1/3}(MgCl_2)_{3.14}(THF)_y \quad (2.2)$$

$$3.14MgCl_2 + TiCl_3 + THF(Sol.) \rightarrow (TiCl_3)(MgCl_2)_{3.14}(THF)z \quad (2.3)$$

Where Sol. = Solvent

In solution or solid state, the complexes in Equation (2.1)-(2.3) may be different. This difference will affect the properties of catalyst directly. In solution, *x*, *y*, and *z* are all relatively big because THF will occupy all the coordination sites of Ti, Mg, and Al together with Cl. In solid state, the percentage of THF is closely related to *x*, *y*, and *z*; consequently, the control of THF percentage in a suitable range is very necessary for catalyst preparation [46].

Prereduction of $TiCl_4(TiCl_3)/MgCl_2/THF$ catalytic systems with cocatalyst (Co-cat.) such as MAO, DEAC, TEA, TiBA, TnOA, etc. A complexation system was formed with the following Equations (2.4)-(2.6):

$$(TiCl_4)(MgCl_2)_{3.14}(THF)x + n\text{Co-cat} \rightarrow (TiCl_4)(MgCl_2)_{3.14}(THF)_{x-n} + n\text{THF}\cdot\text{Co-cat} \quad (2.4)$$

$$(TiCl_3)(AlCl_3)_{1/3}\,(MgCl_2)_{3.14}\,(THF)_y + n\text{Co-cat} \rightarrow (TiCl_3)(AlCl_3)_{1/3}\,(MgCl_2)_{3.14}(THF)_{y-n} + n\text{THF}\cdot\text{Co-cat} \quad (2.5)$$

$$(TiCl_3)(MgCl_2)_{3.14}(THF)z + n\text{Co-cat} \rightarrow (TiCl_3)(MgCl_2)_{3.14}(THF)z\text{-}n + n\text{THF}\cdot\text{Co-cat} \quad (2.6)$$

According to Equations (2.4)-(2.6) prereduction of the catalyst with cocatalyst has at least two influences. First, it reduces Ti(IV) to Ti(III) so that the catalyst has very uniform activity to suit the fluidized bed to increase the stabilization of production and favor the granule morphology of polymer obtained. Second, THF occupies the coordination sites of Ti to make Ti as a center with no activity; cocatalyst can also coordinate with THF, and probably there exist a dynamic equilibrium in which Al and Ti compete for coordination of THF. Therefore some THF would be moved from the Ti center by cocatalyst, and the Ti center will indicate high catalytic activity [46].

- Catalyst based on $MgCl_2$/alcohol complexes or $MgCl_2$•nEtOH adducts

One recipe of ZN catalyst of this kind composes of two steps; the preparation of $MgCl_2$ support and its impregnation with $TiCl_4$. According to the synthesis of $MgCl_2$ support as a carrier, $MgCl_2$ was mixed with ethanol and a dispersant, paraffin oil. After the reaction mass is heated to 120ºC, the melt of the $MgCl_2 \cdot x$EtOH complex (x = 2.8-3.0) was formed. It was thoroughly mixed with the dispersant until the emulsion of molten complex is formed. The emulsion was rapidly dispensed into a large of cold *n*-heptane and the $MgCl_2 \cdot x$EtOH complex crystallizes [47].

$MgCl_2$ formed numerous complexes with alcohols. The [alcohol]:[$MgCl_2$] ratio in the complexes depended on the type of alcohol and the temperature at which the complexes was formed. The complexes usually melt at 80-100ºC, much lower temperature than $MgCl_2$ itself, and they were readily soluble in an excess of alcohol. Both these features were useful for the preparation of Ti-based $MgCl_2$ –supported catalysts.

Two methods were used to synthesize Ti-based catalysts with this support. In the first method, $TiCl_4$ was used to remove ethanol from the solid complex. Spherical particles of the complex was twice treated neat $TiCl_4$, by heating the slurry in *n*-heptane from 20 to 100ºC in the first time and time at 130ºC the second. This treatment created the final ZN catalyst including 7.5 wt.% of Ti [47].

In an alternative method, ethanol was removed from the adduct formed by heating and by treating with an organoaluminum compound. Firstly, the spherical particles were heated from 50 to 150ºC until the (EtOH:$MgCl_2$) ratio in the complex decreased from 2.8 to 1.1. Then the support was dissolved in hexane and the remaining ethanol was removed at 60ºC by treating with TEA. Lastly, the support was treated with $Ti(OBu)_4$ and $SiCl_4$ at room temperature and then heated to 65ºC. The composition of final catalyst was consisted of Ti = 9 wt.%, Mg = 10.6 wt.%, and Cl = 44 wt.%. Moreover, both these catalysts had high activity in polymerization of ethylene (100 kg/g Ti) as well as generated large spherical particles of polymer. The catalysts were similar to catalyst that are used for the synthesis of mixtures of different alkene polymers within a single polymer particle (polyolefin alloys) [47].

It is generally accepted that the alcohol residues remained in this catalyst which led to low activity. Therefore, many published articles are devoted to improve the dealcoholation process and to attempt a suitable of the EtOH/$MgCl_2$ molar ratio in order to develop this method which led to better activity of catalyst as well as property of polymer. Forte and co-worker [48] investigated the effects of the degree of dealcoholation and ethanol content of the support on some physical properties of the catalysts prepared with $MgCl_2$•*n*EtOH complexes. In this work, they were varied the EtOH/$MgCl_2$ molar ratio in the range 1.0-10.0. It could be concluded that the suitable of EtOH/$MgCl_2$ molar ratio were between 2.5 and 4.0. At lower EtOH/$MgCl_2$ ratios than 2.5 it was not probable to gain the adduct in a totally melted form before its precipitation. Nevertheless, at ratios higher than 4.0, it was not probable to obtain good control of the support morphology. Experimentally, it was found that the degree of dealcoholation and ethanol content of the support strongly affected the porosity and surface area of the supports and catalysts. In addition, the description of reactions between the catalyst components during titanation step have been also proposed as observed in Equations (2.7)-(2.13). According to the Equation 2.7, the byproduct $EtOTiCl_3$ was soluble in hot $TiCl_4$ and then it was removed from the catalyst by filtering at high temperature. It is generally accepted that the reaction between titanium tetrachloride and ethanol is highly exothermic; therefore, the introduction of titanium tetrachloride to the support during the catalyst synthesization must be performed at low temperature ($\leq 10^{\circ}C$) to prevent the reactions as presented in Equations (2.7) and (2.8). The treatment of intermediate products including internal donor (ID) in the structures with the addition of $TiCl_4$ led to high surface area and catalytic activity. It could be summarized that the internal donor (Equations (2.9)-(2.12)) were taken to prevent the breakage of catalyst particles, and to control the fixation of $TiCl_4$ on the $MgCl_2$ faces.

$$MgCl_2 \bullet EtOH + TiCl_4 \rightarrow MgCl_2 + EtOTiCl_3 + HCl \tag{2.7}$$

$$MgCl_2 + MgCl_2 \rightarrow MgCl_2(solid) \tag{2.8}$$

$$MgCl_2 \bullet EtOH + ID \rightarrow MgCl_2 \bullet EtOH \bullet ID \quad (2.9)$$

$$MgCl_2 \bullet EtOH \bullet ID + TiCl_4 \rightarrow MgCl_2 \bullet EtOTiCl_3 \bullet ID + HCl \quad (2.10)$$

$$MgCl_2 \bullet EtOTiCl_3 \bullet ID + TiCl_4$$
$$\rightarrow MgCl_2 + MgCl_2 \bullet ID + TiCl_4 \bullet ID + TiCl_4 \bullet EtOTiCl_3 \quad (2.11)$$

$$MgCl_2 \bullet ID + TiCl_4 \rightarrow MgCl_2 \bullet TiCl_4 \bullet ID \quad (2.12)$$

$$MgCl_2(solid) + TiCl_4 \rightarrow MgCl_2(solid) \bullet TiCl_4 \quad (2.13)$$

The alcohol removal is very important to achieve high activities [27, 48-52]. According to published papers, the recrystallization of supports can be performed by the evaporation of the solvent [27, 48, 50, 52-54], or by cooling [27], and then followed by the washing of the substratum before the impregnation stage. However, alcohol elimination is not complete through these techniques and their presence in the support is undesirable as they can react with $TiCl_4$ during impregnation resulting in the formation of titanium alkoxides that are inactive for polymerization [27, 48-52]. For the dealcoholation of support, Chirinos [52] used $SiCl_4$ to react with $MgCl_2 \bullet n$ROH forming the $MgCl_2\text{-}SiCl_{4-n}(OR)_n$. Then, $TiCl_4$ is supported on the alcohol-free recrystallized $MgCl_2\text{-}SiCl_{4-n}(OR)_n$. After a completed dealcoholation, the alkoxysilanes formed remain grafted in the solid catalysts and act as an electron donor in the catalytic polymerization. Currently, the effects of methods for the alcohol removal of $MgCl_2 \bullet n$ROH were investigated by Marques *et al*. [55] and Almeida *et al.* [56]. Either thermal treatment or chemical dealcoholation was employed different substances such as titanium tetrachloride, triethylaluminium, dichlorodimethylsilane, and chlorotrimethylsilane. The supported catalyst, employing the supports which prepared by using the thermal activation of the adduct $MgCl_2 \bullet n OEt_2$ and chemical activation with $TiCl_4$, exhibited a high Ti content. However, the catalyst which prepared by using the treatment of adduct with TEA showed the best activity for both

ethylene and propylene polymerization; even though, this catalyst had relatively low Ti amount fixed on the support surface [55]. Moreover, the catalyst treated with dichlorodimethylsilane was also tested in ethylene and propylene polymerization, it showed low polymerization activity. However, the treatment of catalyst with chlorotrimethylsilane indicated a positive influence on the catalytic activity in ethylene and propylene polymerization. It was suggested that, due to the presence of two chloride atoms in the structure of dichlorodimethylsilane, this became fixed in $MgCl_2$ surface defects in the form of di-ethoxysilane, filling positions where potentially active titanium could be fixed in the support surface which explained the decrease in activity [56]. As proven by SEM measurement, the obtained supported catalysts showed spherical shape and the produced polyethylene particles were also spherically shaped. The catalyst showing the highest Ti content was obtained using the support with largest pores. This one showed the best performance of catalyst in both polymerization of ethylene and propylene, combining high activities and improved polymer properties. That catalyst system was synthesized through thermal dealcoholation instead of chemical [56]. Parada *et al.* [51] studied that the different types of alcoholic solutions of $MgCl_2$, using 1-hexanol, t-butanol, butanol, iso-propanol, propanol, and ethanol, were recrystallized with $SiCl_4$ and thus the supports were subsequently impregnated with $TiCl_4$. As compared in the obtained result, catalysts were generated with from solutions of $MgCl_2$ in 1-hexanol recrystallized by solvent evaporation and quick cooling. The catalytic activity was dependant on the length of the alkyl group and the nature of the isometric alcohol used in the treatment of the support. In addition, the supports and catalysts were characterized by infrared and energy dispersive scanning (EDS). The FT-IR and EDS results could be confirmed the presence of alkoxysilanes in the catalysts treated with $SiCl_4$ as well. Currently, Gopinath ‘s group [57-61] has studied the $MgCl_2$•*n*ROH adduct by various types of alcohol, in order to a deeper understanding of multicomponent complex systems of this type in molecular level properties. Using powder XRD and solid state NMR methods were used to characterize for better understanding of the structural aspects of molecular adducts. However, detailed structural and spectral investigations are important to understand the present catalyst system for better activity.

2.2.2.2 Catalysts Produced by Synthesis of Organomagnesium Compounds

This method for synthesizing the $MgCl_2$ is obtained *in situ* from the reaction of organomagnesium compounds and chlorinating agent in presence of the internal donor [20, 47, 62-65]. In many articles reporting, it has been found that $Mg(OEt)_2$ is one of the most organomagnesium compound for preparing ZN catalysts due to a high activity, more stable activity, as well as replication of precursor morphology to catalyst and to polymer [64, 65].

- Catalyst based on $Mg(OEt)_2$

Tanase *et al*.[63] have investigated in detained the morphology of $Mg(OEt)_2$ as a carrier material and proposed mechanisms for particle growth in $Mg(OEt)_2$ synthesis (Figure 2.9) and chemical reactions (Equations (2.14)-(2.16)), respectively. Elimination of an oxidized layer on a Mg metal surface (e.g., $Mg(OH)_2$) occurred with I_2, activated Mg and EtOH reacted to form $Mg(OEt)_2$ (Equation (2.14)) and amorphous $Mg(OEt)_2$ was immediately precipitated on the Mg surface due to the low solubility of $Mg(OEt)_2$ in EtOH. Simultaneously, I_2 and Mg reacted to form MgI_2 (Equation (2.15)), then $Mg(OEt)_2$, MgI_2 and EtOH formed the quasi-stable complex $nMg(OEt)_2 \bullet MgI_2 \bullet mEtOH$ (Equation (2.16)) and it dissolved to EtOH, and then small plate crystals of $Mg(OEt)_2$ precipitated on the Mg surface from EtOH solution. Some $Mg(OEt)_2$ crystals that had grown on the Mg metal exfoliated as ‘‘lump-like’’ seeds. Large plate crystals subsequently crystallized on the seeds from EtOH solution, and growth on the seeds proceeded to form the round $Mg(OEt)_2$.

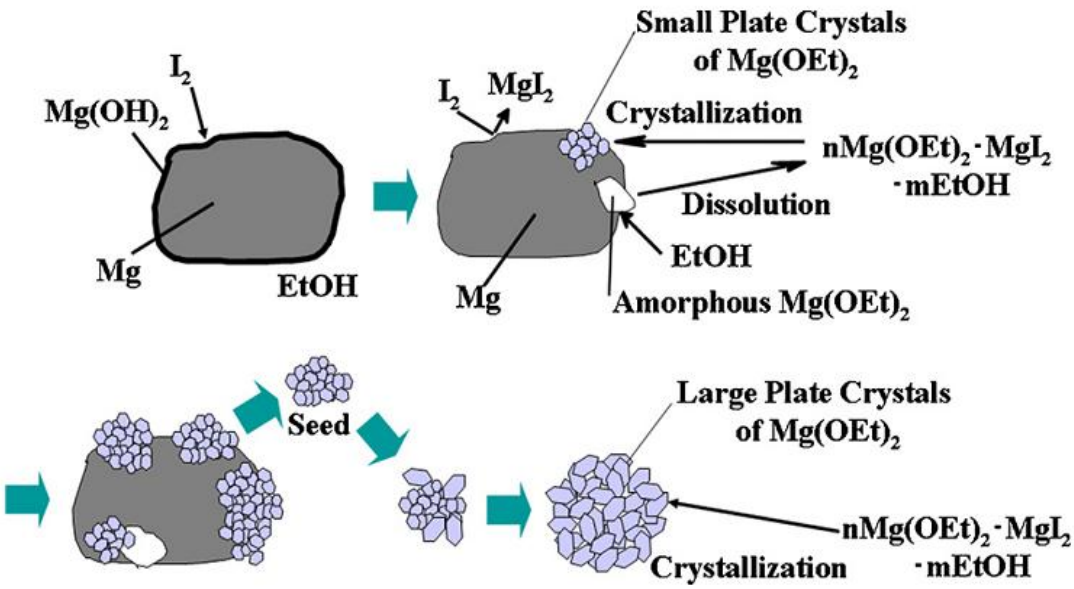

Figure 2.9 Mechanism for particle growth in $Mg(OEt)_2$ synthesis [63].

$$Mg + 2EtOH \rightarrow Mg(OEt)_2 + H_2 \tag{2.14}$$

$$Mg + I_2 \rightarrow MgI_2 \tag{2.15}$$

$$n\mathrm{Mg(OEt)_2} + \mathrm{MgI_2} + m\mathrm{EtOH} \rightarrow n\mathrm{Mg(OEt)_2} \cdot \mathrm{MgI_2} \cdot m\mathrm{EtOH} \tag{2.16}$$

Where n = 1-3, m = 1-6 of integer

Moreover, Tanase *et al.* [20] also have prepared $Mg(OEt)_2$ from the reaction of magnesium with the addition metal dihalide compounds ($MnCl_2$, $FeCl_2$, $CoCl_2$, or $ZnCl_2$). They found that the addition of metal chlorides in the precursor could improve the morphology and particle size. The addition of different types of metal to the crystalline lattice of $Mg(OEt)_2$ (with $CdCl_2$-type hexagonal crystalline structure [66]) through the co-crystallization in $Mg(OEt)_2$ synthesis (Figure 2.10) in order to control the sizes of crystals and the spherical morphology of $Mg(OEt)_2$ particles obtained.

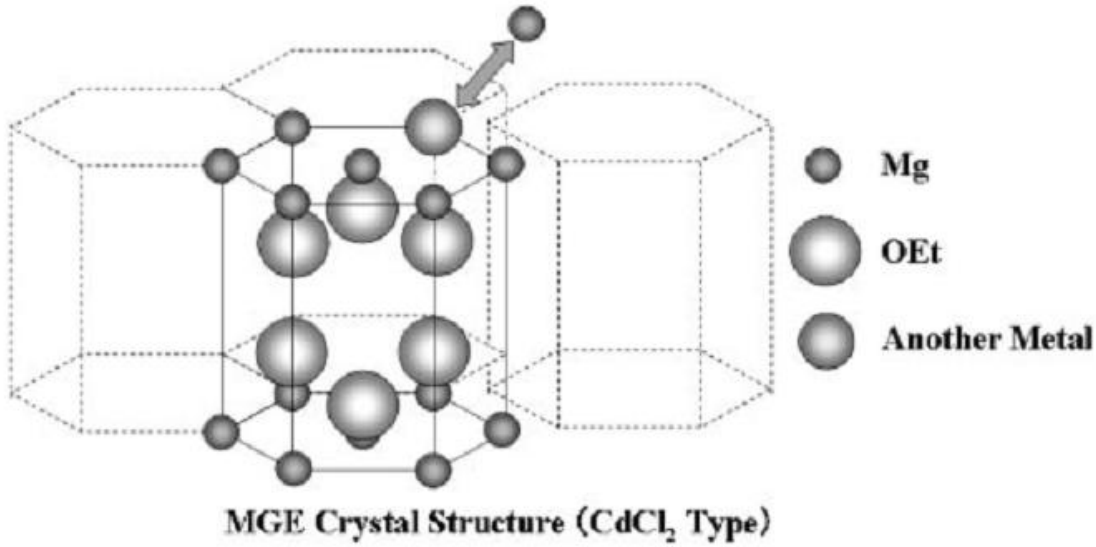

Figure 2.10 The crystalline structure of new carrier material containing a different kind of metal through the co-crystallization in synthesis of $Mg(OEt)_2$ [20].

Joseph *et al*. [62] have also studied the influence of reaction kinetics on morphology of the magnesium ethoxide. They found that magnesium ethoxide formation occurred at the interphase surface of magnesium and ethanol. They was observed that for achieving the desired particle characteristics of magnesium ethoxide from magnesium particles were depended upon the rate of reaction, extent of shearing inside the reactor, agitator rpm, concentration, and viscosity.

The conversion reaction of $Mg(OEt)_2$ to $MgCl_2$ was proposed by Shijing *et al*. [67]. The interaction between $TiCl_4$ and $Mg(OEt)_2$ during catalyst preparations could be explained with the following this reaction:

$$TiCl_4 + Mg(OEt)_2 \rightarrow Ti(OEt)_nCl_{4-n} + Mg(OEt)_mCl_{2-m} \quad (2.17)$$

Where n = 0-2; m = 0-2.

The *n* and *m* values depends mainly on the ratio of [Ti]/[Mg] in the case of other condition being certain. An ethoxyl titanium chloride is presumably formed directly in the course of the transformation of $Mg(OEt)_2$ to $MgCl_2$ ($m = 0$)

$$TiCl_4 + Mg(OEt)_2 \rightarrow Mg(OEt)Cl + Ti(OEt)Cl_3 \text{ or } MgCl_2 + Ti(OEt)_2Cl_2 \quad (2.18)$$

$$2TiCl_4 + Mg(OEt)_2 \rightarrow MgCl_2 + 2Ti(OEt)Cl_3 \quad (2.19)$$

A portion of the obtained ethoxyl Ti chloride dissolves in solvent and was washed off; the other portion as an active centers fixed on the resulting magnesium chloride [67].

According to published patents, many researchers have studied the preparation of ZN catalysts by using $Mg(OEt)_2$ as shown in Table 2.4.

Table 2.4 Ziegler-Natta catalysts based on $Mg(OEt)_2$ as a starting material

Company/ Inventor	Catalyst	Results	Pat. No. /Year
Bernd Diedrich *et al*. (German)	$Mg(OC_2H_5)_2$ + $TiCl_2(O\text{-}iC_3H_7)_2$	The higest activity = 11.7 kgPE/gCat.	3644316 /1972 [68]
Idemitsu Korean Co., Ltd. (Tokyo, JP)	$Mg(OC_2H_5)_2$ + EtOH + $SiCl_4$ + $TiCl_4$	The highest activity in PE (1,250 kgPE/gTi.h), amount of EtOH = 0.5 mmol, Not EtOH = 400 kgPE/gTi.h	4342855 /1980 [69]
Idemitsu Korean Co., Ltd. (Tokyo, JP)	$Mg(OC_2H_5)_2$ + Alcohol + $SiCl_4$ + $TiCl_4$	The highest activity = 350 kgPE/gTi.h when using cyclohexanol	4255544 /1981 [70]
Idemitsu Korean Co., Ltd. (Tokyo, JP)	$Mg(OC_2H_5)_2$ + *n*-Octanol + $TiCl_4$	The highest activity = 337 kgPE/gTi.h	4308170 /1981 [71]

Table 2.4 (Cont.) Ziegler-Natta catalysts based on $Mg(OEt)_2$ as a starting material

Company/ Inventor	Catalyst	Results	Pat. No. /Year
Standard Oil Co., (Indiana, Chicago)	$Mg(OC_2H_5)_2$ + CCl_3COOH + $Ti(O\text{-}nC4H_9)_4$	The highest activity = 36,200 kgPE/gTi.h	4311612 /1982 [72]
Toa Nenryo Koyo Kabushiki Kaisha (Tokyo, JP)	$Mg(OC_2H_5)_2$ + Halogenated HC + EB + $TiCl_4$	The highest activity = 20 kgPE/gCat. (1-hexene as comonomer)	4686265 /1987 [73]
Mansor Izzat Taflaf	$Mg(OC_2H_5)_2$ + $TiCl_4$ + EB + $TiCl_4$ + Benzoyl Chloride + $TiCl_4$	The highest activity = 822.5 kgPE/gTi.h	6692033 /2006 [74]

Dashti *et al.* [64, 65] investigated kinetic and morphological behaviors of using a $Mg(OEt)_2$-based ZN catalyst compared with a conventional ball-milled ZN catalyst for better understanding of catalytic performance. The results indicated that the $Mg(OEt)_2$-based ZN catalyst showed a typical build-up-type kinetics with good polymer morphology. Both the stable kinetics and good replication behavior of the $Mg(OEt)_2$-based ZN catalyst were regarded as originating from the uniform spatial dispersion of active sites in the catalyst particles.

However, One of the key steps to determine the performance of $Mg(OEt)_2$-based ZN catalysts is the chlorination step, an indispensable step to convert $Mg(OEt)_2$ into $MgCl_2$ [65, 68-71, 73-77], where a variety of chlorinating agents have been examined as shown in Table 2.5. It could be concluded that $SiCl_4$ and $TiCl_4$ are preferred as chlorinating agents.

Table 2.5 The improvement of catalytic activity using $Mg(OEt)_2$ by chlorinating agents

Company /Inventor	Catalyst	Chlorinating Agents (CA)	Pat. No. /Year
Solvay & Cie	($Mg(OEt)_2$ + CA) + $TiCl_4$	HCl, $AlCl_3$, Cl_2, $SOCl_2$, NH_4Cl	4144390 /1979 [75]
Idemitsu Kosan Co.,Ltd.	($Mg(OEt)_2$+ $SiCl_4$ + *n*ROH) + $TiCl_4$	$SiCl_4$	4255544 /1981 [69]
Fina Technology,Inc.	$Mg(OEt)_2$+ $TiCl_4$(x3) ($Mg(OEt)_2$+ $SiCl_4$ + *n*ROH) + $TiCl_4$ $Mg(OEt)_2$+ $SiCl_4$ + ID + $TiCl_4$ (x2) $Mg(OEt)_2$+ $SiCl_4$ + ID + $TiCl_4$	$TiCl_4$(x2), $TiCl_4$+$SiCl_4$, $SiCl_4$	5817591 /1998 [71]
Union Carbide Chemicals & Plastics Technology Corporation	$Mg(OEt)_2$+$Ti(OEt)_2$+mixed CA + $TiCl_4$	A multi-step chlorination agents such as $SiCl_4$+EADC, $TiCl_4$+EADC etc.	6511935 /2003 [74]
Idemitsu Kosan Co.,Ltd.	($Mg(OEt)_2$+ $SiCl_4$ + *n*ROH)+ $TiCl_4$	$SiCl_4$	4255544 /1981 [76]
Fina Technology,Inc.	$Mg(OEt)_2$+ $TiCl_4$(x3) ($Mg(OEt)_2$+ $SiCl_4$+ *n*ROH) + $TiCl_4$ $Mg(OEt)_2$+ $SiCl_4$+ ID + $TiCl_4$(x2) $Mg(OEt)_2$+ $SiCl_4$+ ID + $TiCl_4$	$TiCl_4$(x2 or x3), $TiCl_4$+ $SiCl_4$, $SiCl_4$	5817591 /1998 [77]

2.2.3 Lewis Acid as the Third Component

The addition of a third component to the metal-alkyl is a widespread practice with $MgCl_2$ catalysts in order to their performance and to control the polymer molecular structure [37]. In ethylene polymerization the introduction of alkyl halides

modification (Lewis acids such as $AlCl_3$, halogens and others) is rather limited and is principally used to modify the MWD and chain structure distribution of the polymer are mainly determined by the active center distribution (ACD) of the catalyst. It is widely accepted that a large percentage of active sites are formed at the edges, cuts, and surface defects of $MgCl_2$ crystallites. Doping $MgCl_2$ with inorganic salts can change the distribution of these defects and thus change the ACD of the catalyst [11]. On the other hand, the addition of modifiers is almost indispensable to obtain satisfactorily stereoregular propylene polymers. The additives used for this purpose are generally electron donor compounds (Lewis bases) [37]. However, this work has been involved to study the effect of Lewis acid halides on Ziegler-Natta catalyst as described in patent and scientific literature.

The influence of different Lewis acids such as $AlCl_3$, $AlEtCl_2$, $SnCl_4$, $TiCl_4$ and BF_3 were studied on the ethylene polymerization activities in the soluble system of Cp_2TiCl_2-DEAC. It was found that modification with a Lewis acid increased the number of active sites, the rate constant of chain propagation and the molecular mass of polymer. The authors attributed both effects to enhance in the degree of polymerization activities due to its complexing with the Lewis acid compound.

On ethylene polymerization in the soluble $TiCl_4$-AlR_3-Ph_2Mg catalytic system the addition of a strong Lewis acid ($SbCl_5$) to a molar ratio $SbCl_5$: $TiCl_4$ = 1:1 increased both the rate of polymerization and the molecular mass of the polymer obtained.

$Ti(OBu)_4 \cdot AlEt_2Cl$ catalytic system with weak Lewis acids such as $MgCl_2$, $MnCl_2$, $CoCl_2$, and $NiCl_2$ accelerated the propylene polymerization. The addition stronger Lewis acids such as $FeCl_3$, $GaCl_3$, $HfCl_4$, $ZrCl_4$, $TaCl_5$, and $NbCl_5$ in contrast impeded polymerization. From the results it was assumed that Lewis acid form a complex with the titanium atom of the active centre.

Modification of $TiCl_4/MgCl_2$ by a stronger Lewis acid ($SnCl_4$) decreased the catalytic activity. At the same time, $TiCl_3$ catalyst modified with $SnCl_4$ could be

increase catalytic activity. Possibly the fall in the activity of $TiCl_4/MgCl_2$ in the in the presence of $SnCl_4$ was due to a change the interaction of $TiCl_4$ with the $MgCl_2$ surface in the presence of $SnCl_4$.

$TiCl_4/MgCl_2$ catalytic system modified with $NiCl_2$, $CoCl_2$, and $FeCl_3$ on ethylene polymerization enhanced the catalytic activity and the molecular mass of the polymer obtained. A similar effect was observed on ethylene polymerization in solution catalysts based on titanium tetraalkoxides on $MgCl_2$ carrier modified by $NiCl_2$ obtained *in situ*. Simultaneous rise in the molecular mass of the polymer and the polymerization rate suggested that on modification of $TiCl_4/MgCl_2$ with $NiCl_2$, $CoCl_2$, and $FeCl_3$ the chain propagation rate constant increased. At the same time on ethylene polymerization in the presence of solid $TiCl_3$ solutions in metal chlorides the activity of the catalyst diminished in the order: $MgCl_2)_{1.5}TiCl_3$ >> $MnCl_2 \cdot TiCl_3$ > $FeCl_2 \cdot 2TiCl_3$ > $MnCl_2 \cdot 2TiCl_3$ > $CoTi_{1.6}Cl_{6.6}$ > $GeCl_3 \cdot 3TiCl_3$ > $NiCl_2 \cdot 3TiCl_3$ > $NiCl_2 \cdot 2TiCl_3$ > $MoCl_3 \cdot TiCl_3$.

In all likelihood the modifying action of the chlorides of the transition metals did not boil down to direct interaction with $TiCl_4$ and was determined by the interaction, as a minimum, between the three components of the catalyst including the modifying compound, $MgCl_2$ as well as the chloride of the transition metal [78].

According to the effect of $MnCl_2$ adding on the catalytic activity for olefin polymerization were reported by Garoff and Leinonen [25]. The catalyst added with 10 mol% of $MnCl_2$ indicated increasing activities while at higher Mn concentrations activity decreased linearly.

The influences of $ZnCl_2$ doping on the catalytic performance for olefin polymerization were reported by Fregonese and Bresadola [26]. The catalyst doped with 0.73 wt.% of $ZnCl_2$ exhibited the highest activity, whereas the use of higher $ZnCl_2$ concentrations caused lower activities. In addition, the introduction of $ZnCl_2$ into $MgCl_2$ support could promote the structural defects in the support indicating that

the replacement of a partial Mg by Zn was occurred. This phenomenon is possibly occurred because their ionic radii are very similar (Zn^{2+} = 0.88 Å, Mg^{2+} = 0.86 Å).

To modify $MgCl_2$ support with $AlCl_3$ by co-ball milling method, it was found that the addition of a little amount of $AlCl_3$ in the process of the ball milling promotes the crystal lattice destroy of $MgCl_2$ [79]. Due to the lower lattice energy of $AlCl_3$lattice than that of $MgCl_2$ lattice, the lattice defects of $AlCl_3$ lattice is more prone to be formed than those of $MgCl_2$ lattice (Reaction (A) and (B), Figure 2.11). The chlorine vacancies formed due to the defects of $AlCl_3$ lattice may attract the chlorine atoms of $MgCl_2$ lattice and in turn the attraction promotes the formation of the defects of $MgCl_2$ crystal lattice (Reaction (C), Figure 2.11). Therefore, $TiCl_4$ can be dispersed more uniformly and fixed more firmly on the support of $AlCl_3/MgCl_2$-supported catalyst than that of the $MgCl_2$-supported catalyst. However, the excess amount of $AlCl_3$ leads to the decrease of the polymerization activity. This can be explained that $AlCl_3$ is not an ideal support as $MgCl_2$. Moreover, the addition of $AlCl_3$ of $AlCl_3/MgCl_2$ sup-ported catalyst has little influence on the isotactic index of polypropylene in comparison with $MgCl_2$ supported catalyst.

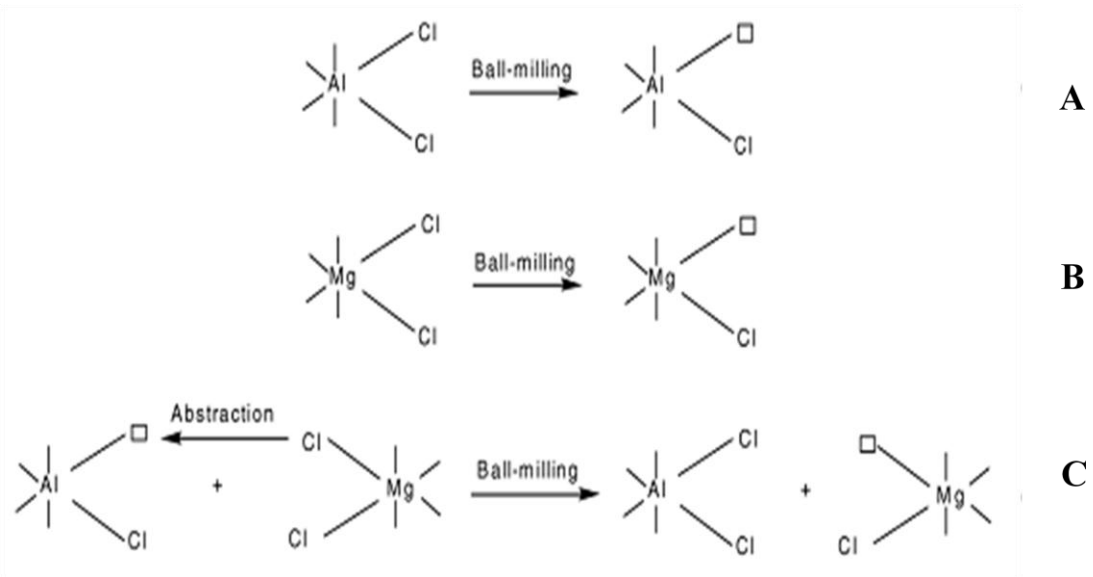

Figure 2.11 The formation of defect of $MgCl_2$ lattice during the co-milling of $MgCl_2$ and $AlCl_3$ **[**79**].**

According to Chen *et al.* [11] showed that the doped on $MgCl_2$ supported on Ziegler–Natta catalysts with $AlCl_3$ in ethylene polymerization. The results showed that the catalysts based on $AlCl_3$-doped $MgCl_2$ support exhibited a slightly higher activity than did the $MgCl_2$-supported catalyst and the molecular weight distribution (MWD) of polyethylene markedly increased (from 10.8 to 47.9) with the increase of $AlCl_3$ content in catalysts. In the meantime, Chen and Fan [28] investigated Ti-based Ziegler–Natta catalysts supported on $MgCl_2$ doped with $AlCl_3$ in Ethylene/1-hexene copolymerization. The $TiCl_4/MgCl_2$ catalyst doped with $AlCl_3$ results showed slightly higher efficiency and higher 1-hexene incorporation than the $TiCl_4/MgCl_2$ catalyst without doped $AlCl_3$ due to the effect of doped $AlCl_3$ that there are two possible points to explain the effect of doped $AlCl_3$:

The first, $AlCl_3$ has higher Lewis acidity than $MgCl_2$: its presence in the catalyst might reduce electron density on some types of active center, which is beneficial to the coordination of more electron-donating olefin on active center than ethylene. And the second, the doping $AlCl_3$ in the catalyst may change the active center distribution, resulting in formation of more active centers with high copolymerization ability [28]. In addition to the addition of $AlCl_3$ mixed with cocatalyst found that the molecular weight distribution (MWD) of polyethylene increased [37].

Ribour and his co-worker [23] provided a method for improving and controlling the activity for Ziegler-Natta catalyst systems. A Ziegler-Natta pre-catalyst is activating by adding a Lewis acid (MX_n). The BCl_3 was the most preferred Lewis acid due to the size of and the oxidation state of metal B played a role on the distribution and activation of the active sites several other metals have been tested such as Si and Sn but B had by far the best performance as activator. Similarly, other halogens or alkyl groups have been tested for X, but chlorine gives the best results: the activities obtained with various X can be ranked as follows: Cl > Br > F > Ethyl. Consequently, the treatment with BCl_3 improved the activity by 2 with respect to the same untreated catalyst system. Treating catalyst with BCl_3, it showed that the productivity increased with increasing amount of BCl_3 in homopolymerization of

ethylene and copolymerization of ethylene with 1-hexene. According to copolymerization of ethylene and 1-hexene found that at the first the productivity increased with increasing amount of BCl_3, it reached a maximum and then decreased slowly. The position of the maximum varied with the nature of the pre-catalyst. Ribour *et al*. [80] investigated the modification of heterogeneous Ziegler-Natta pre-catalysts by treatments with BCl_3 (2 hours in heptane; T = 20–90 °C; B/Ti = 0.1–5) before their use in the polymerization of propylene to modify the active sites distribution and without drastic modifications of polypropylenes properties (tacticity, molecular weight distribution).

Ribour *et al.* [23] provided a method for improving the tacticity of Ziegler-Natta catalyst systems and for controlling the behavior of the active sterospecific sites. A Ziegler-Natta pre-catalyst is activated by adding a Lewis acid (MX_n) such as $SiCl_4$ and $SnCl_4$ due to the size of and the oxidation state of metal M played a role on the distribution and activation of the active sites. Si and Sn indicated the best performance for reducing the amount of atactic polymer while keeping a reasonable productivity Similarly, other halogens or alkyl groups have been tested for X, but chlorine gives the best results: the activities obtained with various X could be ranked as follows: Cl > Br > F > Ethyl. Besides, Lewis acid is also used to remove alcohol from recrystallization step of $MgCl_2$ ($MgCl_2.n$ROH adduct).The catalyst obtained from $SiCl_4$ recrystallization was not only to provide the highest activity, but it also showed the highest isotacticity index in polymer [52].

2.2.4 Cocatalyst

A general feature of the Ti based ZN catalysts is activation by alkylaluminum compound in order to change the oxidation state of titanium. It is well known that the different characteristics in Ziegler-Natta catalysts depend on the oxidation state of titanium during polymerization. The titanium valences including Ti^{4+}, Ti^{3+} and Ti^{2+} are produced by reacting $TiCl_4$ with activator such as AlR_3, where R represents different alkyl groups or Cl ligands. Ti^{3+} species are active species for the polymerization of both ethylene and propylene while Ti^{2+} which is the over-reduction

of Ti^{3+} is also active for ethylene polymerization [37, 81]. However, the activity of the catalyst and its stereospecificity (higher when the activity decreased) are strongly dependent on different kinds of AlR_3 compounds. Nooijen [82] performed an experimental study on various the different types of alkylaluminum compounds such as triethylaluminium (TEA), triisobutylaluminium (TIBA), trioctylaluminium (TOA), and iso-prenylaluminium (IPRA). It could be concluded that the catalytic activities increased in the order: TEA, TIBA, TOA, and IPRA. This results obtained suggested that increasing molecular dimensions of the cocatalyst increased diffusion limitations leading to a decrease in the rate of activation of the catalyst precursor. In addition, there other parameters are also affected on the performance of catalyst such as ratio of Al/Ti, temperature and time of mixing of all components, concentration of reactants, duration of polymerization [83], etc.

Specialized $TiCl_3 \cdot xAlCl_3$ composition is formed from $TiCl_4$ by a very specific reduction process involving the aluminum alkyl or aluminum metal. This reaction involves the alkylation of $TiCl_4$ with aluminum alkyl molecules followed by a dealkylation reduction to a trivalent state as in the following equations:

- Alkylation reactions:

$$TiCl_4 + AlEt_3 \rightarrow EtTiCl_3 + AlEt_2Cl \tag{2.20}$$

$$TiCl_4 + AlEt_2Cl \rightarrow EtTiCl_3 + AlEtCl_2 \tag{2.21}$$

$$TiCl_4 + AlEtCl_2 \rightarrow EtTiCl_3 + AlCl_3 \tag{2.22}$$

- Reduction reactions:

$$EtTiCl_3 \rightarrow TiCl_3 + Et\cdot \tag{2.23}$$

$$2Et \rightarrow \text{Ethane} + \text{ethylene} \tag{2.24}$$

Under drastic conditions, $TiCl_3$ can be similarly reduced to $TiCl_2$. The above equation only suggested the basic steps which occur; the actual mechanistic process is very complex and not well understood.

The actual $TiCl_3$ product formed is a composition containing $AlCl_3$ as alloy and probably some chemisorbed $AlEt_2Cl$ and $AlEtCl_2$. If the reduction is incomplete, the unreacted $AlEt_3$ and $TiCl_4$ are also present. Some $EtTiCl_3$ species may also be adsorbed on the $TiCl_3$.

It is understandable that different catalytic mixtures will be formed when the components $AlEt_3$ (or $AlEt_2Cl$) and $TiCl_4$ are mixed and used under different conditions. The nature of the catalyst changes with polymerization time. Some researchers stabilized the preparations by a prepolymerization aging at ambient or higher temperatures, but this produced only a partial improvement [83].

On the other hand, the external donor which can be used appears to be dependent on the type of internal donor. If ID is an aromatic monoester (EB is the most usual), esters of the same type are normally required, such as methyl-*p*-tolulate (MPT), ethylanisate (EA), *p*-ethoxy-ethylbenzoate (PEEB) and the like, whereas alkoxysilanes are required with phthalates (or diethers). Hindered piperidines, such as 2,2,6,6-tetramethylpiperidine (TMP), on the other hand, seem to work well with diethers, but not as well with monoesters. Whichever is the external donor, however, owing to its basic nature and the acidic nature of the AlR_3, a more or less complex interaction between the two components takes place [84].

In conclusion, it can be stated that all types of external donor easily form complexes with the AlR_3 cocatalyst. These complexes are rather stable for silanes, whereas in the case of aromatic esters, they further react, leading to the partial destruction of the ester and its replacement with significantly less stereoregulating products. The true cocatalyst is, in this case, a mixture including free AlR_3, unconverted AlR_3/ester complex, and a mixture of Al-alkoxides of different bulkiness. Some free ED also can be present if the Al/ED ratio is very low [84].

2.3 Mechanism of Ethylene Polymerization

Usually, Ziegler-Natta catalyst consists of two components (i.e., a transition metal salt such as a $TiCl_3$ or $TiCl_4$ (catalyst) and main-group metal compounds involving alkyl-Al (cocatalyst). It is generally accepted that the formation of active sites on Ziegler-Natta catalysts for olefin polymerization is accomplished through reduction and alkylation of surface Ti species by interaction of the catalyst with Al-alkyl cocatalyst.

2.3.1 Ethylene Polymerization

Despite passage of more than 60 years since the basic discoveries, the mechanism of ZN polymerization is still not fully understood. As in all chain-growth polymerizations, the basic steps are composed of initiation, propagation, and termination (chain transfer) as shown below:

- Initiation:

$$\text{Cat*-R} + CH_2 \doteq CH_2 \rightarrow \text{Cat*-}CH_2CH_2\text{R}$$

or $$\text{Cat*-H} + CH_2 = CH_2 \rightarrow \text{Cat*-}CH_2\text{-}CH_2$$

- Propagation:

$$\text{Cat*-}(CH_2\text{-}CH_2)_n\text{-R} + CH_2 = CH_2 \rightarrow \text{Cat*-}(CH_2\text{-}CH_2)_{n+1}\text{-R}$$

- Termination:

(i). Spontaneous

$$\text{Cat*-}(CH_2\text{-}CH_2)_n\text{-R} \rightarrow \text{Cat-}(CH_2\text{-}CH_2)_n\text{-R}$$

(ii). By transfer with hydride β-elimination

$$\text{Cat*-}(CH_2\text{-}CH_2)_n\text{-R} \rightarrow \text{Cat*-H} + CH_2 = \text{CH-}(CH_2\text{-}CH_2)_{n-1}\text{-R}$$

(iii). By transfer with aluminium alkyl

$$\text{Cat*-(CH}_2\text{=CH}_2\text{)}_n\text{-R} + \text{AlR}'_3 \rightarrow \text{Cat*-R}' + \text{R}'_2\text{Al-(CH}_2\text{-CH}_2\text{)}_n\text{-R}$$

(iv). By transfer with hydrogen

$$\text{Cat*-(CH}_2\text{-CH}_2\text{)}_n\text{-R} + \text{H}_2 \rightarrow \text{Cat*-H} + \text{CH}_3\text{-CH}_2\text{-(CH}_2\text{-CH}_2\text{)}_{n-1}\text{-R}$$

(v). By transfer with monomer

$$\text{Cat*-(CH}_2\text{-CH}_2\text{)}_n\text{-R} + \text{CH}_2 = \text{CH}_2$$

$$\rightarrow \text{Cat*-CH}_2\text{-CH}_2\text{-CH}_3 + \text{CH}_2\text{= CH-(CH}_2\text{-CH}_2\text{)}_{n-1}\text{-R}$$

Where Cat* is an active center; Cat is a deactivated center; R and R' are alkyl groups [85].

The mechanisms of chain propagation can be divided into two groups according the role of the catalyst and the cocatalyst interaction. In monometallic mechanisms, the cocatalyst creates the active species from the transition metal, however; is not involved in the chain growth reaction itself. Bimetallic mechanisms postulate an electron deficient bridge complex between Ti and Al components and favor propagation at the Al-C bond [29, 36].

In most bimetallic mechanism, the transition metal has the function of complexing and of polarizing the monomer, thereby preparing it for insertion into the Al-alkyl (polymer) bond. Most of these mechanisms were proposed by early workers in this area searching for similarities between ZN polymerization and the “Aufbau reaction” [29].

However, the mechanism of Cossee and Arlman is the most widely accepted one and many other monometallic mechanisms are variations of its basic assumption. The Cossee-Arlman proposal involves a “migratory alkyl transfer” [29] and, with some refinements, remains the most widely cited mechanism for ZN catalysis. A summary is shown below.

The reduced form of titanium is octahedral and contains open coordination sites (□) and chloride ligands on crystallite edges. Initiation begins by formation of an active center, believed to be a titanium alkyl. Alkylation by TEA cocatalyst produces an active center as seen Figure 2.12.

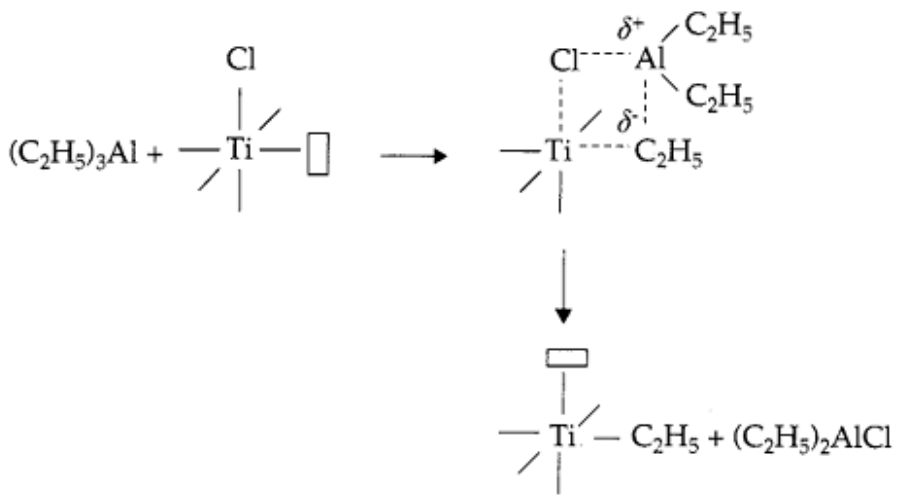

Figure 2.12 Formation of an active center by the reaction between a titanium alkyl and TEA cocatalyst [29].

The alkyl migrates (rearranges) such that an open coordination site moves to a crystallite edge position. Coordination of an ethylene monomer occurs to generate a π-complex as in Figure 2.13. Subsequent addition across ethylene results in the propagating species:

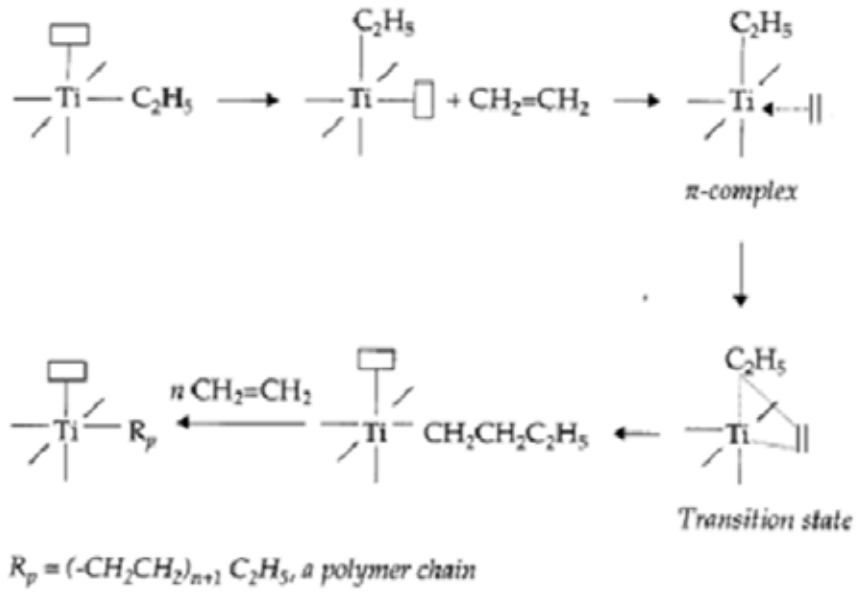

Figure 2.13 Propagation of ethylene monomer to generate a long-chain polymer [29].

Because titanium-carbon σ-bonds are known to be unstable, a different mechanism that invokes coordination of the aluminum alkyl to the titanium alkyl has been hypothesized. It is suggested that the titanium alkyl is stabilized by association with the aluminum alkyl. Coordination also accommodates the well-known propensity of aluminum alkyl to associate. This is known as the "bimetallic mechanism" and essential features were originally proposed by Natta and other workers in the early 1960s. Basic steps are similar to the Cossee-Arlman mechanism. The principal difference is participation of the aluminum alkyl. However, polymerization is still believed to occur by insertion of C_2H_4 into the Ti-C bond (rather than the Al-C bond). Key steps are represented in Figure 2.14 below:

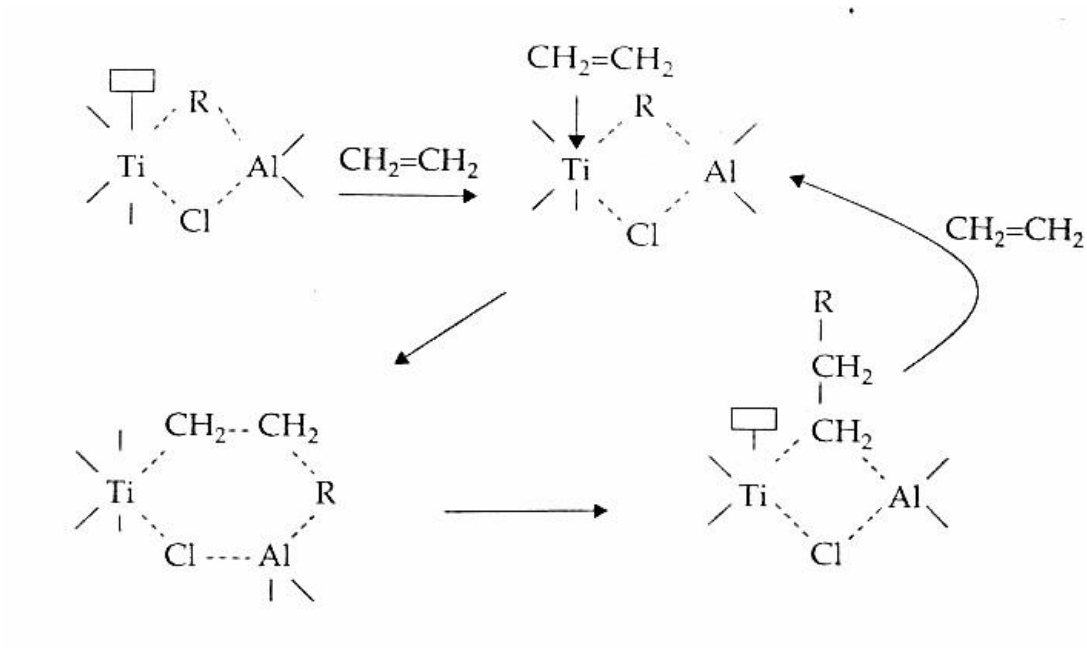

Figure 2.14 Bimetallic polymerization mechanism [29].

Termination occurs primarily through chain transfer to hydrogen, that is, hydrogenolysis of the R_p-Ti bond as in Figure 2.15. The titanium hydride may add ethylene to produce another active center for polymerization.

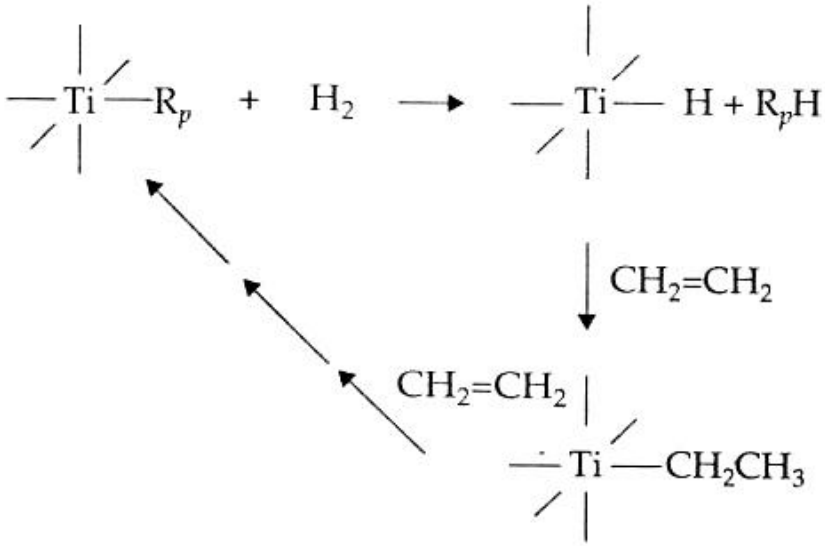

Figure 2.15 Schematic representation of hydrogenolysis chain transfer reaction [29].

Chain termination may also occur by β-elimination with hydride transfer to titanium (Figure 2.16 (A)), by β-elimination with hydride transfer to monomer (Figure 2.16 (B)), and chain transfer to aluminum alkyl (Figure 2.16 (C).

The aluminum alkyl product from Figure 2.16 (C) containing the polymeric chain (R_p) will undergo hydrolysis or oxidation/hydrolysis when the resin is exposed to ambient air. This chemistry results in polymer molecules with methyl and $-CH_2OH$ end groups, respectively. However, concentrations are miniscule, since the vast majority of chain termination occurs by Figure 2.15 and Figure 2.16 (A-B).

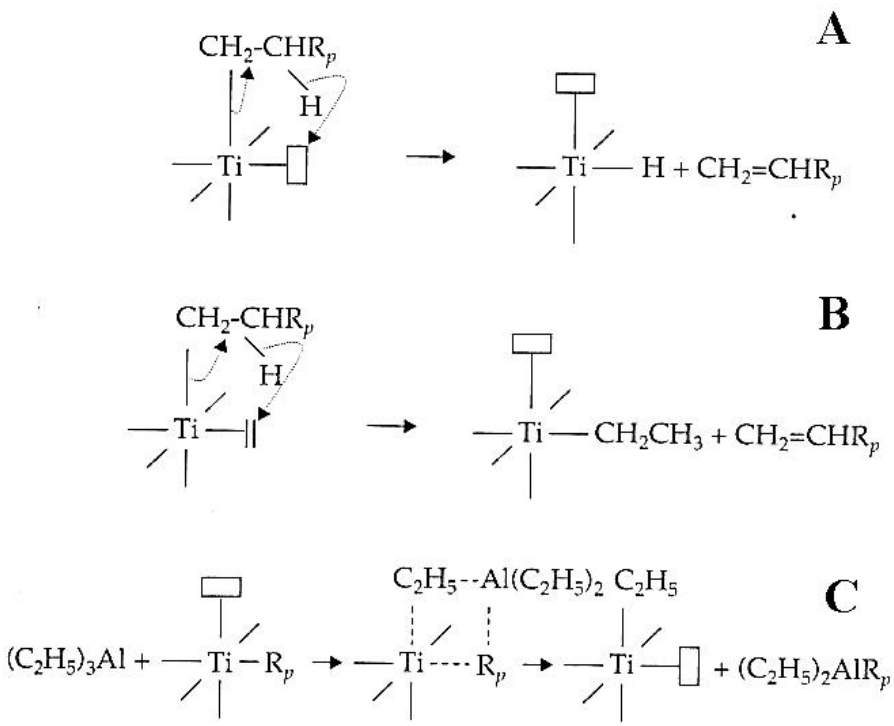

Figure 2.16 Schematic representation of chain termination reaction [29].

In chain transfer/terminations presented in Figures 2.15 and 2.16, the component containing the transition metal is still an active catalyst. Thus, each active center may produce hundreds or thousands of polymer chains.

The mechanism for polymerization of propylene using ZN catalysts is analogous to that discussed in this section with ethylene. However, unlike ethylene,

propylene can be said to have “head” and “tail” portions and regiochemistry can vary. More importantly, the orientation (stereochemistry) of the methyl group in the polymer has a dramatic effect on polymer properties. These factors make polymerization of propylene (and other α-olefins) more complex. However, ZN catalysts are the most important transition metal catalysts for production of polyethylene and other poly-α-olefins. Indeed, at this writing, it would not be practicable to manufacture the quantities of stereogular polypropylene needed for the global market without ZN catalysts. This may change as single site catalyst technology continues to evolve, but ZN catalysts will remain essential to polyolefin manufacture well into the 21st century [29].

2.3.2 Ethylene Copolymerization

It is well known that linear low-density polyethylene (LLDPE) is synthesized by copolymerization of ethylene with α-olefins. According to published papers, it was found that α-olefins have been used in ethylene copolymerization such as propylene, 1-butene, 1-pentene, 1-hexene, 1-octene, 1-decene, and so on [86-90]. An introduction of α-olefins to copolymer brings about to change of polymer properties (i.e. crystallinity, melting point, and density) [89-93]. Therefore, various copolymer properties are more advantageous than polyethylene generating from homopolymerization process such as better flexibility, lower viscosity, more excellent mechanical properties, and easier recycling [93]. However, the properties of copolymer depend largely on the amount of comonomer content in polymer chains [89-93]. In literature reviews, comonomer contents are based on several factors including structure of catalysts, types of cocatalyst as well as concentrations of comonomers in feed) [89-93]. In addition, the enhancement of catalytic activities by the introduction of a small amount 1-olefins can found both metallocene and ZN catalyst system is named the “comonomer effect” [28, 42, 94-96] catalyst case, the mechanism of this effect is shown in Figure 2.17.

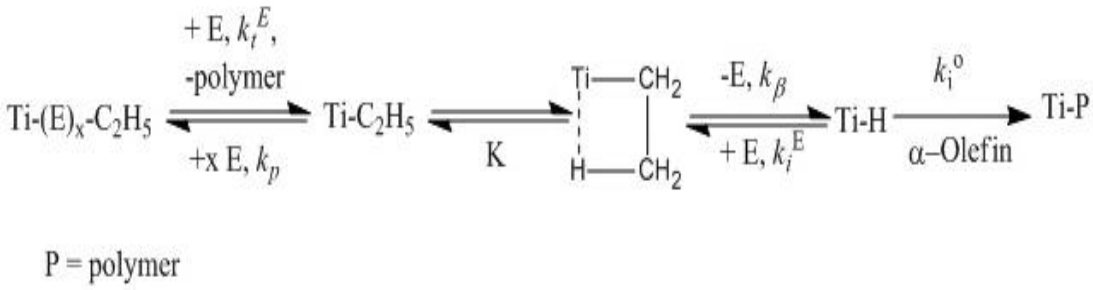

Figure 2.17 The kinestic mechanism of ethylene copolymerization reaction [94, 96].

In 1999, Kissin *et al*. [94, 96] proposed that a large amount of the sleeping active centers were generated from the β-agostically stabilized Ti-C_2H_5 group which were reduced the activity in ethylene homopolymerization. When the addition of any alpha-olefins in polymerization of ethylene, it added into the Ti-H bond and formed in polymer chain. Therefore, the activity of catalyst in ethylene/1-olefins copolymers was increased.

On the other hand, some researchers believe that the increase in polymerization activity is due to physical effects, others argue that chemical effects play a more important role [28]. Recently, Taniike, *et al.* [97] concluded that mechanistic explanations of the comonomer effect can be classified by chemical and physical origins. For the chemical origins were composed of two explanations:

(i) An increment of propagation rate constant because of reactivation of reactivation of dormant sites by ethylene in ethylene/propylene copolymer. When comparison with propylene, ethylene has a smaller size and higher reactivity, and hence it can be incorporated into dormant sites, which might be formed by a regioirregular propylene incorporation.

(ii) An enhancement of active-site proportion per Ti [C^*], based on some chemical reasons. Lost activity for homopolymerization of α-olefin remain active for ethylene copolymerization which reported by Spitz *et al*. [98]. Moreover,

agglomerated Ti species are dissociated in the presence of α-olefin leading to increase in the number active sites [99].

In general, the physical factors can be frequently separated in two main explanations such as:

(i) Enhancement of monomer diffusion through the decreased crystalline polymer by the insertion of comonomer. This attributes to an increase in the monomer concentration at the active centers [97] .

(ii) The disintegration of catalyst particles during copolymerization thus exposing new potential active centers, hence, increasing the diffusion of cocatalyst through copolymer [97].

2.4 Catalyst Particle Morphology

The possibility of controlling the polymer shape, size, and PSD to some extent through the catalyst has been known since the very beginning of the PP industry. It is based on the fact that the polymer usually tends to duplicate, on a large scale, the physical characteristics (shape and texture) of the parent catalyst. This phenomenon, usually named “replication”, is closely associated the particle growth mechanism of the polymerization. From the mechanism mentioned below, an extensive and well-controlled catalyst fragmentation and a uniform polymer growth seem to be the key parameters for a faithful replication. The catalyst has been required in the following:

- High surface area
- Proper porosity with a net of pore evenly distributed throughout the particle
- Appropriate mechanical strength, it has to be strong enough to withstand handling, but low enough to breakage to microparticle during polymerization
- Homogeneous distribution of the active sites
- Free access of the monomer to the inner most zones

2.5 Particle Growth Mechanism

To control the particle morphology, the thorough understanding about particle growth is important. Being aware of this important, from the beginning of 1970s, several models have been proposed to clarify the evolution of polymer particles from the original catalyst. The most representative ones can be divided into three types of physical models: Solid core" model, Polymer flow model, and Multigrain model [100] .

In the “Solid core” model, polymer is formed and accumulated of the surface of a nonfriable catalyst particle. In the "Polymer flow model", catalyst particle is completely fragmented in the polymerization, these fragments move outward with the same velocity of the surrounding polymer. The "Multigrain model" (MGM) seems to be more sophisticated, where the catalyst particle composes of numerous microparticles bearing active sites on their surface. The monomer diffuses into the catalyst volume and polymerizes on the surface of those microparticles, forming a micro-shell surrounding them and filling pore volume. After filling the pores, continuously formed polymer builds up stressing forces inside of the particle, when the forces become large enough to overcome the stand of catalyst structure, they break the catalyst particle into many small fragments, which are held together by the initially formed polymer. As the polymerization proceeds, the polymer particles expand continuously to the end of polymerization. From 1980s, Ray et al. introduced a mathematical framework for MGM to simulate many aspects of polymerization process, such as molecular weight distribution, heat and mass transfer limitation, particle fragmentation and etc [101]. Recently, Rajez et al. further realized MGM by giving the third dimension in calculation [102]. The images of three models are represented in Figure 2.18

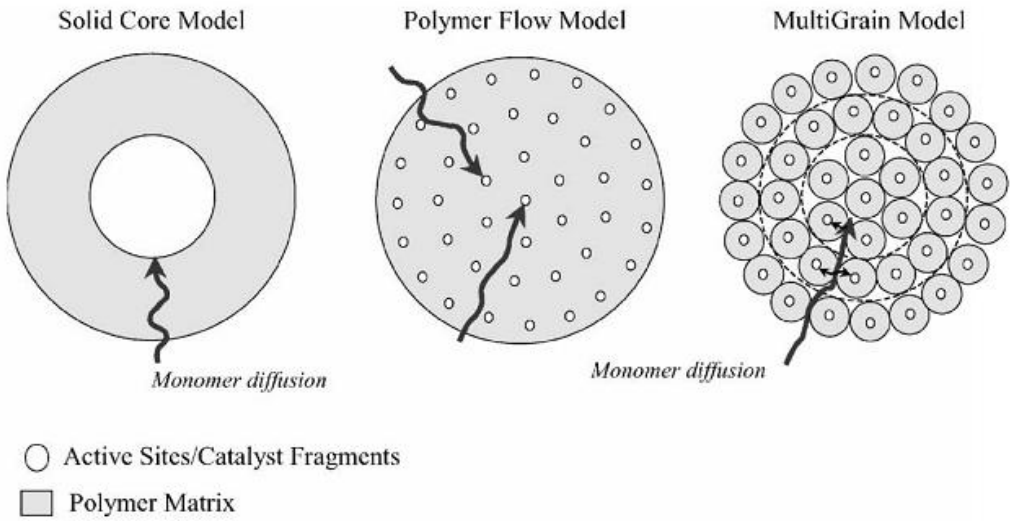

Figure 2.18 Schematic of three types of physical models including the solid core model, the polymer flow model, and the multigrain model [100].

Even though MGM is quite sophisticated, it is still very far from real mechanism. The empirical researchers, by direct observation, proposed more realistic models to explain for the particle growth. Bukatov et al.[103] considered that each microparticle is further made up of many catalyst crystallites, namely primary particles. In polymerization, the microparticles are fragmented, the crystallite are separated from each other and become a solid core for each primary polymer particle. This model can be called as "double grain model with solid microcore". Kakugo et al. observed that after microparticle being fragmented, the catalyst crystallite move to the surface of microparticle to sustain the polymerization, so-call "double grain model with expanding microcore" [104]. This model then was confirmed by Cecchin et al. [105]. The images about these two models are presented in Figure 2.19.

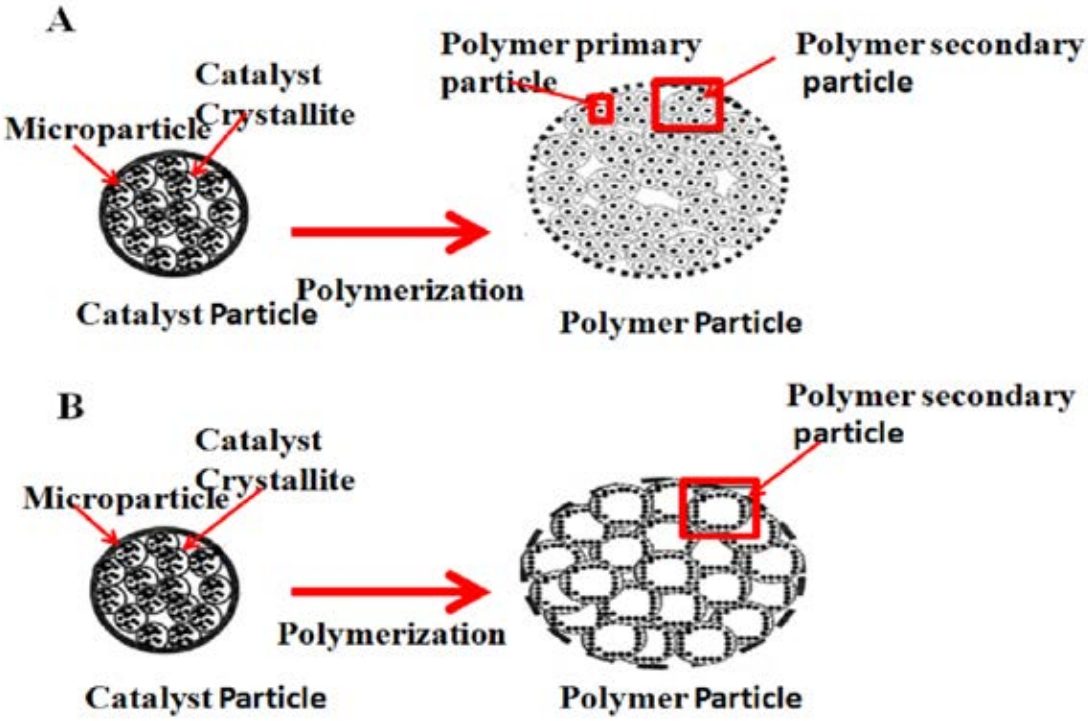

Figure 2.19 (A) Double grain model with solid microcore, (B) double grain model with expanding microcore [105].

CHAPTER III
EXPERIMENTAL

To achieve the research objectives and research scope, the research methodology is provided in this chapter which comprises of chemicals, catalyst preparation, and ethylene polymerization.

First of all parts depicted chemicals used for this work. The second part demonstrated the catalyst preparation. Next, the instruments and apparatuses were used to characterize the catalysts. The last part was provided the reaction procedure for ethylene polymerization.

3.1Chemicals

3.1.1 Chemical 1

The chemicals employed during the experimental research at Terano Laboratory, School of Materials Science, Japan Advanced Institute of Technology, Japan. Only critical materials are summarized in the following lists:

1. Ethylene of research grade, donated by Asahi Kasei Chemical Corp., was used without further purification.
2. Chlorinating agents ($SiCl_4$, $FeCl_2$, $ZnCl_2$, and $MnCl_2$) were purchased from Wako Pure Chemical Industries Ltd.
3. Anhydrous magnesium ethoxide [$Mg(OEt)_2$] was donated by Toho Titanium Co. Ltd. and used without further purification.
4. Titanium tetrachloride ($TiCl_4$) was purchased from Wako Pure Chemical Industries Ltd. and used as received.

5. Cocatalyst agents such Triethylaluminium (TEA), Triisobutylaluminium (TIBA), Trioctylaluminium (TNOA), and Diethylaluminum chloride (DEAC) was donated by Tosoh FineChem Corp.
6. *n*-Heptane and toluene, purchased from Wako Pure Chemical Industries Ltd., as solvents were purified by passing through molecular sieves 4A column.
7. High purity nitrogen, purchased from Uno Sanso Co., was used without further purification.
8. 1-hexene as comonomer was dehydrated in Schlenk tube containing 4A molecular sieves and then bubbled with N_2 for 2h.

3.1.2 Chemical 2

The chemicals used in these experiments, carried out at the Center of Excellence on Catalysis and Catalytic Reaction Engineering, were specified as follows:

1. Polymerization-grade ethylene (C_2H_4) from Thai Industrial Gas Co., Ltd was used as received.
2. Ultra high purity argon (99.999%) was purchased from Thai Industrial Gas Co., Ltd. (TIG) and was further purified by passing through the column packed with molecular sieve 3Å, BASF Catalyst R3-11G (copper catalyst), sodium hydroxide (NaOH) and phosphorus pentoxide (P_2O_5) in order to remove traces of oxygen and moisture.
3. Anhydrous magnesium chloride ($MgCl_2$) was purchased from Sigma-Aldrich Inc.
4. Titanium tetrachloride ($TiCl_4$) was purchased from Merck Ltd.
5. Triethylaluminum (TEA) in hexane solution, was donated by Tosoh Finechem, Japan.
6. Polymerization-grade *n*-hexane (C_6H_{14}) and *n*-Heptane (C_7H_{14}) were donated from SR Lab. They were purified by refluxing over sodium/benzophenone under argon atmosphere prior to use.

7. Benzophenone (purum 99.0%) was obtained from Fluka Chemie A.G. Switzerland.
8. Sodium (lump in kerosene, 99.0%) was supplied from Aldrich chemical Company, Inc.
9. Commercial-grade methanol was purchased from SR lab.
10. Hydrochloric acid (Fuming 36.7%) was supplied from Sigma-Aldrich Inc.
11. Comonomer (1-hexene, 1-octene) were purchased from Sigma-Aldrich Inc.
12. Chlorinating agents ($SiCl_4$, $FeCl_2$, and $ZnCl_2$) were purchased from Sigma-Aldrich Inc.
13. The purified grade of tetrahydrofuran (THF) was used without further purification.
14. Ethanol (C_2H_5OH) was purchased from Merck Ltd.

3.2 Preparation of Catalyst

3.3.1 Preparation of $TiCl_4/MCl_x/MgCl_2$ Catalytic System

A $TiCl_4/SiCl_4/MgCl_2$ catalyst (termed as Si-MGE) was synthesized according to the procedure in the literature [70]. 10 g of $Mg(OEt)_2$ suspended in 150 ml of toluene was charged into 500 ml three-necked round bottom flask equipped with a mechanical stirrer under N_2 atmosphere. 2.55 ml of ethanol (the molar ratio of ethanol to $Mg(OEt)_2$ = 0.5) and 1.25 ml of $SiCl_4$ as the chlorinating agent (the molar ratio of $SiCl_4$ to $Mg(OEt)_2$ = 0.125) were subsequently added. The mixture was once reacted at 80ºC under stirring for 2 h. Thereafter, 25 ml (227 mmol) of $TiCl_4$ was dropwisely added to the mixture at 0ºC over a period of 2 h, followed by slowly raising the temperature to 100ºC. The mixture was allowed to react at this temperature for 2 h. Finally, the resultant solid was repetitively washed with hot toluene and *n*-heptane and kept as slurry in heptane.

A $TiCl_4/MgCl_2$ catalyst without other chlorinating agents beside $TiCl_4$ (termed as None-MGE) was prepared based on the procedure described above except the addition of EtOH and $SiCl_4$ as well as the heat treatment at 80ºC.

The catalysts with metal halide components (MCl_x, where M is Fe, Mn and Zn) were prepared based on the procedure described above except the addition of $SiCl_4$ as well as the heat treatment at 80ºC. The resultant catalysts were termed as Fe-MGE, Mn-MGE, and Zn-MGE for $FeCl_2$, $MnCl_2$, and $ZnCl_2$, respectively.

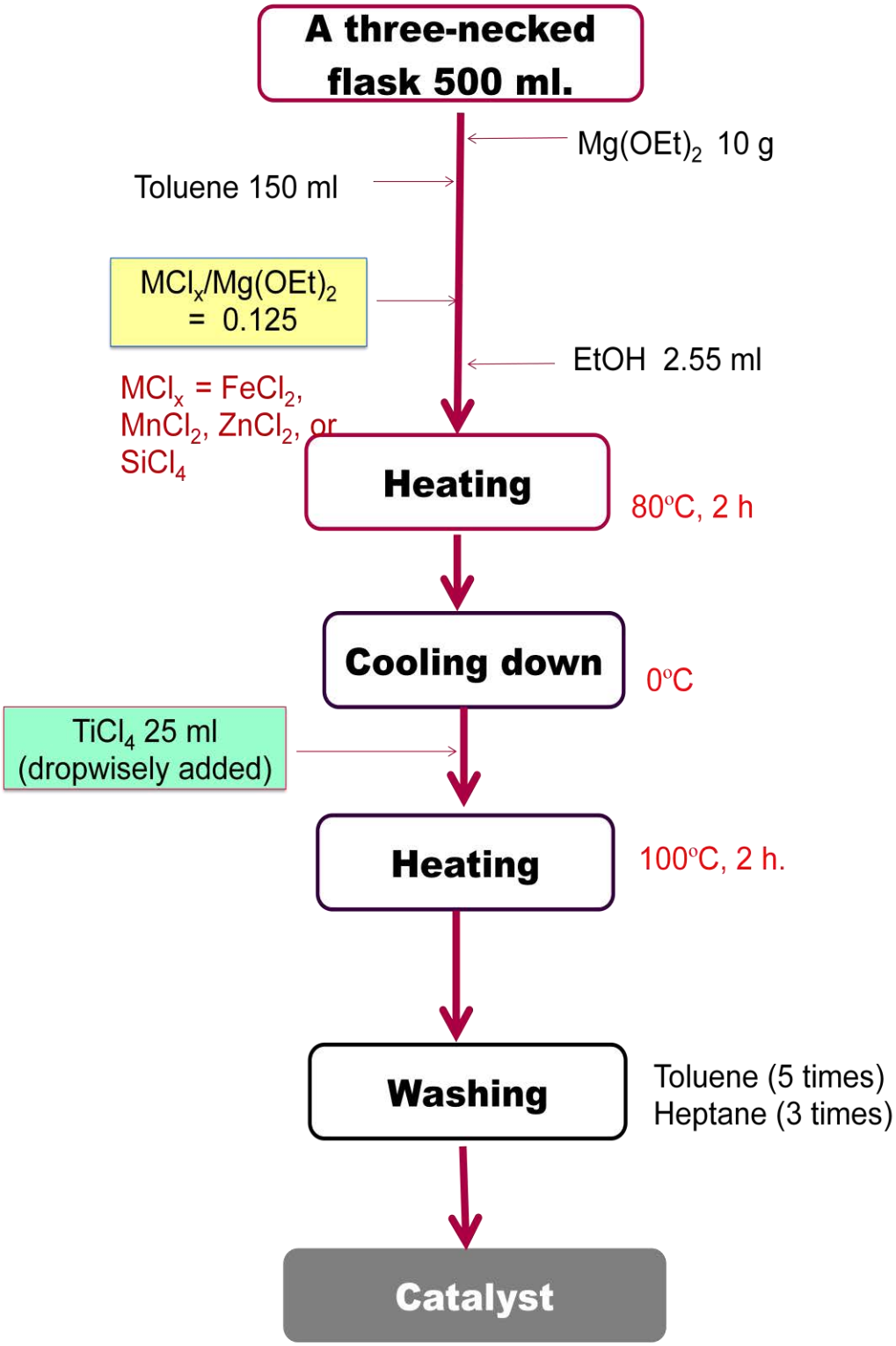

Figure 3.1 Experimental flow of preparation of $TiCl_4/MgCl_2$ catalytic system by various single metal chlorides in the chlorination stage of $Mg(OEt)_2$.

3.3.2 Preparation of $TiCl_4/MCl_x+SiCl_4/MgCl_2$ Catalyst System

The catalysts modified with metal halide components (MCl_x, where M is Fe, Mn and Zn) and $SiCl_4$were also prepared based on the same procedure with that of Si-MGE catalyst except 0.063 mol/mol of $MCl_x/Mg(OEt)_2$ and 0.063 mol/mol of $SiCl_4/Mg(OEt)_2$ were added instead of 0.125 mol/mol of $SiCl_4/Mg(OEt)_2$ for Si-MGE. The resultant catalysts were termed as FeSi-MGE, MnSi-MGE, and ZnSi-MGE for $FeCl_2$, $MnCl_2$, and $ZnCl_2$, respectively.

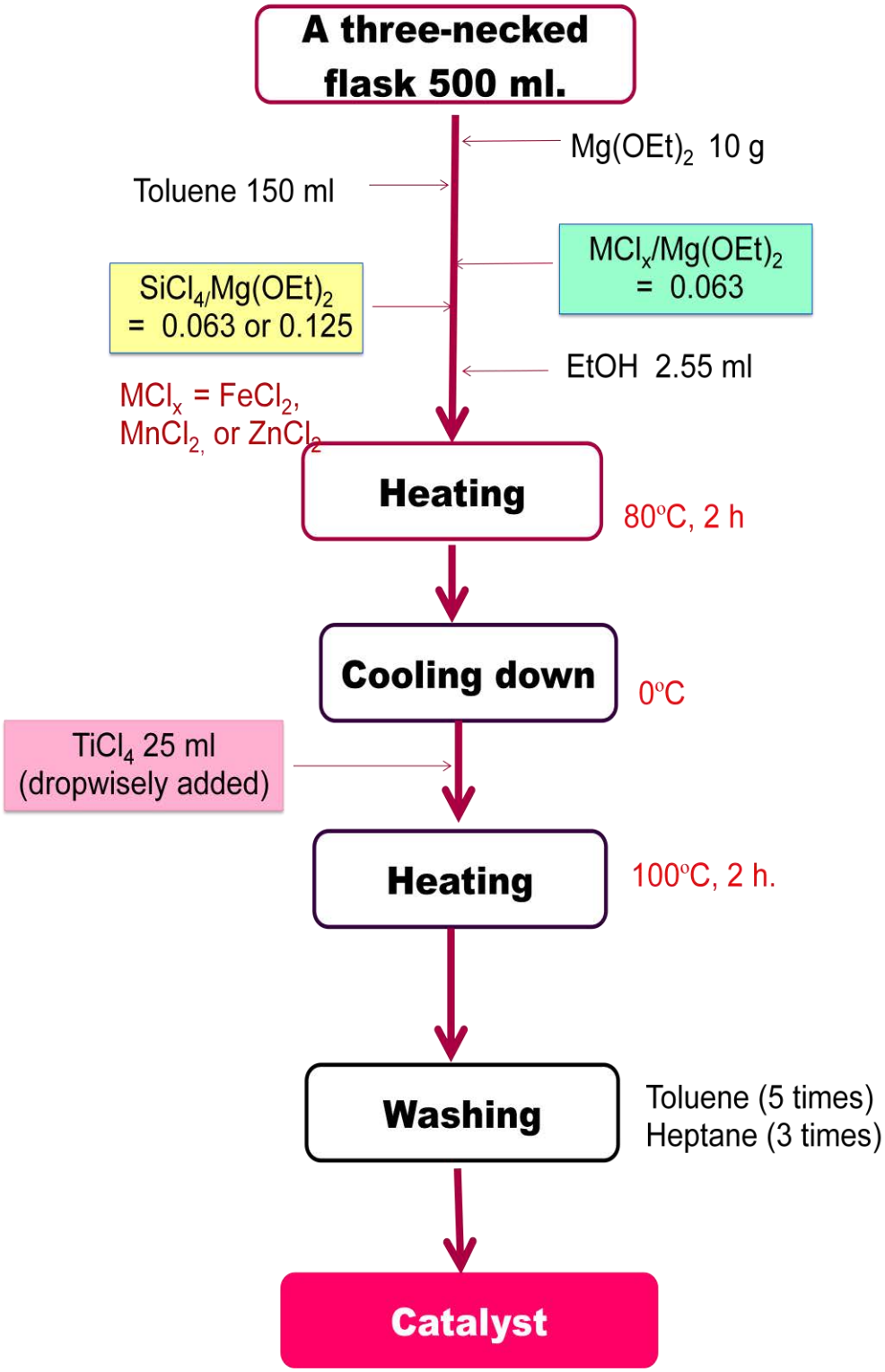

Figure 3.2 Experimental flow of preparation of $TiCl_4/MgCl_2$ catalytic system by various metal chlorides added together with $SiCl_4$ in the chlorination stage of $Mg(OEt)_2$

3.3.3 Preparation of $TiCl_4/MgCl_2/THF$ Catalyst System

The $TiCl_4/MgCl_2/THF$ catalyst (None-THF) was prepared by anhydrous $MgCl_2$ (2 g) and THF (150 ml), which were added into a 500 ml four-necked round bottom flask equipped with mechanical stirrer and cooling system. Then, 2 ml of $TiCl_4$ was injected into the flask. The mixture was continuously stirred and the temperature was heated up to 68-69°C for 3 h. After cooling the solution at 40°C, the part of liquid was siphoned off and the part of solid was washed several times with 100 ml of dry n-heptane. Then, the obtained catalyst was dried under a vacuum at room temperature. The catalyst powder was kept under argon atmosphere.

The $TiCl_4/FeCl_2/MgCl_2/THF$, the $TiCl_4/ZnCl_2/MgCl_2/THF$, the $TiCl_4/SiCl_4/MgCl_2/THF$, and the $TiCl_4/SiCl_4/ZnCl_2/MgCl_2/THF$ catalysts were denoted as Fe-THF, Zn-THF, Si-THF, ZnSi-THF, respectively. All modified catalysts were synthesized by the same procedure as used for the preparation of the unmodified catalyst (None-THF) excepting for adding anhydrous $ZnCl_2$ for Zn-THF, and $SiCl_4$ for Si-THF, with 0.063 mol/mol of Lewis acid/$MgCl_2$. Moreover, the ZnSi-THF was prepared using anhydrous $ZnCl_2$ and $SiCl_4$ having the amount of chemical substances as same as for Zn and Si as mentioned above. The addition of $FeCl_2$ for Fe-THF was prepared with 0.125 mol/mol of Lewis acid/$MgCl_2$.

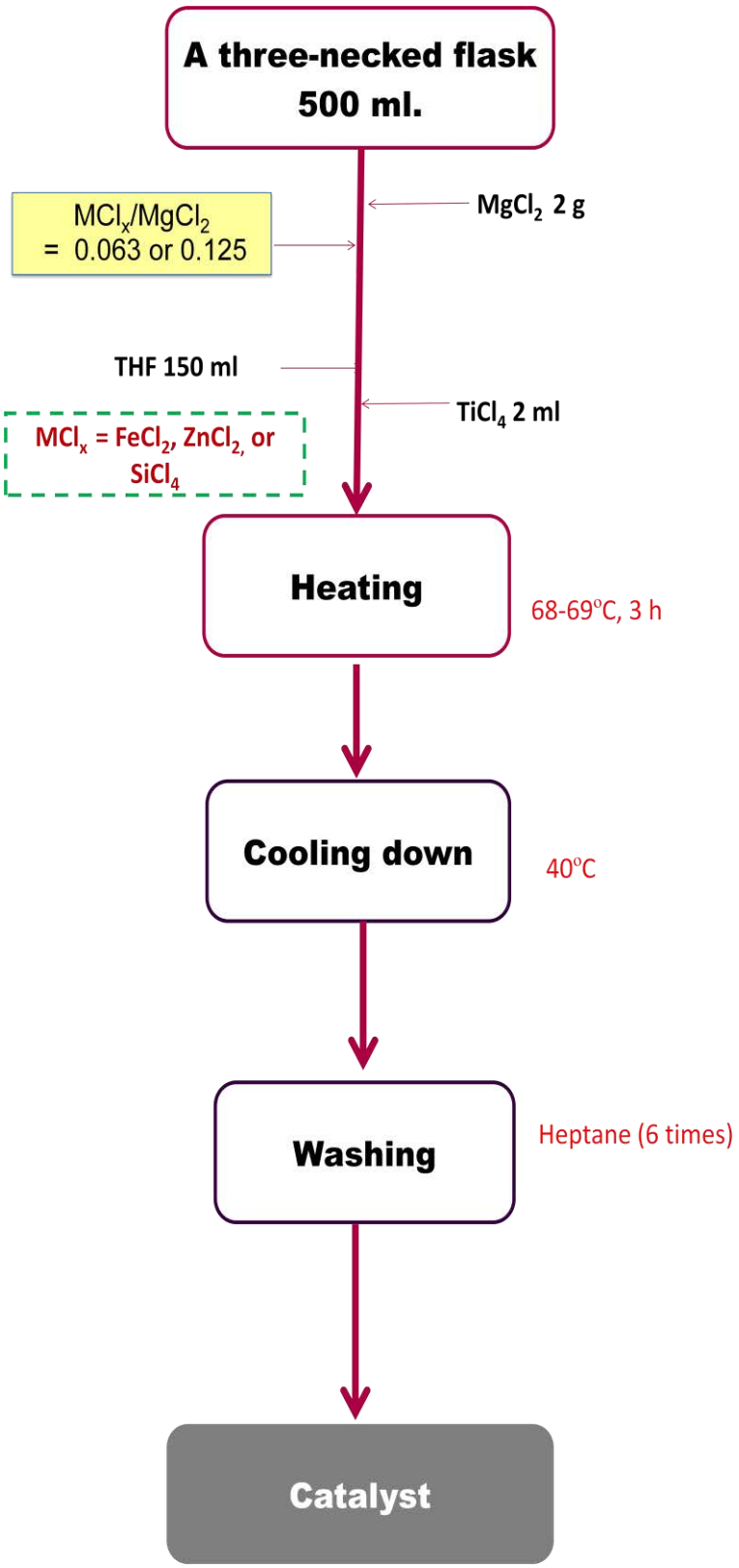

Figure 3.3 Experimental flow of preparation of $TiCl_4/MgCl_2/THF$ catalytic system by various metal chlorides.

3.3.4 Preparation of $TiCl_4/MgCl_2$ Catalyst System (Recrystallization Method)

A catalyst of type of $TiCl_4/MgCl_2$ (None-EtOH) was prepared in a 500 ml four-necked round bottom flask, which was equipped with mechanical stirrer and a condenser. Under the argon atmosphere, anhydrous $MgCl_2$ (2g) and ethanol (EtOH) in mole ratio of 1:10 were added into the flask, and 13.3 ml of dry *n*-heptane was also introduced. The mixture was then heated to 80°C under stirring, until $MgCl_2$ was completely dissolved. After that, the system was cooled to -20°C and 26 ml of $TiCl_4$ was injected into the flask. The temperature was slowly increased to 80°C and hold for 1 h. The solid was washed with *n*-heptane for 3 times. 18 ml of *n*-heptane was introduced into the flask. Another 18 ml of $TiCl_4$ was impregnated into the slurry mixture at 95°C and the reaction system was stirred for 1 h. The liquid part was removed and the solid part was washed several times with *n*-heptane. Finally, the obtained catalyst was vacuum dried at room temperature. The catalyst powder was transferred into a glass bottle and stored under argon atmosphere [106]. The obtained catalyst was designated as None-EtOH.

$TiCl_4/FeCl_2/MgCl_2$ (Fe-EtOH) catalyst was prepared by the same procedure as used for the preparation of the unmodified catalyst (None-EtOH), except for adding $FeCl_2$ along with $MgCl_2$. The amount of $FeCl_2$ was 0.125 (molar ratio of $FeCl_2$ to $MgCl_2$). The resulting catalyst was designated as $FeCl_2$-EtOH.

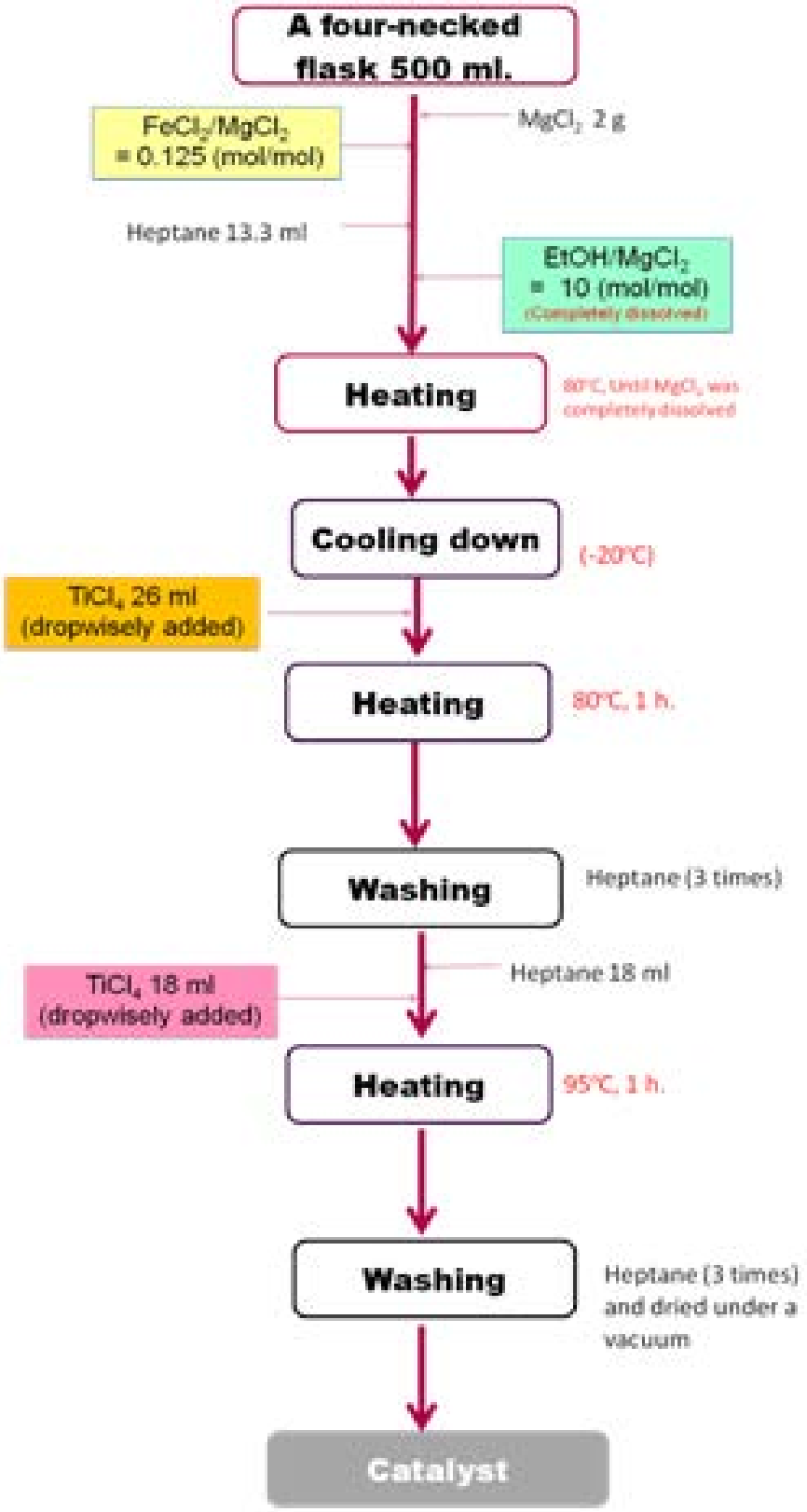

Figure 3.4 Experimental flow of preparation of $TiCl_4/MgCl_2$ catalytic system by Recrystallization method modified with $FeCl_2$.

3.5 Polymerizations

3.5.1 Reactor 1: One Liter Stainless Steel Reactor (High Pressure)

For homopolymerization of ethylene, one liter stainless steel rector fitted with mixing propellers was used for the polymerization of ethylene at 50ºC under a nitrogen atmosphere. First, 490 ml of heptane (total volume of solvent being 500 ml) was introduced into a reactor, and then ethylene gas was saturated at 5 atm for 30 min. 5 ml of TIBA (10 mmol/l) as cocatalyst and the catalyst (5 mL of the concentration of slurry of prepared catalyst = 1mg/ml) were injected into the reactor in order to start ethylene polymerization. After 30 min, a continuous ethylene feeding was stopped reaction by adding acidic ethanol.

For copolymerization of ethylene/1-hexene, 66 ml of heptane (total volume of solvent being 200 ml) was injected into a reactor. After feeding ethylene for 20 min at 50ºC, 130 ml of 1-hexene (5 mol/l) was introduced in the reactor. The ethylene was flowed in the reactor in order to get ethylene saturated solvent. The concentration of cocatalyst in solvent was 10 mmol/l. After that, 2 ml of the catalyst (the concentration of slurry of prepared catalyst being 1mg/ml) was added into the reactor, and then the copolymerization was started by the continuous introduction of ethylene gas until 30 min. The copolymerization of ethylene was terminated by the addition of acidic ethanol. All of the obtained polymers were then filtered, washed with methanol and dried in a vacuum oven at 60ºC for 6 h.

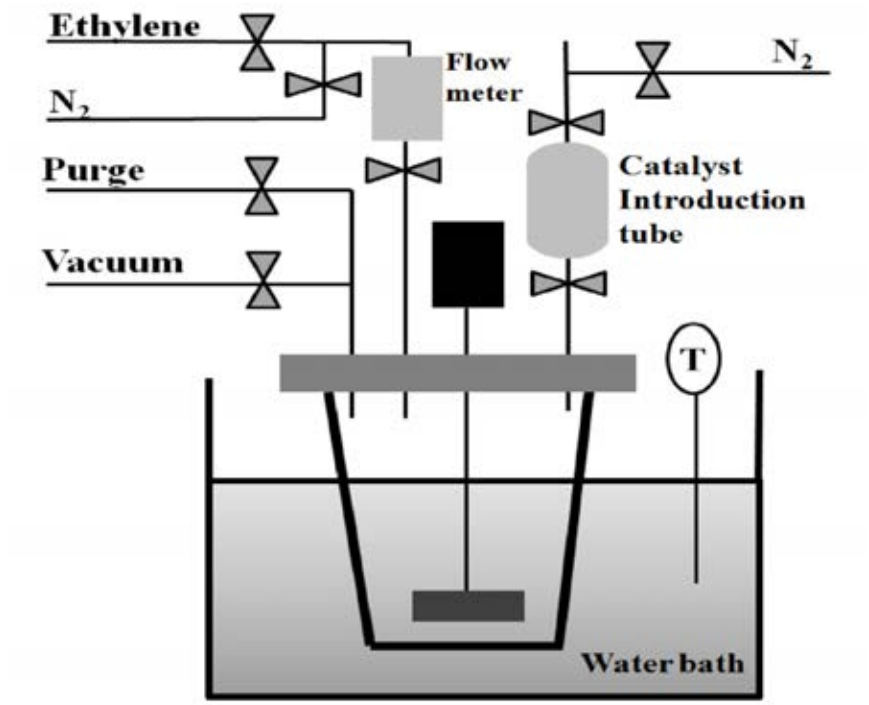

Figure 3.5 Schematic illustration of one liter stainless steel rector.

3.5.2 Reactor 2: Autoclave Reactor

Ethylene homo- and copolymerization were carried out in a 100 ml semi-batch stainless steel autoclave reactor equipped with magnetic stirrer. Firstly, the desired amounts of hexane (total volume of 30 ml) and TEA as cocatalyst were injected into the reactor. Then, 10 mg of catalyst powder was added into the autoclave. After that, the reactor was immersed in liquid nitrogen to stop reaction and the amount of α-olefins of 0.3 mol/l was introduced into the reactor. After evacuating the argon removal, the reactor was heated up to 80°C. The polymerization was started by continuous feeding ethylene gas until the consumption of 0.018 moles of ethylene (6 psi was observed from the pressure gauge) was reached and the reaction time was recorded for the calculating activity of catalysts. Finally, the terminal reaction was stopped by addition of acidic methanol [93]. The copolymer obtained was washed with methanol, filtered, and dried under vacuum at 60°C for 6 h.

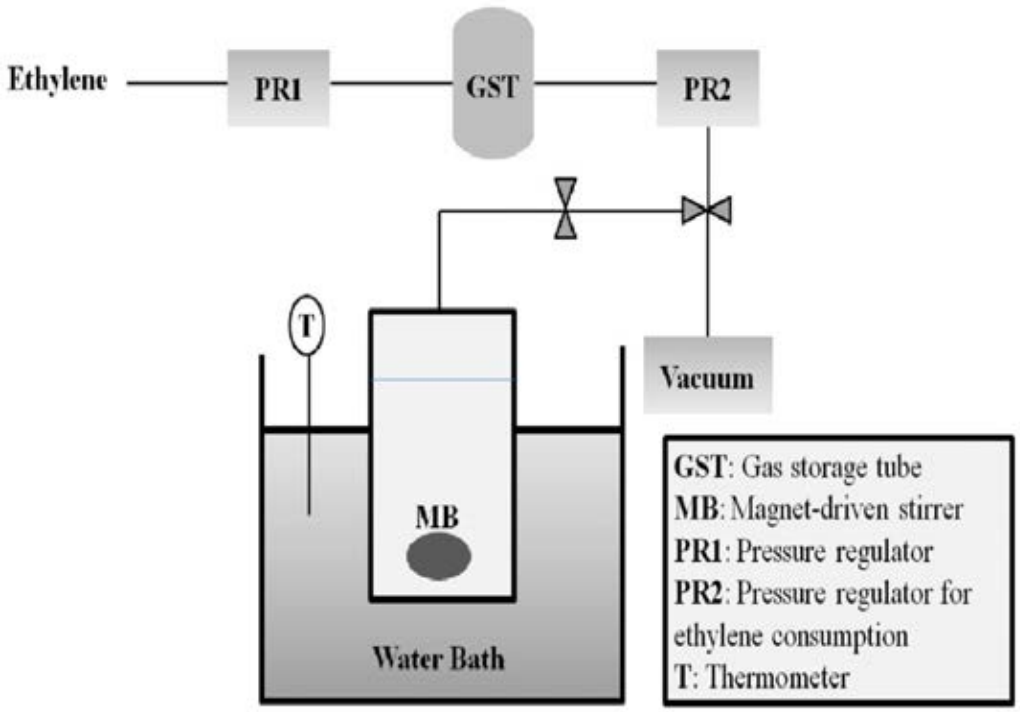

Figure 3.6 Schematic illustration of a 100 ml semi-batch stainless steel autoclave reactor.

3.6 Characterizations

3.6.1 The Catalyst Composition

3.6.1.1 Titanium Titration

The titanium content of the prepared catalysts was measured by titration method. The catalyst was dissolved in sulfuric acid and hydrochloric acid. The reduction of Ti^{4+} to Ti^{3+} was carried by excess of Al. The solution was then heated to remove hydrogen production and dissolved remained Al. Titration was performed at room temperature. The introduction of $Fe_2(SO_4)_3$ sulfuric acid aqueous solution in the presence of NH_4SCN was used as an indicator [107].

3.6.1.2 Inductively Coupled Plasma Spectroscopy (ICP)

The composition of catalyst such as Ti, Mg, Fe, Si, and Zn, were determined by inductively coupled plasma atomic emission spectroscopy equipment (ICP-OES optima 2100 DV from PerkinElmer). The catalyst was digested with hydrochloric (HCl). After catalyst was completely dissolved, the solution sample was then diluted with DI water.

3.6.1.3 Gas Chromatography (GC)

The amount of THF in the catalysts was determined by gas chromatography (GC), using a SHIMADZU GC-14B equipped with a flame ionization detector (FID) and N_2 as carrier.

3.6.2 Surface Area Measurement

3.6.2.1 N_2 Physisorption 1

N_2 adsorption experiment was performed on Belsorp-max at -196ºC in order to calculate the surface area and pore volume of catalysts. Prior to the measurements, catalyst samples were added in a tube under N_2 atmosphere and then degassed at 80 °C for 2 h [108].

3.6.2.2 N_2 Physisorption 2

The specific surface area was determined by nitrogen physisorption method. The single point specific surface area of the catalysts was performed on Micromeritics Chemisorb 2750 at -196ºC. Prior to the measurement, the catalyst sample was added into a tube under N_2 atmosphere.

3.6.3 X-ray Photoelectron Spectroscopy (XPS)

X-ray photoelectron spectroscopy (XPS) was taken on Krato Analytical Shimadzu spectrometer (Axis Ultra DMD model) with a monochromatic Al Kα source in order to investigate the composition of surface catalysts. Samples for XPS measurements were attached on a carbon tape and fixed on a sample holder. The sample holder was put into transfer chamber under inert atmosphere. After evacuating, the holder was transferred to analysis chamber under operating pressure 10^{-9} Torr. Then X-ray gun was turned on, neutralizer was used to reduced the charging effect to obtain better signal to noise ratio, and the sample was subjected to XPS data acquisitions. Survey scan was carried out between 0-1000 eV BE on each sample with a resolution of pass energy 160 and step size 1 eV for a preliminary survey.

3.6.4 X-ray Diffraction (XRD) Analysis

X-ray diffraction (XRD) was performed to determine the bulk crystalline phases of samples. It was carried out using a Bruker D8 Advance Diffractometer at 40 kv, 40 mA with CuK_{α} radiation (λ = 1.54056 A°). Diffraction patterns were recorded in the reflection mode at room temperature with the scans from diffraction angle 2θ = 10 to 60° with scan speed of 0.3 sec/step and a step size of 0.02. All powder samples were prepared in glove box under argon atmosphere and loaded into a holder covered with a Mylar film to prevent air and moisture during the experiment.

3.6.5 Scanning Electron Microscopy (SEM) and Energy Dispersive X-ray Spectroscopy (EDX)

SEM and EDX were used to determine the morphologies and elemental distribution throughout the catalyst samples, respectively. The SEM was performed with a JEOL mode JSM-6400. The EDX of Link Isis series 300 program was applied. The catalyst samples were conducted with argon overflow to protect air and moisture during the experiment.

3.6.6 Scanning Electron Microscopy (SEM)

The morphologies of catalysts were investigated using scanning electron microscope (SEM, Hitachi S-4100 Field Emission Electron Microscope). The samples were prepared in a glove bag under inert atmosphere, then transferred to a deposition device (Hitachi E-1030 Ion Sputter) for the Pt-Pd coating, and finally transferred to a SEM equipment, during which the contact with air was minimized [109].

3.6.7 Fourier Transforms Infrared Spectroscopy (FT-IR)

The Fourier transforms infrared spectroscopy (FT-IR) was applied with Nicolet 6700 FT-IR spectrometer. The catalyst powder was casted as thin film on NaCl disk in a glove box and kept under argon atmosphere during the experiment. A scanning range from 400 to 4000 cm^{-1} with scanning of 400 times was applied.

3.6.8 Thermal Gravimetric Analysis (TGA)

Thermal gravimetric analysis (TGA) was performed by a SDT analyzer Model Q 600 from TA Instrument. The catalyst sample of 10 mg and temperature ramping from 30 to 500 °C at 5°C/min was used in the operation. The carrier gas was N_2 UHP.

3.6.9 ^{13}C Nuclear Magnetic Resonance (^{13}C NMR)

3.6.9.1 ^{13}C NMR 1

The content of 1-hexene units in copolymers were measured by ^{13}C NMR using 400 MHz Brucker 3 at 120ºC. 100 mg of samples was dissolved in hexachloro-1,3-butadiene as a diluent and 1,1,2,2-tetrachloroethane-d_2 for internal lock and internal chemical shift reference.

3.6.9.2 ^{13}C NMR 2

Nuclear magnetic resonance spectrometer (^{13}C NMR) spectra were recorded at 110°C using a Bruker Advance II 400 operating at 100 MHz with an acquisition time of 1.5 s [93]. The solution of ethylene-1-hexene and ethylene-1-octene copolymers were prepared in 1,2,4-trichlorobenzene and $CDCl_3$ for an internal lock solvent. The microstructure of copolymers were characterized with ^{13}C NMR following each method reported by Randall [110], Soga *et al*. [111], and Zhikang *et al*. [112]

3.6.10 The Molecular Weight of Polymers

The molecular weights of polymers obtained in this study were determined by solution viscosity. Samples were dissolved in 1,2,4-trichlorobenzene and measured at 150 °C with a capillary viscometer. The efflux time was recorded. The data were used for viscosity calculations and converted to the viscosity average molecular weight (M_v).

3.6.11 Differential Scanning Calorimeter (DSC)

The Perkine Elmer Pyris Diamond Differential Scanning Calorimeter (DSC) was used to study the melting point (T_m) and the percentage of crystallinity (χ_c) of polymers. A standard heating and cooling were operated at 20°C/min in the temperature range of 50-200ºC under nitrogen flow. T_m was determined in the second scan. From the endothermic curve, result was referred to the heat of fusion (*H*). The percentages of crystallinity of the polymers were determined with the following this equation:

% Crystallinity (χ_c) =) 100 (3.1)

Where ° = 290 J/g is the heat of fusion of linear PE as reported in ref. [113]. For density of polymer (d), it was calculated from the following semiempirical equation:

Density (d) = [(2195+)/2500] (3.2)

CHAPTER IV
RESULTS AND DISCUSSION

In this chapter, it can be mainly divided into three sections. The first section can be roughly separated into two parts: (i) the influence of metal chlorides on activity of $Mg(OEt)_2$-based Ziegler-Natta catalyst for ethylene homo- and copolymerization and (ii) the effects of various mixed metal chlorides-$SiCl_4$ on activity of $Mg(OEt)_2$-based Ziegler-Natta catalyst for ethylene homo- and copolymerization as presented in Section 4.1. Section 4.2 explains the effects of $FeCl_2$ doping on characteristics and catalytic properties of Ziegler-Natta catalyst prepared by different catalyst preparation methods and the last part in Section 4.3, the synergistic effects of the $ZnCl_2$-$SiCl_4$ modified $TiCl_4/MgCl_2$/THF catalytic system on ethylene homo- and copolymerization are elucidated.

4.1 Influence of Metal Chloride Compounds on Activity of $Mg(OEt)_2$-based Ziegler-Natta Catalyst for Ethylene Homo- and Copolymerization

It has long been known that ZN catalytic systems are composes of titanium tetrachloride supported on a magnesium chloride ($TiCl_4/MgCl_2$), which is activated by cocatalyst. Many studies have been devoted in academic and industrial fields not only for better understanding of catalytic mechanisms, but also for specific targets such as higher activity [1, 2], better morphology control (shape, size, distribution, bulk density etc.) [7-9], higher hydrogen response [3, 9, 10], adjustments in molecular weight (MW) and molecular weight distribution (MWD) [2, 3, 7, 10-17], enhanced comonomer incorporation efficiency, and more uniform chemical composition distribution (CCD) [18, 19]. In order to achieve these targets, the choice of starting materials to obtain $MgCl_2$ carrier is one of the most substantial parameters [20]. In general, it has been accepted that the $Mg(OEt)_2$–based catalyst exhibits a high activity, good replication, and more stable activity [20, 64, 65]. One of the key steps

determining the performance of $Mg(OEt)_2$-based ZN catalysts is the chlorination step, an indispensable step to convert $Mg(OEt)_2$ into $MgCl_2$ [65, 68-71, 73-77], where a variety of chlorinating agents have been examined. Concerning the chlorinating agent, Derroitte *et al.* [75] investigated various chlorination agents (HCl, $AlCl_3$, Cl_2, $SOCl_2$, NH_4Cl) to obtain $TiCl_4/MgCl_2$ catalysts and they found that the addition of HCl in the chlorination step exhibited the highest PE yield. Moreover, Akimoto *et al*. [69] employed $SiCl_4$ as a chlorinating agent and revealed that the co-addition of ethanol during the catalyst preparation provided the highest activity in ethylene polymerization. In addition, various alcohols added together with $SiCl_4$ during the chlorinating step was further investigated [70]. It was concluded that the co-addition of a suitable amount of alcohol can improve the activity, compared to the absence of alcohol case. In summary, the most efficient chlorination of $Mg(OEt)_2$ into $MgCl_2$ is achieved by $SiCl_4$ in the presence of alcohol [70]. Although $SiCl_4$ is regarded as the most efficient chlorinating agent, the $SiCl_4$ remaining in the obtained catalysts affects on the activity and polymer properties as so-called a third component [77]. Such "doped" ZN catalysts with other metal halides such as $ZnCl_2$ and $MnCl_2$ were studied by Fregonese and Bresadola and Garofi and Leinonen, respectively. It was found that the addition of a suitable amount of metal chloride components in ZN catalysts not only enhanced the catalyst activity, but also improved the surface structure of resultant $MgCl_2$ support [25, 26].

The aim of the present study is to investigate the influences of metal chloride components i.e., $FeCl_2$, $MnCl_2$, $ZnCl_2$, and $SiCl_4$ on ethylene homo- and copolymerization activities of $Mg(OEt)_2$-based ZN catalysts and the properties of obtained polymers. It can be separated roughly into two parts. Firstly, the influences of different types of single metal chlorides on activity of $Mg(OEt)_2$-based Ziegler-Natta catalyst for ethylene homo- and copolymerization are considered. Due to high efficiency of $SiCl_4$ to cleave poisoning OEt, $SiCl_4$ is selected as reported from the first part. Therefore, the second part further focuses on the investigation of various metal chlorides added together with $SiCl_4$ in the chlorination stage of $Mg(OEt)_2$. All catalysts are tested for ethylene homo- and copolymerization as well as the properties and morphology of the polymer obtained, are investigated and discussed further.

4.1.1 Effects of Types of Single Metal Chlorides on Activity of $Mg(OEt)_2$-based Ziegler-Natta Catalyst for Ethylene Homo- and Copolymerization

4.1.1.1 Effect of the Alkylaluminium Structure on the Catalytic Activity

In this part, it is intended to evaluate the catalyst efficiency with various types of alkylaluminiums. Typically, alkylaluminium compounds can be divided into two types, three trialkylaluminium compounds having different alkyl group such as TEA, TIBA, and TNOA and an alkylaluminium halide (DEAC). The structures of all alkylaluminiums are shown in Figure 4.1

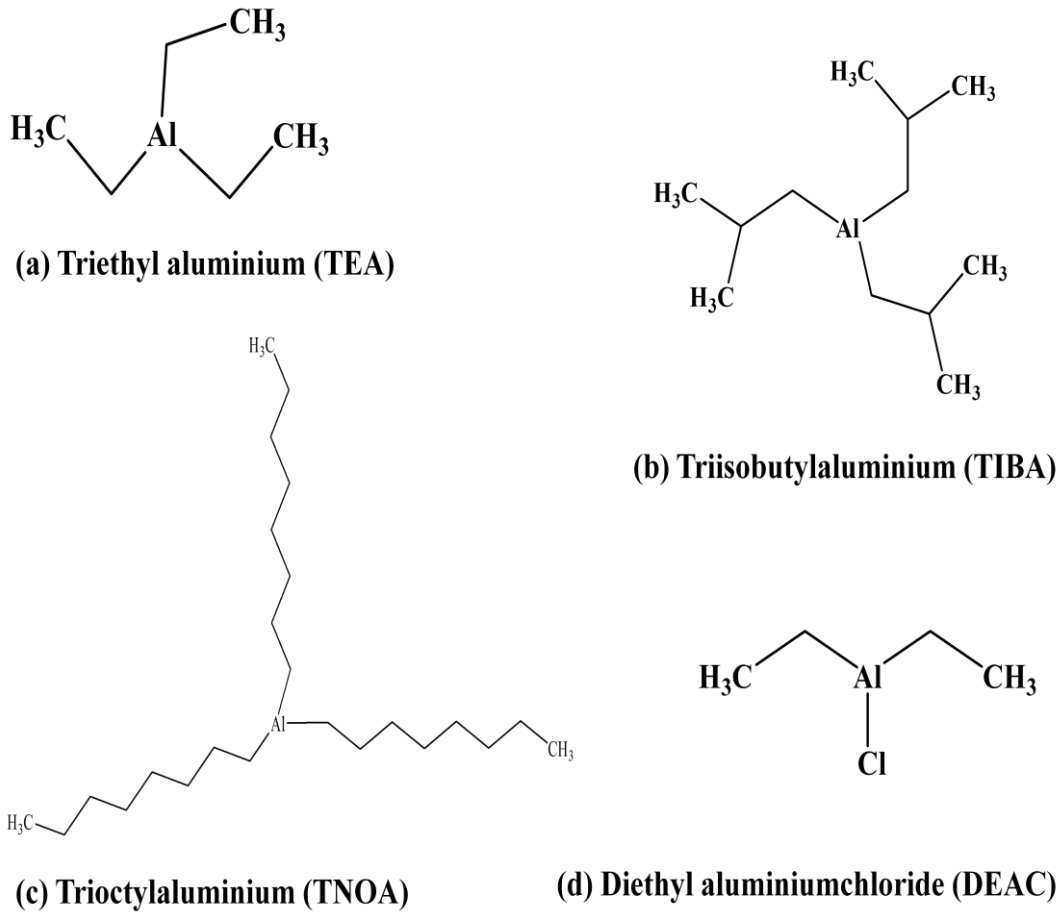

Figure 4.1 Structures of different kinds of alkylaluminium compounds.

As reported in Table 4.1, the catalytic activities order of Si-MGE > None-MGE > Zn-MGE was not dependent on the alkylaluminium type. The highest activity could be achieved from Si-MGE due to higher efficiency of $SiCl_4$ to cleave poisoning OEt. In the comparative study with different types of alkylaluminium compounds, the activity order is TEA > TIBA > TOA > DEAC, regardless of the catalyst type. This phenomenon could be explained that the catalytic activities drastically decreased with the increase in the bulkiness of the alkyl group of the aluminium compound [114]. Nooijen [82] reported that the different types of alkyl groups could be explained in terms of increasing diffusion limitations with the increased molecular dimensions of the cocatalysts. In addition, the increase in alkyl size resulted in the reduction in the tendency of association [115]. Therefore, TEA showed the highest activity among other cocatalysts. On the other hand, it was observed that DEAC gave less effective cocatalyst than TNOA because trialkyl aluminum compounds are usually preferred over the halogen-containing analogues [116]. In addition, Haward *et al.* [117] explained that there was an optimal ligand size for producing maximum catalyst activity.

Table 4.1 The effects of single metal in ethylene polymerization at different types of cocatalyst[a]

Catalyst abbreviation	Components	Ti content[b] (%wt.)	Cocatalyst	Activity (kg PE/mol Ti·h·atm)
None-MGE	$TiCl_4/MgCl_2$	10.4	TEA	101.1
			TIBA	30.2
			TNOA	19.9
			DEAC	14.9
Si-MGE	$TiCl_4/SiCl_4/MgCl_2$	7.2	TEA	445.3
			TIBA	152.1
			TNOA	78.5
			DEAC	23.0
Zn-MGE	$TiCl_4/ZnCl_2/MgCl_2$	14.7	TEA	34.7
			TIBA	19.7
			TNOA	12.5
			DEAC	4.7

[a] Ethylene polymerization condition: Weight of catalyst = 5 mg, [Cocatalyst] = 10 mmol/l, heptane volume = 0.5 l, pressure of ethylene = 5 atm, T = 50 ºC, t = 0.5 h.
[b] Determined by titration method.

4.1.1.2 Influences of Single Metal Chloride Modified Ziegler-Natta Catalysts for Ethylene Homo- and Copolymerization with 1-Hexene

Table 4.2 shows the effects of single metal chlorides in ethylene homo- and copolymerization with 1-hexene. For ethylene homopolymerization, it was found that the homopolymerization activity followed in the order of Si-MGE > Mn-MGE > Fe-MGE > None-MGE > Zn-MGE, while the copolymerization activity increased in the following order: Si-MGE > Mn-MGE > Fe-MGE > None-MGE > Zn-MGE. According to the result of homopolymerization activity, it indicated that Si-MGE provided the highest activity due to higher efficiency of $SiCl_4$ to cleave poisoning

OEt. Considering catalytic activity for copolymerization, it has been well known that the incorporation of Lewis acidic halides increases comonomer incorporation as a result of an ability to attract higher olefin (1-hexene), which has higher electron density than ethylene. Consequently, the introduction of Lewis acidic halides was likely more important than the monomer diffusion for the comonomer incorporation. On the other hand, None-MGE and Zn-MGE catalysts showed the reduction in copolymerization activity because it could be formed an inactive or less active titanium alkoxides from the incomplete chlorination during the catalyst preparation [27, 49, 51]. Due to the steric hindrance of inactive species, the monomer diffusion was impeded in difficult access to the active centers, leading to a decrease in copolymerization activity and comonomer incorporation of None-MGE and Zn-MGE. However, the effect of titanium alkoxides causing the reduction in the activity of ethylene/1-olefins copolymerization or 1-olefins polymerization was already reported in the previous investigations [27, 49, 51]. Regarding to Table 4.2, it could be seen that the addition of Lewis acid compounds increased 1-hexene insertion as mentioned earlier.

Table 4.2 The effects of single metal chloride in ethylene homo- and copolymerization with 1-hexene[a,b]

Catalyst abbreviation	Components	Ti content[c] (%wt.)	[1-hexene] (mol/L)	Activity[a,b] (kg PE/mol Ti·h·atm)	H[d] (mol%)
None-MGE	$TiCl_4/MgCl_2$	10.4	0	30.2	-
			5	11.1	5.2
Si-MGE	$TiCl_4/SiCl_4/MgCl_2$	7.2	0	152.1	-
			5	502.2	5.4
Fe-MGE	$TiCl_4/FeCl_2/MgCl_2$	6.5	0	30.7	-
			5	249.6	9.1
Mn-MGE	$TiCl_4/MnCl_2/MgCl_2$	4.9	0	31.7	-
			5	444.2	6.1
Zn-MGE	$TiCl_4/ZnCl_2/MgCl_2$	14.7	0	19.7	-
			5	6.6	5.9

[a] Homopolymerization conditions: Catalyst amount = 5.0 mg, [TIBA] = 10 mmol/l, heptane volume = 0.5 l, ethylene pressure = 5 atm, T = 50 ºC, t = 0.5 h.

[b] Copolymerization conditions: Catalyst amount = 2.0 mg, [TIBA] = 10 mmol/l, (heptane and 1-hexene) volume = 0.2 l with 5.0 mol/l of 1-hexene, ethylene pressure = 5 atm, T = 50 ºC, t = 0.5 h.

[c] Determined by titration method.

[d] Calculated by ^{13}C NMR spectroscopy.

^{13}C NMR is one of the most powerful techniques to analyze the microstructure of ethylene/α-olefin [111, 118]. Hence, the microstructures of copolymers obtained from all catalysts were determined by means of ^{13}C NMR. The results of ethylene copolymerization with 1-hexene can be listed in Table 4.3. Ethylene incorporation for all systems gave copolymers with similar triad distribution regardless of acidic modification. No HHH sequence obtained from all catalysts was detected.

Table 4.3 Results of ethylene/1-hexene copolymerization together with the analytical data of copolymer[a]

Catalysts	[HHH]	[HHE]	[HEH]	[EHE]	[HEE]	[EEE]
None-MGE	0.0000	0.0294	0.0030	0.0223	0.0680	0.8773
Si-MGE	0.0000	0.0278	0.0020	0.0261	0.0756	0.8682
Fe-MGE	0.0000	0.0645	0.0000	0.0263	0.1289	0.7803
Mn-MGE	0.0000	0.0399	0.0000	0.0206	0.0811	0.8584
Zn-MGE	0.0000	0.0334	0.0002	0.0258	0.0845	0.8526

[a] Content of 1-hexene units in copolymers calculated by ^{13}C NMR spectroscopy.

4.1.2 Effects of Various Mixed Metal Chlorides-$SiCl_4$ on Activity of $Mg(OEt)_2$-based Ziegler-Natta Catalyst for Ethylene Homo- and Copolymerization

As considered the results from the previous section, it was found that the addition of $SiCl_4$ gave the highest activity because of higher efficiency of $SiCl_4$ to cleave poisoning OEt among the other Lewis acid compounds. Nonetheless, the addition of Lewis acid compounds exhibited the positive effect on the comonomer insertion and copolymer activity. Consequently, $SiCl_4$ was mainly used as chlorinating agent accompanied with another metal chloride component in order to develop the chlorinating stage of $Mg(OEt)_2$ and to create the additional efficient supported ZN catalyst. Besides, $FeCl_2$, $MnCl_2$ or $ZnCl_2$ was employed together with $SiCl_4$ to modify $Mg(OEt)_2$ for examining the impact on ethylene homo- and copolymerization with 1-hexene in terms of catalytic activity and polymer properties. Table 4.4 presents the characteristics of the different types of all catalysts studied in this part.

Table 4.4 Characteristics of the different kinds of catalysts

Catalyst abbreviation	Components	Ti content[a] (wt.%)	BET surface area[b] (m^2/g)
None-MGE	$TiCl_4/MgCl_2$	10.4	220
Si-MGE	$TiCl_4/SiCl_4/MgCl_2$	7.2	283
FeSi-MGE	$TiCl_4/FeCl_2/SiCl_4/MgCl_2$	2.1	295
MnSi-MGE	$TiCl_4/MnCl_2/SiCl_4/MgCl_2$	4.3	180
ZnSi-MGE	$TiCl_4/ZnCl_2/SiCl_4/MgCl_2$	2.3	95

[a] Determined by titration.

[b] Determined by N_2 physisorption at -196ºC.

In this study, Table 4.4 summarizes the Ti contents and the surface areas of the prepared catalysts. It is interesting to note that when $SiCl_4$ was introduced in the chlorination step, the Ti content became lower than the catalyst synthesized without the presence of $SiCl_4$, even if the surface area was rather enlarged. More interestingly, The Ti contents became much lower than that of None-MGE and Si-MGE, when $SiCl_4$ was added together with metal halides ($FeCl_2$, $MnCl_2$ or $ZnCl_2$). It could be presumed that $SiCl_4$ and the metal halides could be adsorbed on $Mg(OEt)_2$ and further reacted to form alkoxy-containing compounds on the surface [70], which might competitively block the adsorption of $TiCl_4$. Based on the N_2 physisorption measurement, it was found that FeSi-MGE catalyst exhibited the highest surface area, while ZnSi-MGE catalyst had the lowest surface area. Therefore, the addition of the metal halides affected not only the chemical composition, but also the physical structures of the catalysts in a complicated manner.

Table 4.5 Elemental analysis of catalysts by means of XPS measurements

Catalysts	Chemical composition (atomic%)					Ti/Mg
	Ti 2p	Cl 2p	Si 2s	Mg 2s	M[a]	(atomic%/atomic%)
None-MGE	15.5	54.2	-	30.3	-	0.51
Si-MGE	10.5	25.4	50.3	13.8	-	0.77
FeSi-MGE	18.0	30.2	35.0	16.5	0.3	1.09
MnSi-MGE	13.9	21.7	22.7	41.4	0.1	0.34
ZnSi-MGE	9.8	28.2	39.5	22.7	n.d.	0.43

[a] Binding Energy of Metal 2p : Fe (721.5 eV), Mn (658.3 eV), and Zn (n.d.).

The XPS measurement is recognized as one of the most powerful techniques for analyzing catalyst surfaces [119-122]. It was used to analyze the surface chemical composition of the prepared catalysts as summarized the results in Table 4.5. It was found that the catalysts synthesized with the presence of $SiCl_4$ exposed a significant amount of Si atoms on the surfaces. Moreover, the atomic ratios of Mg and Cl atoms were obviously reduced. For another information from XPS analysis, the Ti/Mg atomic ratio is important factor to infer how much Ti species are exposed on the outermost surface of the catalyst. The highest of Ti/Mg atomic ratio was obtained from FeSi-MGE, while MnSi-MGE and ZnSi-MGE showed lower the Ti/Mg atomic ratio compared to Si-MGE.

SEM images were presented in order to study the morphologies of the catalyst particles (Figure 4.2). Irrespective of different chlorinating steps, all of the catalysts exhibited similar morphologies: Most of the catalyst particles replicated the spherical shape of the $Mg(OEt)_2$ precursor, while a few to several particles form agglomerates probably during the $TiCl_4$ treatment [64, 65]. It is interesting to note that MnSi-MGE and ZnSi-MGE with diminished surface areas also exhibited similar particle morphologies, suggesting that the modification with metal might exert influences in a more microscopic manner.

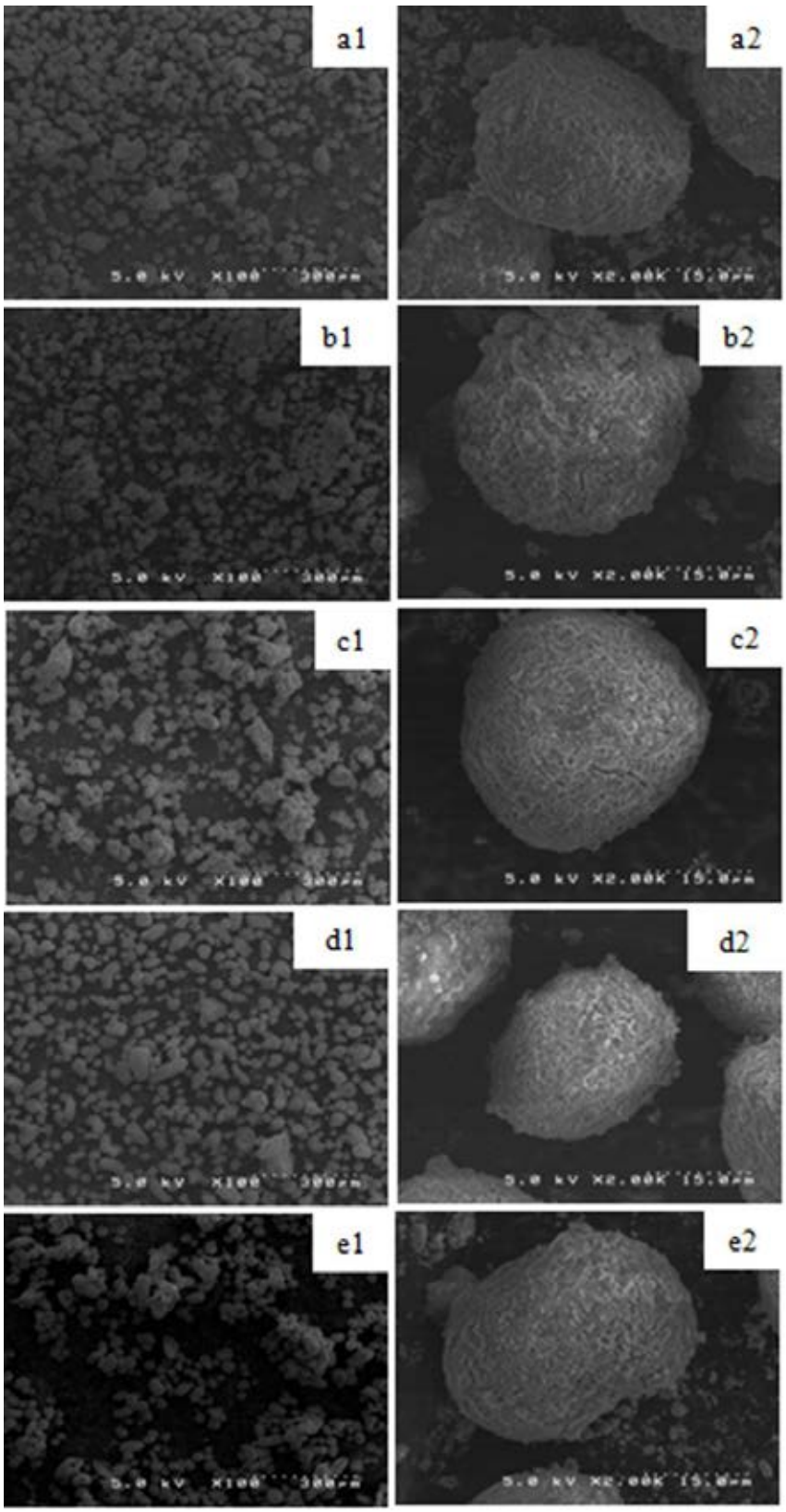

Figure 4.2 SEM images of catalyst particles at magnification 100x and 2000x: a) None-MGE, b) Si-MGE, c) FeSi-MGE, d) MnSi-MGE, and e) ZnSi-MGE.

All the catalysts were subjected to ethylene homopolymerization and ethylene/1-hexene copolymerization. Table 4.6 collects the catalytic activities in both the gPE/gcat·h·atm and kgPE/molTi·h·atm units. For the ethylene homopolymerization, the co-addition of $FeCl_2$ and $SiCl_4$ in the chlorination step exhibited the highest activity per gcat, which was three times greater than the catalyst prepared only with $SiCl_4$. On the contrary, the other metal chlorides ($MnCl_2$ and $ZnCl_2$) were less effective in boosting up the catalytic activity. It is interesting to note that the homopolymerization activities per Ti except for None-MGE were correlated with the Ti/Mg atomic ratio determined by XPS (Table 4.5), following the same order of FeSi-MGE > Si-MGE > ZnSi-MGE > MnSi-MGE. The exception of None-MGE, which gave the lowest activity, could be explained by the formation of inactive or less active titanium alkoxide species due to incomplete chlorination [64, 65]. Similar results on activity enhancements in ethylene homopolymerization were found by many researchers, mostly accompanied by a higher surface area and a larger Ti/Mg ratio of catalysts [123-125]. A higher homopolymerization activity accompanied by a greater exposure of Ti atoms on outer surfaces could be thought as a sign of easier mass transfer to the active center.

The introduction of 5.0 mol/l of 1-hexene remarkably enhanced the activities from 2 to 7 times compared with the homopolymerization activities for all the catalysts except for None-MGE. This phenomenon is generally understood as a consequence of physical factors [97]:

(i) Enhancement of monomer diffusion through the decreased crystalline polymer by the insertion of comonomer. This attributes to an increase in the monomer concentration at the active centers [97].

(ii) The disintegration of catalyst particles during copolymerization thus exposing new potential active centers, hence, increasing the diffusion of cocatalyst through copolymer [97].

The introduction of any metal chlorides (MCl_2) such as $FeCl_2$, $MnCl_2$, and $ZnCl_2$, markedly enhanced the insertion of comonomer (Table 4.6) as compared with the other two catalysts, independently of the Ti/Mg ratio and the polymerization activities. It is generally known that the incorporation of Lewis acidic halides enhances comonomer incorporation due to an ability to attract higher olefin (1-hexene), which has higher electron density than ethylene. Therefore, the introduction of Lewis acidic halides is likely more important than the monomer diffusion for the comonomer incorporation.

Table 4.6 Ethylene homopolymerization and ethylene/1-hexene copolymerization results

Catalysts	**[1-hexene] (mol/L)**	**Activity[a,b]**		**H[c] (mol%)**
		g PE/g cat·h·atm	**kg PE/mol Ti·h·atm**	
None-MGE	0	65	30	-
	5	24	11	5.2
Si-MGE	0	227	152	-
	5	751	502	5.4
FeSi-MGE	0	182	421	-
	5	438	1012	8.4
MnSi-MGE	0	84	94	-
	5	532	595	7.0
ZnSi-MGE	0	68	144	-
	5	467	989	7.7

[a] Homopolymerization conditions: Catalyst amount = 5.0 mg, [TIBA] = 10 mmol/l, heptane volume = 0.5 l, ethylene pressure = 5 atm, T = 50 ºC, t = 0.5 h.

[b] Copolymerization conditions: Catalyst amount = 2.0 mg, [TIBA] = 10 mmol/l, (heptane + 1-hexene) volume = 0.2l with 5.0 mol/l of 1-hexene, ethylene pressure = 5 atm, T = 50 ºC, t = 0.5 h.

[c] Determined by ^{13}C NMR.

In addition, the microstructures of resulting copolymers of all catalysts were determined by ^{13}C NMR measurement. The results of ethylene copolymerization with 1-hexene can be observed in Table 4.7. Ethylene incorporation in all systems showed copolymers with similar triad distribution regardless of acidic modification. No HHH sequence of all catalysts was also detected.

Table 4.7 Results of ethylene-1-hexene copolymerization together with the analytical data of copolymers[a]

Catalysts	[HHH]	[HHE]	[HEH]	[EHE]	[HEE]	[EEE]
None-MGE	0.000	0.0501	0.0028	0.0250	0.0466	0.8755
Si-MGE	0.000	0.0305	0.0057	0.0282	0.0553	0.8804
FeSi-MGE	0.000	0.0528	0.0046	0.0313	0.0584	0.8530
MnSi-MGE	0.000	0.0432	0.0037	0.0263	0.0503	0.8765
ZnSi-MGE	0.000	0.0424	0.0059	0.0345	0.0657	0.8516

[a] Content of 1-hexene units in copolymers calculated by ^{13}C NMR spectroscopy.

The melting temperature and crystallization behavior of ethylene homo- and copolymers were investigated by DSC analysis. As presented in Table 4.8, the melting temperature and crystallinity of all copolymers were decreased, compared to those of homopolyethylene. It was evidently disclosed that the crystallinity and other properties are only influenced by the amount of insertion of 1-hexene, but not by the type of support modification.

Table 4.8 Properties of polymers measured by DSC method

Catalysts	**Comonomer**	**Melting temp. (T_m)[a] in °C**	**Crystallinity (χ_c)[b] in %**	**Density (d)[c] in g/cm^3**
None-MGF	0	139.77	37.85	0.922
	1-hexene	126.42	19.62	0.900
Si-MGE	0	139.13	37.13	0.921
	1-hexene	126.12	20.54	0.902
FeSi-MGE	0	139.66	35.05	0.919
	1-hexene	125.86	16.10	0.897
MnSi-MGE	0	139.81	38.46	0.923
	1-hexene	124.05	20.94	0.902
ZnSi-MGE	0	140.38	34.48	0.918
	1-hexene	125.78	18.98	0.900

[a] Melting temperature was characterized by DSC analysis;

[b] The percentage of crystallinity was determined by the following equation:

$(\Delta H/\Delta H\ )$ 100, where ° = 290 J/g;

[c] The density of copolymer was calculated according to the semi-empirical equation:

d = (2195+ΔH)/2500.

4.2 Effects of $FeCl_2$ Doping on Characteristics and Catalytic Properties of Ziegler-Natta Catalyst Prepared via Different Catalyst Preparation Methods

It has been well-known that anhydrous magnesium chloride is an ideal support, which is suitable for $TiCl_4$ due to its crystal and electronic structure [2, 26, 126, 127]. Therefore, there are many different procedures that have been used to produce $MgCl_2$ particles for catalyst synthesis [128]. Ziegler-Natta catalysts comprised $TiCl_4$, $MgCl_2$ as a support and Lewis base are a popular effective catalyst system which has been widely used for olefin polymerization [42, 43]. Lewis base such as alcohols, ethers, esters, and ketones are frequently added for preparing the Ziegler-Natta catalysts [129, 130]. Moreover, the complex of $TiCl_4/MgCl_2$ catalysts prepared via the reaction between $MgCl_2$ and $TiCl_4$ in tetrahydrofuran (THF) solution has been extensively studied [42, 43] due to its benefits such as good hydrogen response ability, low cost, being suitable for copolymer, and providing moderate catalytic activity [46, 131]. However, it was found that the $TiCl_4/MgCl_2$/THF catalyst system has a major disadvantage which is the coordinated THF molecules in the catalyst structure leading to a decrease in activity [46, 131, 132]. In general, this catalytic system is activated by the addition of alkylaluminium compounds (strong Lewis acid) such as $AlEt_2Cl$, MAO, $AlEt_3$, $AlEt_2Cl$, and $AlMe_3$ [133] in order to remove some coordinated THF molecules in the catalyst structure leading to high catalytic activity for ethylene polymerization [42,132]. However, these alkylaluminium compounds still have disadvantages including high cost, hazardous organic compounds, and decreasing activity with its large amounts [42, 43, 132]. Therefore, one of the promising alternative ways to overcome these drawbacks is to add Lewis acid in the catalyst system.

According to alcohol adduct-based solution, it can provide a good polymer morphology and high efficiency [57-61]. However, it was found that the $MgCl_2 \cdot n$ROH adduct obtained from recrystallization method, had small amounts of

residual alcohol and titanium chloride alkoxides in the support acting as catalytic poisons [27, 48, 50-52, 134]. In order to achieve good activity of the catalyst and morphology of the polymer, an intermediate dealcoholation step is applied [27, 48, 50-52, 134]. Moreover, the obtained support with the increased specific surface area and modifying porosity leads to the increase in the incorporation of titanium after titanation step. Therefore, the removal of the alcohol is very important for preparing the catalyst. There are three methods to dealcoholate support: (i) dealcoholation under hot nitrogen flow, (ii) dealcoholation under vacuum with the controlled heat, and (iii) reaction of support particles with TEA [27, 48, 50-52, 55, 134].

Currently, some additives or promoters are required for catalyst modification in order to achieve better catalytic performance. Moreover, several researchers claimed the addition of $AlCl_3$, $MnCl_2$, and $ZnCl_2$ to generate the defect on $MgCl_2$ support which eventually contributed to the improvement of catalytic activities and polymer properties in Ziegler-Natta catalyst system [11, 25, 26].

This section focuses on the effect of $FeCl_2$ on Ziegler-Natta catalyst with two different catalyst preparation techniques in order to improve the catalytic activities and polymer properties. The catalyst modification with $FeCl_2$ was selected due to its advantages over the alkylaluminium compounds such as lower cost and less hazardous organic compound, and having potential to improve the catalyst activity. In this work, two methods of catalyst modification with $FeCl_2$ i.e. $TiCl_4/MgCl_2$ complexes in THF soluble ($TiCl_4/MgCl_2$/THF) and recrystallization method with ethanol, was investigated. To understand the effect of $FeCl_2$ between both catalyst preparation methods, the obtained catalysts were characterized by SEM/EDX, XRD, and FT-IR measurements. Moreover, all catalysts were determined by means of TGA in order to relate the structure of the support precursor with the catalyst properties. Finally, these catalysts were conducted in ethylene polymerization and the catalyst activity and polymers properties were then compared.

4.2.1 Characteristic of the Prepared Catalysts

In this study, the doped $FeCl_2$ into two catalyst systems was used to prepare the ZN catalyst for ethylene polymerization. The influence of adding $FeCl_2$ on the compositions of catalysts is shown in Table 4.9. As seen in None-THF and Fe-THF catalysts, the amount of Ti and Mg and Ti/Mg ratio of the unmodified catalyst and $FeCl_2$-modified catalyst were similar, indicating that the addition of $FeCl_2$ into $TiCl_4/MgCl_2/THF$ catalytic system did not affect on those compositions. For None-EtOH and Fe-EtOH catalysts, it was found that the presence of $FeCl_2$ causes the increase in titanium content. The addition of $FeCl_2$ into EtOH solution for preparing ZN catalyst might affect on the degree of disorder in $MgCl_2$ support. As reported previously [27, 52], the enhancement of degree of disorder of $MgCl_2$ crystals by adding Lewis acid halides may help more $TiCl_4$ incorporation on the $MgCl_2$ support [27, 52].

Table 4.9 The characteristic and abbreviation of two systems of the obtained catalysts[a]

Catalyst code	Components	Ti (wt.%)	Mg (wt.%)	Fe (wt.%)	Ti/Mg (mol/mol)
None-THF	$TiCl_4/MgCl_2/THF$	5.5	6.5	0.0	0.43
Fe-THF	$TiCl_4/FeCl_2/MgCl_2/THF$	5.4	6.3	1.0	0.43
None-EtOH	$TiCl_4/MgCl_2$ (EtOH)	7.2	15.0	0	0.24
Fe-EtOH	$TiCl_4/FeCl_2/MgCl_2$(EtOH)	11	14.7	2.3	0.38

[a] Determined by ICP technique.

The external surface compositions of Fe and Ti measured by EDX technique are summarized in Table 4.10. Considering THF system, the results showed that the Fe-THF catalyst has higher amount of Ti than None-THF catalyst. Comparing with ICP method which can be evaluate the Ti amounts in terms of bulk analysis, the Fe-THF catalyst had higher amount of Ti on the surface than that in the bulk, suggesting that this catalyst mostly contained Ti atoms on the catalyst surface. For

alcohol adduct system, it could be observed that Fe-EtOH catalyst has also higher amount of Ti than None-EtOH catalyst. However, the Fe-EtOH catalyst had lower Ti amount on the surface than that in the bulk, indicating that a portion of Ti atoms was presumably located in the catalyst pores. These phenomena were dependent on the different methods to synthesize ZN catalyst. It has been well-known that the recrystallization technique by ethanol caused in higher in Ti amounts in terms of bulk because Ti atoms were located in the catalyst pores and on the surface [7]. It was suggested that dealcoholation step for this method could be resulted in increasing the porosity of $MgCl_2$ support [7] leading to the insertion of Ti atoms into the pores of support after the impregnation of $TiCl_4$. However, it should be noted that the incorporation ability of Ti on the catalyst surface increased with an introduction of $FeCl_2$. Consequently, the studied catalysts with different amounts of the Ti on surface were carried out for ethylene polymerization in order to test their catalytic performance, as further mentioned in Section 4.2.2.

Table 4.10 Energy dispersion X-ray analysis (EDX) of the catalysts

Catalysts	Cl (wt.%)	Mg (wt.%)	Ti (wt.%)	Fe (wt.%)	Ti/Mg (mol/mol)
None-THF	47.44	13.56	7.86	-	0.28
Fe-THF	47.81	13.80	9.40	3.13	0.34
None-EtOH	47.17	14.68	6.43	-	0.22
Fe-EtOH	49.92	13.50	7.28	1.52	0.27

Figures 4.3 and 4.4 illustrate the XRD patterns of None-THF, Fe-THF, None-EtOH and Fe-EtOH catalysts. As seen in figure 4.3, it was found that the XRD pattern of None-THF catalyst exhibited the $MgCl_2$/THF complex at 2θ = 10.4 , 20.2 and 32.3°. The XRD peaks at 2θ = 11.1° and 13.2° were assigned to the complex of $TiCl_4$ with THF [42, 135]. The $TiCl_3$/THF complexes of both None-THF and Fe-THF catalysts were identified by XRD peaks at 2θ = 12.2°, 16.7°, and 16.9°. Both None-THF and Fe-THF catalysts indicated the diffraction peaks around 2θ = 11.5

and 18.3°, corresponding to the structure of the $TiCl_4/MgCl_2/THF$ complex [135]. In addition, it was also found that some THF in the structure of $MgCl_2/THF$ complex could be removed by adding the $FeCl_2$. It could be verified by the disappearance or decreasing of the intensity of the diffraction peaks at 2θ = 10.4°, 20.2°, and 32.2° which was assigned to the $MgCl_2/THF$ structure. The XRD patterns of None-EtOH and Fe-EtOH catalysts are presented in Figure 4.4. Their broad peaks centered at 2θ = 15°, 30-35°, and 50.5° were similar for both catalysts. It was suggested that high disorder of δ-form of $MgCl_2$ species is referred to high surface defects $MgCl_2$ crystallites. It was accepted that a lot of Ti atoms can incorporate at the $MgCl_2$ defects as confirmed the Ti contents from the ICP and EDX measurements. However, the XRD patterns of ZN catalysts relied on the natural of catalyst preparation and the amount of coordinated base (internal donor) in the support [40]. Experimentally, the addition of $FeCl_2$ into two different catalyst preparations could not be detected the $FeCl_2$ peak of XRD spectra. This result revealed that $FeCl_2$ with high dispersion could not be displayed by means of XRD technique [136].

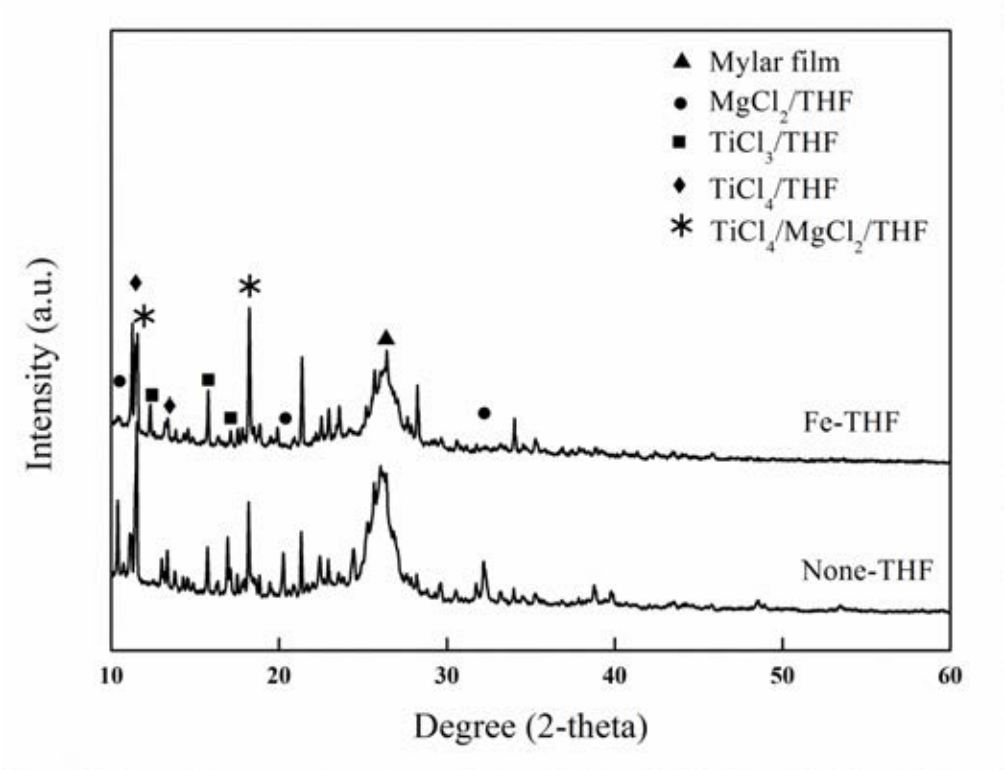

Figure 4.3 XRD patterns of None-THF and Fe-THF catalysts.

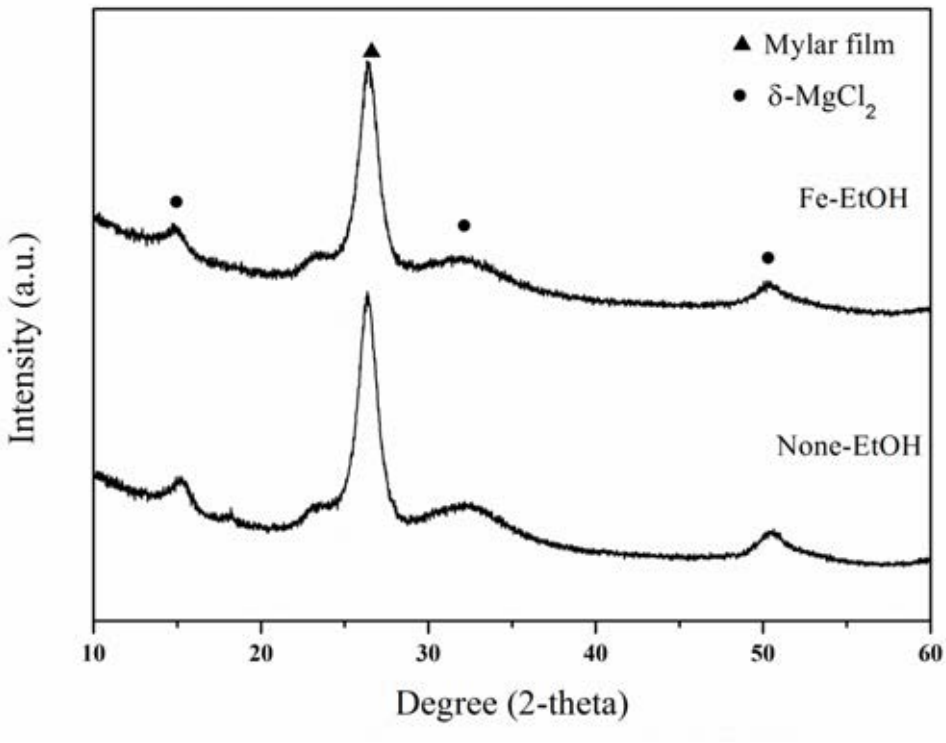

Figure 4.4 XRD patterns of None-EtOH and Fe-EtOH catalysts.

In order to investigate the interaction of ZN catalysts between $TiCl_4$ and $MgCl_2$ on the catalyst surface after the modification with $FeCl_2$ into $TiCl_4/MgCl_2/THF$ catalyst, the absorption bands of THF were examined by FT-IR technique as shown in Figure 4.5. None-THF catalyst indicated that the absorption bands at 875, 913, and 1031 cm^{-1} are attributed to THF. However, after $FeCl_2$ was introduced into the ZN catalyst in the THF solution, the IR peaks of the C-O-C stretching bands of THF were slightly shifted from 875 cm^{-1} to 866 cm^{-1}, from 913 cm^{-1} to 909 cm^{-1}, and from 1031 cm^{-1} to 1015 cm^{-1} as a result of the strong Lewis acidity of Ti and Mg [137]. Moreover, the modified $FeCl_2$ catalyst exhibited the split of C-O-C stretching band of THF at 953 cm^{-1}, representing the occurrence of the reaction with $FeCl_2$. This was probably due to the partial removal of THF weakly coordinated with Ti or Mg [137]. The FT-IR results as mentioned above could be confirmed with the XRD results that some THFs were removed from the structure of $MgCl_2/THF$ complex by the modification of $FeCl_2$. It was found that the introduction of $FeCl_2$ did not destroy the structure of $MgCl_2/THF$ complex which was similar to the addition of a small amount of DEAC, helping the enhancement of rate of ethylene homopolymerization [42, 43]. In addition, this results was corresponded to those from other works [42, 43, 137].

None-EtOH and Fe-EtOH catalysts prepared from recrystallization method via ethanol are shown in Figure 4.6. Only None-EtOH showed the strong absorption band between 3349 cm^{-1} and 3507 cm^{-1}, assigned to O-H stretching of EtOH [138]. It was obviously found that the removal of EtOH from the catalyst was occurred with the presence of $FeCl_2$.

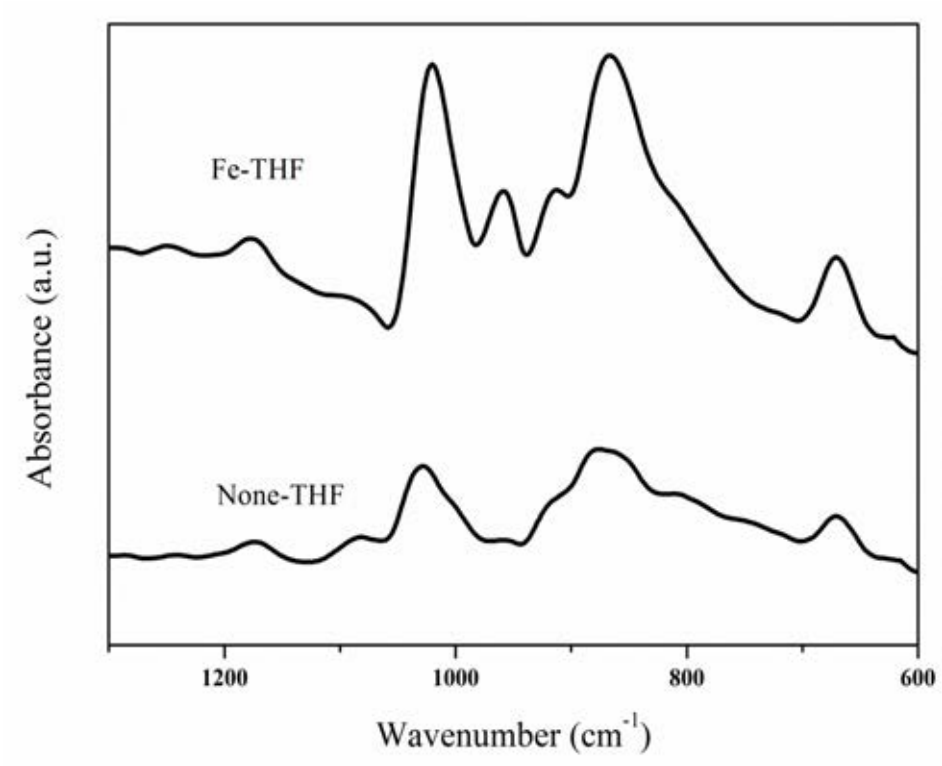

Figure 4.5 IR spectra of None-THF and Fe-THF catalysts.

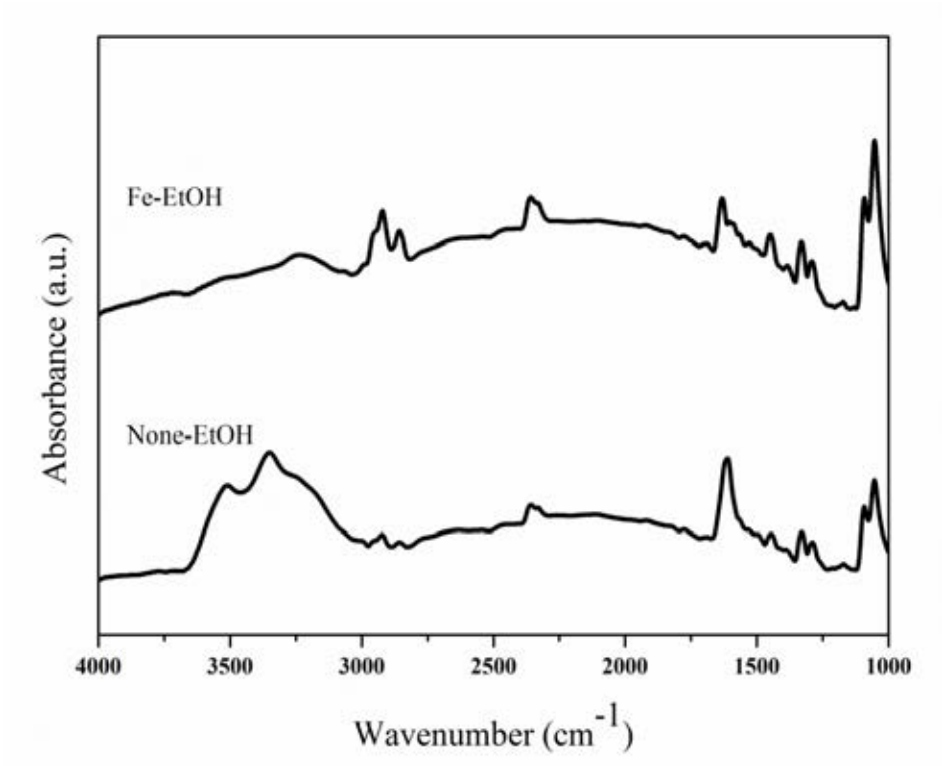

Figure 4.6 IR spectra of None-EtOH and Fe-EtOH catalysts.

4.2.2 Catalytic Activity of Different Catalysts

The unmodified catalyst and $FeCl_2$-modified catalyst were conducted in the ethylene polymerization at the similar condition to determine the activities of catalysts that were affected by $FeCl_2$ modification of the $TiCl_4/MgCl_2/THF$ catalyst. The catalytic activities are presented in Table 4.11. It could be observed that the $FeCl_2$-modified catalyst exhibited the highest activity, more than twice of the unmodified catalyst. It was because the $FeCl_2$ had an efficiency to remove a partial THF which covered the catalyst reasonably as confirmed by XRD and FT-IR, resulting in the activity increment. This result was similar to Chang *et al.* [42] that reported about the removal of THF from $TiCl_3(AA)/3MgCl_2/THF$ catalyst system by the addition of a small amount of DEAC. The highest activity of ethylene polymerization could be achieved with the optimum amount of THF removal. It should be noted that a suitable amount of THF removal with the incorporation of $FeCl_2$ led to an increase in the catalytic activity as well as the active sites.

In addition, $FeCl_2$ modification of $TiCl_4/MgCl_2$ by recrystallization method, catalysts were also performed for the ethylene polymerization at the same condition to examine the catalytic activity as reported in Table 4.11. According to the catalytic activities from this table, it was found that the $FeCl_2$-modified catalyst exhibited a slight increase in polymerization activity when comparing to None-EtOH catalyst. This phenomenon was presumably occurred due to having an ability of EtOH removal from the catalyst surface obtained from the addition of $FeCl_2$. This result was in a good agreement with Parada *et al*. [27, 50, 52] that claimed the dealcoholation via the use of $SiCl_4$ in the recrystallization of $MgCl_2$ from its solution in alcohol. The activity of ethylene polymerization increased with the eliminated alcohol from $MgCl_2$•*n*ROH adduct from help of $SiCl_4$. It could be concluded that $FeCl_2$ could enhance the catalytic activity due to alcohol removal from the $MgCl_2$•*n*ROH adduct.

Table 4.11 The effect of $FeCl_2$ as an additive metal halide on the catalytic activity[a]

Catalysts	Activity (kg PE/mol Ti. h)	Activity Ratio[b]
None-THF	406	1.00
Fe-THF	831	2.05
None-EtOH	427	1.00
Fe-EtOH	471	1.10

[a] Ethylene polymerization conditions: Weight of catalyst = 10 mg, [TEA] = 200 mmol/l, Al/Ti = 140, total volume of hexane = 30 ml, T = 80 ºC, [ethylene] = 0.018 mol.

[b] Activity ratio = Activity $_{(Fe\text{-}THF\ or\ Fe\text{-}EtOH)}$/ Activity $_{(None\text{-}THF\ or\ None\text{-}EtOH)}$

Moreover, another factor involving the degree of interaction between Ti species and $MgCl_2$ support, should be considered as the possible reason for the activity enhancement. This interaction can be examined by the TGA measurement in order to provide a better understanding on the influence of $FeCl_2$-modification on the catalyst surface. According to the report from Terano *et al.* [139], the interaction between $MgCl_2$ and $TiCl_4$ was proposed. The TGA results can provide the information the degree of $TiCl_4$ bound to $MgCl_2$ support in terms of weight loss and the removal temperature. As a matter of fact, the strong interaction leads to the difficulty for the $TiCl_4$ bound to the $MgCl_2$ for reacting with cocatalyst during the polymerization, eventually resulting in lower polymerization activity. On the other hand, the leaching of $TiCl_4$ could be appeared owing to weak interaction between $MgCl_2$ and $TiCl_4$. Hence, the optimum interaction between $MgCl_2$ and $TiCl_4$ was as important factor in order to achieve high activity. Figure 4.6 shows TGA profiles of unmodified and $FeCl_2$-modified $TiCl_4/MgCl_2$/THF catalysts. It was found that the weight losses of $TiCl_4$ presented in each support were in the order of None-THF (59.3%) > Fe-THF (41.5%). The $TiCl_4$ species with strong interaction with $MgCl_2$ support was removed at ca. 229 and 236 °C for None-THF and Fe-THF, respectively. This result indicated that the $TiCl_4$ presented on $MgCl_2$ support with $FeCl_2$-modification exhibited the stronger interaction and then provided higher in the catalytic activity. A similar behavior was investigated by Kaivalchatchawal *et al.*

[140], indicated that the incorporation of Ga and BCl_3 into metallocene catalysts for their modification led to an increase in the catalytic activity for ethylene/1-hexene copolymerization. The reason was Ga and BCl_3 had an efficiency to enhance the interaction between the support and MAO obtained from the formation of more acidic sites which could promote MAO to activate this catalyst during polymerization.

Figure 4.7 shows the results obtained from TGA analysis of None-EtOH and Fe-EtOH catalysts prepared by the recrystallization method. It was found that the weight losses of $TiCl_4$ presented in each support were in the order of None-EtOH (31.39%) > Fe-EtOH (27.08%). The $TiCl_4$ species having strong interaction with $MgCl_2$ support was removed at ca. 264 and 272 °C for None-EtOH and Fe-EtOH, respectively. This result indicated that the $TiCl_4$ presented in $MgCl_2$ support with $FeCl_2$ modification exhibited slightly increased interaction, and then provided higher catalytic activity, which was similar to the result of $TiCl_4/MgCl_2/THF$ catalytic system with the presence of $FeCl_2$. In this case, it showed that $FeCl_2$ could reduce the amount of EtOH remaining in this catalyst as confirmed by FT-IR measurement, leading to a slightly increased interaction.

From the comparison between two methods of $FeCl_2$ modification, it could be noted that the $TiCl_4/MgCl_2/THF$ catalytic system exhibited lower interaction with higher catalytic activity, comparing to the recrystallization method by ethanol. This was probably due to the preparation procedures were different in solvent mediums to make the different interaction between $TiCl_4$ and $MgCl_2$. However, it was worth noting that the addition of $FeCl_2$ into two techniques increased the interaction between $TiCl_4$ and $MgCl_2$ leading to improve the catalytic activities.

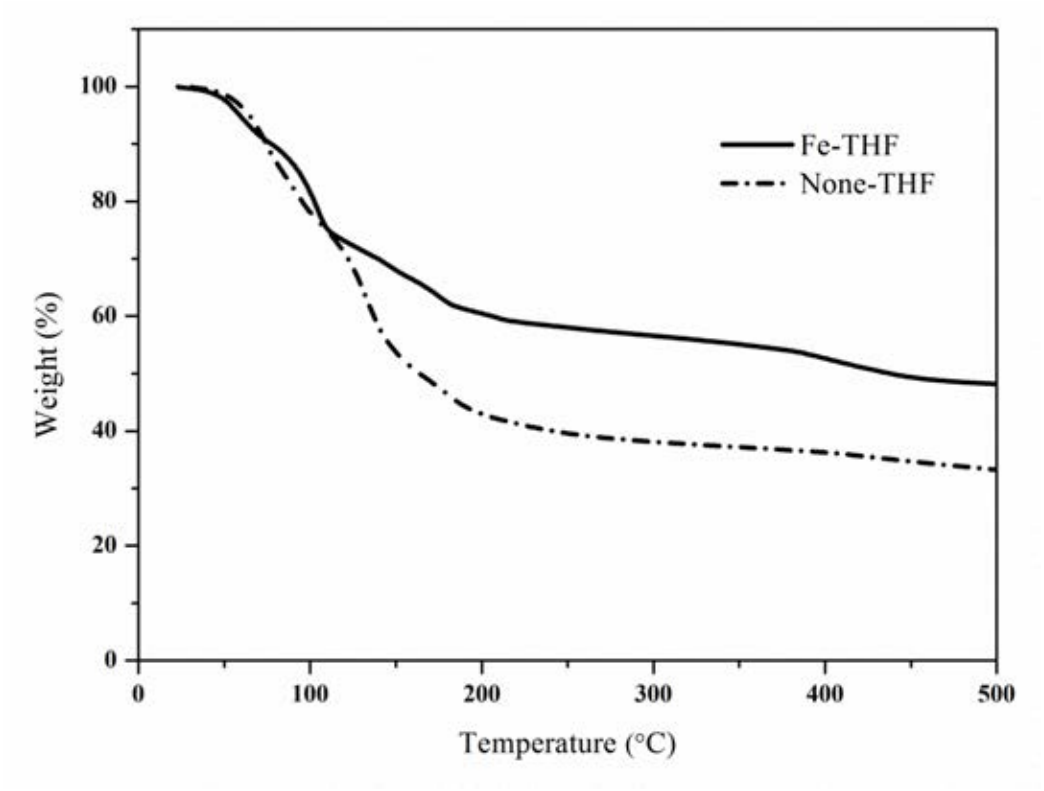

Figure 4.7 TGA profiles of None-THF and Fe-THF catalysts.

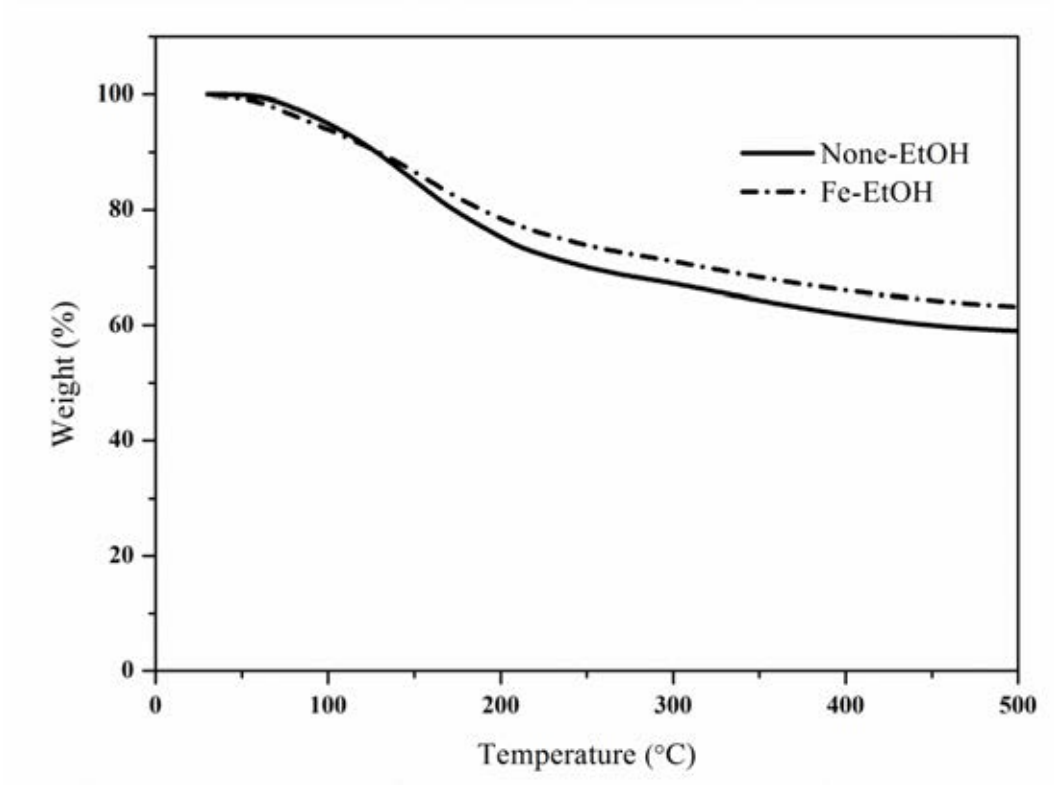

Figure 4.8 TGA profiles of None-EtOH and Fe-EtOH catalysts.

It could be summarized that the addition of the $FeCl_2$ into $TiCl_4/MgCl_2/THF$ catalytic system led to an increase in the catalytic activity of the catalyst (Table 4.11). It was reasonably due to the role of $FeCl_2$ which could remove the THF from the catalyst. The ability to remove THF from the catalytic structure of DEAC and TEA were investigated in several works [42, 131, 141]. The modification with $FeCl_2$ could remove some THF from $MgCl_2$ support that probably led to $MgCl_2$-$FeCl_2$ complexes interacted with $TiCl_4$ to generate the active sites for ethylene polymerization as a result of strong interaction with increasing Ti on the catalyst surface. In order to give a better understanding of the effect of $FeCl_2$-modification on the surface and strong interaction, the proposed model is presented in Figure 4.9.

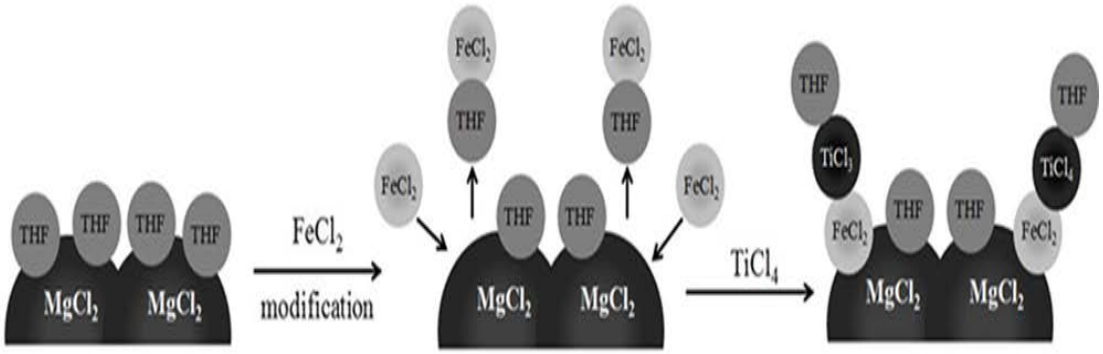

Figure 4.9 The plausible effect of $FeCl_2$ adding on the $TiCl_4/MgCl_2/THF$ catalytic system.

Regarding to the recrystallization method, the porosities of support could be increased by the dealcoholation step [7]. As previously reported, thermal dealcoholation [50] and chemical dealcoholation (cocatalyst agents, $SiCl_4$ and $TiCl_4$, etc.) [27, 55] have been employed for completely removing EtOH from the $MgCl_2$•*n*EtOH complex. In this study, $FeCl_2$ was added into $MgCl_2$•*n*EtOH complex before adding the $TiCl_4$ in the dealcoholation step, causing partial removal of EtOH. The addition of $FeCl_2$ could remove EtOH from $MgCl_2$ support, leading to increasing the porosities of support. It was further found that more Ti atoms could be inserted in the pores of $MgCl_2$. This result could be confirmed by ICP and EDX measurements. Hence, it could be concluded that the activity of ethylene polymerization depended on the exposure of Ti species on the outer surface [123-125]. This result could be

explained by the mass transfer issue. It could be observed in the degree of the activity enhancement of the catalyst modified with $FeCl_2$ in THF system that the value was higher than the catalyst modified with $FeCl_2$ in EtOH system due to the amount of Ti atom located on the catalyst surface. However, the model of $FeCl_2$ modification in the recrystallization method can be proposed as depicted in Figure 4.10

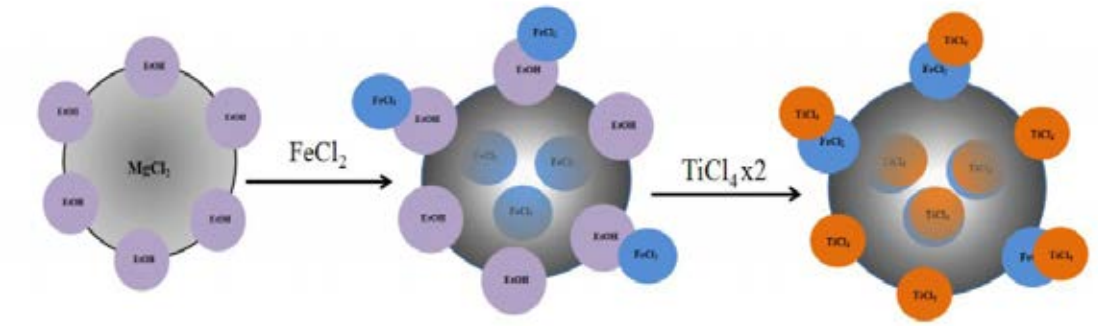

Figure 4.10 The Plausible effect of $FeCl_2$ adding on the $TiCl_4/MgCl_2$ catalytic system prepared by the recrystallization method.

4.2.3 Effect of $FeCl_2$ on Polymer Properties

The obtained polymers from None-THF, Fe-THF, None-EtOH, and Fe-EtOH catalysts were determined by means of DSC and SEM. Table 4.12 shows the DSC analysis results for polyethylene synthesized by None-THF and Fe-THF catalysts. It showed that T_m and T_c of $FeCl_2$-modified catalysts were similar to those of the unmodified catalysts, while the crystallinity of PE with $FeCl_2$ modification slightly increased when compared to the unmodified catalyst. Since the polymer properties obtained from None-EtOH and Fe-EtOH catalysts were similar, it was reasonably suggested that $FeCl_2$ did not affect on the polymer properties.

Table 4.12 Results of thermal analysis of polyethylenes obtained from various catalysts

Catalysts	Melting temp. (T_m) in °C	Crystallization temp. (T_c) in °C	Crystallinity (X_c) in %
None-THF	133.8	112.1	52.7
Fe-THF	133.6	112.3	55.3
None-EtOH	133.7	112.3	52.8
Fe-EtOH	133.2	112.5	53.2

The morphologies of the obtained polymers from SEM technique prepared by the catalysts with and without $FeCl_2$ modification are shown in Figure 4.11. No significant morphologies of polyethylene were observed, suggesting that the addition of $FeCl_2$ in two different methods could not change the morphologies of the obtained polymers.

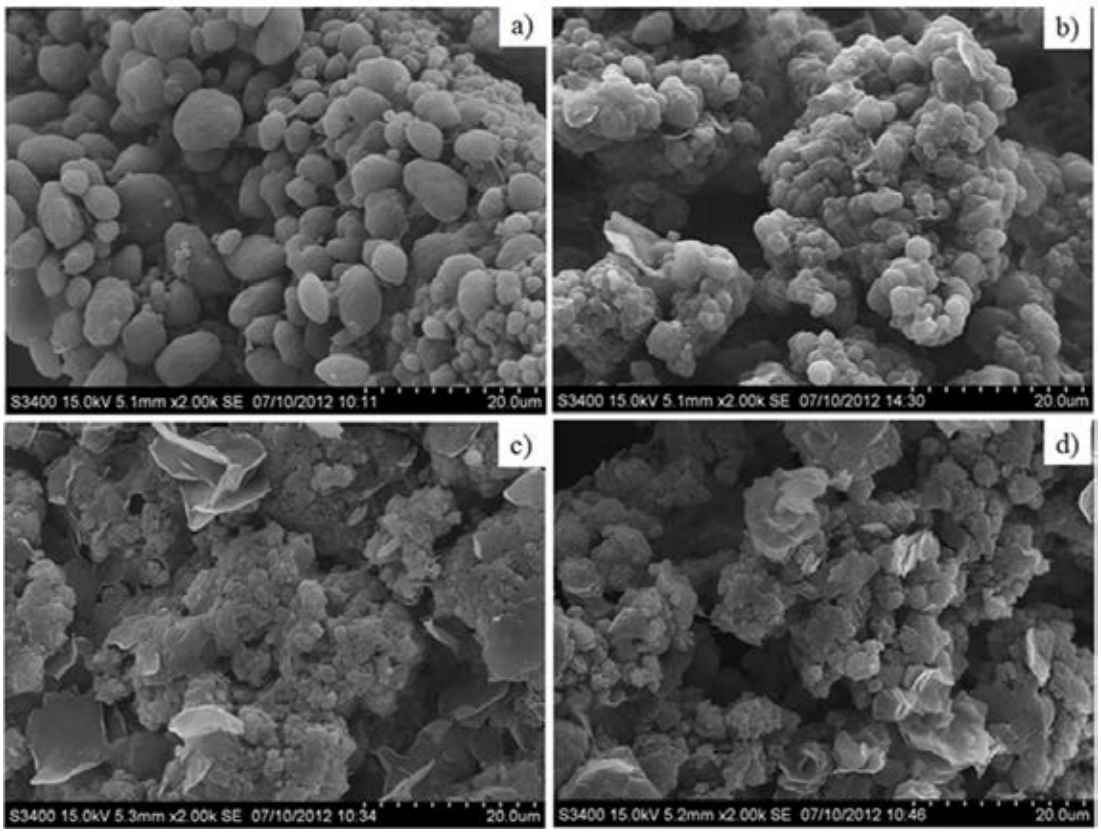

Figure 4.11 SEM micrographs of the polyethylene particles of a) None-THF, b) Fe-THF, c) None-EtOH, and d) Fe-EtOH catalysts.

4.3 Synergistic Effects of the $ZnCl_2$-$SiCl_4$ Modified $TiCl_4/MgCl_2$/THF Catalytic System on Ethylene Homo- and Copolymerization

In general, Lewis acid halide additives added into $MgCl_2$ support have the ability to change the surface properties of $MgCl_2$ crystalline, resulting in the modification of active center distribution of catalysts. It consequently leads to the improvement in catalytic performances and polymer properties [11]. The influences of $ZnCl_2$ doping on the catalytic performances for olefin polymerization were reported by Fregonese and Bresadola [26]. The catalyst doped with 0.73 wt.% of $ZnCl_2$ exhibited the highest activity, whereas the use of higher $ZnCl_2$ contents caused lower activities. In addition, the introduction of $ZnCl_2$ into $MgCl_2$ support could promote the structural defects in the support indicating that the replacement of a partial Mg by Zn was occurred. This phenomenon is possibly occurred because their ionic radii are very similar (Zn^{2+} = 0.88 A°, Mg^{2+} = 0.86 A°). Besides, Lewis acid was also used to remove alcohol from recrystallization step of $MgCl_2$ ($MgCl_2$•*n*ROH adduct). The catalyst obtained from $SiCl_4$ recrystallization was not only to provide the highest activity, but it also showed the highest isotacticity index in the polymer [27].

Therefore, this study focuses on the ethylene homo- and copolymerization of ethylene with the long chain α-olefins (1-hexene or 1-octene) by $TiCl_4/MgCl_2$/THF catalytic system modified with Lewis acid compounds such as $ZnCl_2$, $SiCl_4$, and $ZnCl_2$-$SiCl_4$ mixtures. Up to now, there has not been any papers reported in the $ZnCl_2$-$SiCl_4$ mixtures compared to a single Lewis acid ($ZnCl_2$ or $SiCl_4$) for improving the $TiCl_4/MgCl_2$/THF catalytic system in ethylene polymerization. In particular, it has been expected that the $ZnCl_2$-$SiCl_4$ modification should improve the activity of this catalytic system by more THF removal than that of single metal chloride. In addition, the modification of $TiCl_4/MgCl_2$/THF catalytic system with Lewis acid compounds is interested in due to their many advantages such as good hydrogen response ability, low cost, suitable for copolymers, and moderate activity of catalysts [42, 43, 131].

Moreover, this system is easy to prepare and the Lewis acid could be also dissolved in THF solvent leading to good dispersion of active sites and Lewis acid on the support. All synthesized catalysts were tested in order to investigate the effect of Lewis acid on ethylene homopolymerization and to compare the comonomer types on ethylene copolymerization with 1-hexene or 1-octene at certain polymerization condition. The influences of Lewis acid modifications were investigated by means of N_2 physisorption, ICP, GC, XRD, SEM/EDX, and FT-IR analysis. All resulting polymers were further characterized by viscosity method, DSC, and SEM. In addition, the comonomer content was examined via ^{13}C NMR.

4.3.1 Characterization of Catalysts

The abbreviation of the modified catalysts with the different additives ($ZnCl_2$, $SiCl_4$, and the combined $ZnCl_2$-$SiCl_4$) is listed in Table 4.13.

Table 4.13 Abbreviation of the prepared catalysts

Catalyst Abbreviation	Components
None-THF	$TiCl_4/MgCl_2/THF$
Zn-THF	$TiCl_4/ZnCl_2/MgCl_2/THF$
Si-THF	$TiCl_4/SiCl_4/MgCl_2/THF$
ZnSi-THF	$TiCl_4/ZnCl_2/SiCl_4/MgCl_2/THF$

Table 4.14 presents the chemical compositions of all catalysts determined by ICP. It was found that the titanium contents and the ratios of Mg/Ti of None-THF, Zn-THF and Si-THF catalysts were similar. However, the titanium content of ZnSi-THF decreased by 29 %, while its Mg/Ti ratio increased by 34%, when compared to None-THF. It is interesting to note that the addition of $ZnCl_2$-$SiCl_4$ mixture in this catalyst might reduce free-vacancies of $MgCl_2$ crystallization and Ti insertion, which is corresponding to the result of Coutinho and Xavier [42]. It was disclosed that the

addition of PCl_3 in $TiCl_4/MgCl_2$ via ball milling method decreased the incorporation of Ti on this catalyst system. In addition, the content of THF decreased with the Lewis acid modification, suggesting that the Lewis acids could remove some THF in the catalyst structure. According to the information in Table 4.14, the $ZnCl_2$-$SiCl_4$ mixture showed the highest amount of THF removal from the catalyst structure. It was also observed that the amount of Zn was higher than that of Si in ZnSi-THF catalyst, even though their amounts were added equally in the catalyst preparation step (Lewis acid/$MgCl_2$ of 0.063). Owing to higher acidity of $SiCl_4$ than $ZnCl_2$, more removal ability of THF from $MgCl_2$ was achieved. Moreover, a portion of $SiCl_4$ content could possibly remove THF as well. In accordance with the similar ionic radii of Zn and Mg [26], $ZnCl_2$ was more efficient to incorporate with $MgCl_2$ support than $SiCl_4$. Therefore, it was reasonable to obtain higher content of Zn in ZnSi-THF catalyst.

Table 4.14 Elemental composition of all prepared catalysts in this work

Catalysts	**Ti[a] (wt.%)**	**Si[a] (wt.%)**	**Zn[a] (wt.%)**	**Mg[a] (wt.%)**	**Mg/Ti[a] (mol/mol)**	**THF[b] (wt.%)**
None-THF	5.5	-	-	6.5	2.33	32.7
Zn-THF	5.0	-	4.9	6.2	2.44	30.6
Si-THF	5.4	4.9	-	6.5	2.37	26.5
ZnSi-THF	3.9	1.1	5.5	6.2	3.13	21.6

[a] Determined by ICP.

[b] Measured by GC.

The XRD patterns of all catalysts are shown in Figure 4.12. The broad peak around 2θ = 26 was assigned to a Mylar film used for prevention of air and moisture. The precursor, anhydrous $MgCl_2$, exhibited the strongest reflections at 2θ of ca. 15.1 , 30.3°, 35°, and 50.5°. The characteristic peaks of $MgCl_2$/THF complex were presented at 2θ = 10.4 , 20.2 and 32.3 [42]. All catalysts showed the XRD patterns around 2θ = 11.5 and 18.3 indicating the formation of the $TiCl_4/MgCl_2$/THF

complex [135]. Moreover, all catalysts exhibited the peaks around 2θ = 11.1° and 13.2° indicating the $TiCl_4$/THF complex and the $TiCl_3$/THF complex showed XRD peaks at 2θ = 16.7° [42, 135]. The disappearance of Lewis acid spectra was occurred when $ZnCl_2$ and $SiCl_4$ were incorporated in $TiCl_4/MgCl_2$/THF system due to its well-dispersed form. It can be explained that the crystallite sizes of $ZnCl_2$ and $SiCl_4$ are smaller than 3 nm, which are restricted by means of XRD technique [136]. Nevertheless, it was found that the introduction of Lewis acid compounds probably broke the crystalline structure of $MgCl_2$/THF complex, attributing to the reduction or disappearance of the intensity of XRD patterns at 2θ = 10.4 , 20.2 , and 32.3 . The $ZnCl_2$-$SiCl_4$ mixture (ZnSi-THF catalyst) had high efficiency to decrease the peak intensity of $MgCl_2$/THF complexes when compared to that with single metal chloride modification (Zn-THF and Si-THF catalysts).

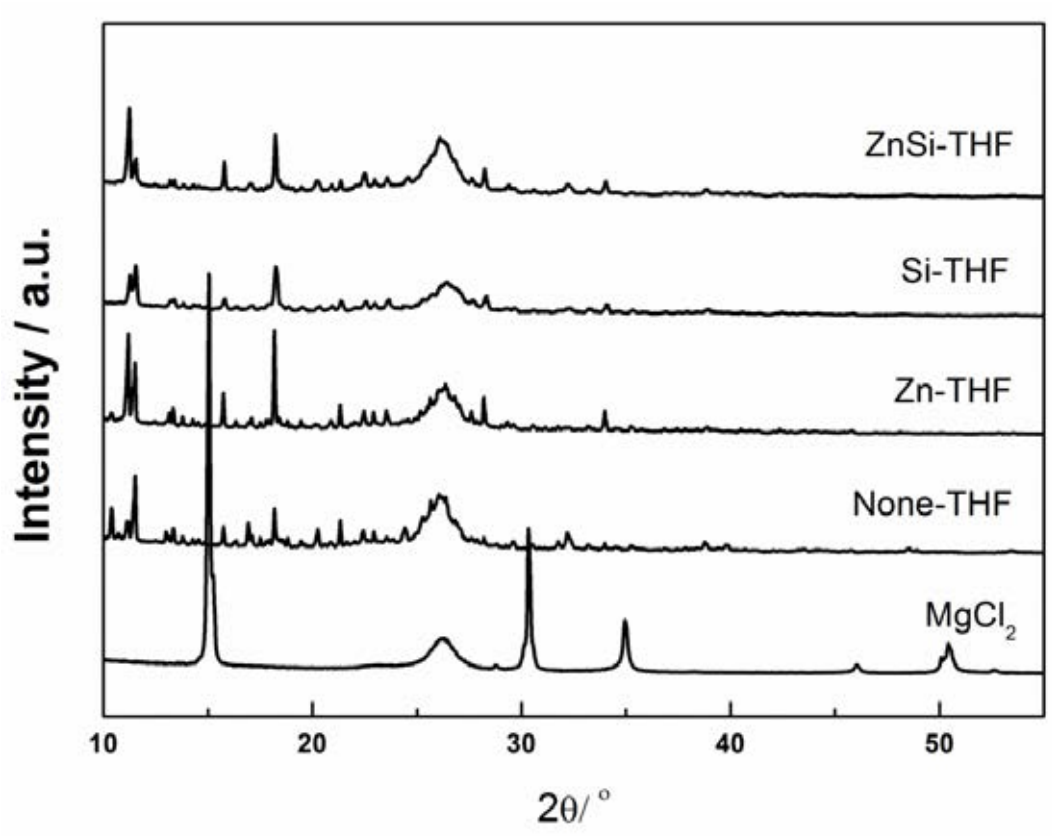

Figure 4.12 XRD patterns of α-$MgCl_2$, None-THF, Zn-THF, Si-THF and ZnSi-THF catalysts.

The single point specific surface area of the catalysts was determined using the nitrogen physisorption method as shown in Table 4.15. The modified catalysts with Lewis acids had a higher surface area than that of the unmodified catalyst. This indicated that the addition of Lewis acid possibly broke the crystal growth or prevented the aggregation of $MgCl_2$/THF support leading to increased surface area. This result was similar to Kang *et al*. [142], who reported that Lewis acids could extract EB in the support to make the high surface area of catalyst as well. Moreover, the result of catalyst surface area is in good agreement with XRD results as mentioned earlier.

Table 4.15 The surface area of catalysts measured by the N_2 physisorption

Catalysts	**Surface area (m^2/g)**
None-THF	4.4
Zn-THF	6.5
Si-THF	7.6
ZnSi-THF	11.3

In order to investigate the surface of catalysts, especially the Ti content on catalyst surface, EDX technique was used. Table 4.16 displays the Ti content of catalysts doped and undoped with the Lewis acid. It can be seen that the Ti concentration in each catalyst was varied upon different electronic environment of catalyst. These results indicated that ZnSi-THF exhibited the highest amount of Ti on surface, suggesting that the concentration of Ti on surface can be increased by the addition of double metal chlorides ($ZnCl_2$-$SiCl_4$). Moreover, the tendency of Ti content on the surface of each catalyst was in the range of ZnSi-THF > Si-THF > Zn-THF > None-THF. However, when compared with ICP result, it can be observed that titanium atoms at surface was higher than that in the bulk because the addition of Lewis acids could remove THF from the structure of $MgCl_2$/THF (as shown in Table 4.14).

In addition, the distribution of elements on catalyst surface should be considered. The EDX mapping for all catalysts was used for this objective as shown in Figure 4.13. It can be clearly seen that the dispersion of Ti modified with Lewis acids was better especially for the modification of mixed metal chlorides (ZnSi-THF) on the catalyst granule than the one without Lewis acid modification. Then, the different catalysts doped and undoped with Lewis acid modification were evaluated for ethylene polymerization.

Table 4.16 Ti content of all catalysts measured by the EDX analysis

Catalysts	Ti (wt.%)
None-THF	7.86
Zn-THF	10.28
Si-THF	10.72
ZnSi-THF	12.70

FT-IR spectroscopy was used to characterize the interaction of $TiCl_4$ with supports in the presence of THF. Several researchers claimed that the complex of $TiCl_4/MgCl_2$ with THF could be observed at IR bands in the range of 1100–700 cm^{-1}, suggesting the most sensitive to THF complexes with a metal center [43, 135, 137]. In general, pure THF has an asymmetrical and a symmetrical C-O-C stretching bands around 913 cm^{-1} and 1071 cm^{-1}, respectively [137]. However, these two peaks were shifted to the lower wavenumber and splitted into several components, suggesting that THF forms a complex with a metal center [135]. Experimentally, IR spectra of all catalysts in the range of 1100-800 cm^{-1} are represented in Figure 4.14. The C-O-C stretching bands of THF in None catalyst showed the characteristic peaks around 1027.9 and 877.5 cm^{-1}, which were similar to the result of Chu *et al.*[43] referred to the bimetallic complex of Ti-Mg-THF. However, $TiCl_4/MgCl_2$/THF catalysts modified with different additives ($ZnCl_2$, $SiCl_4$, and the combined $ZnCl_2$-$SiCl_4$) exhibited the slight shift of the peaks to lower wavenumber when compared to the None-THF catalyst, indicating that metal halides (Zn or Si) coordinated in the

bimetallic complex of Ti-Mg-THF could bring lower wavenumber of the C-O-C stretching bands of THF. This result may cause an increase in the Lewis acidity of the active center [137].

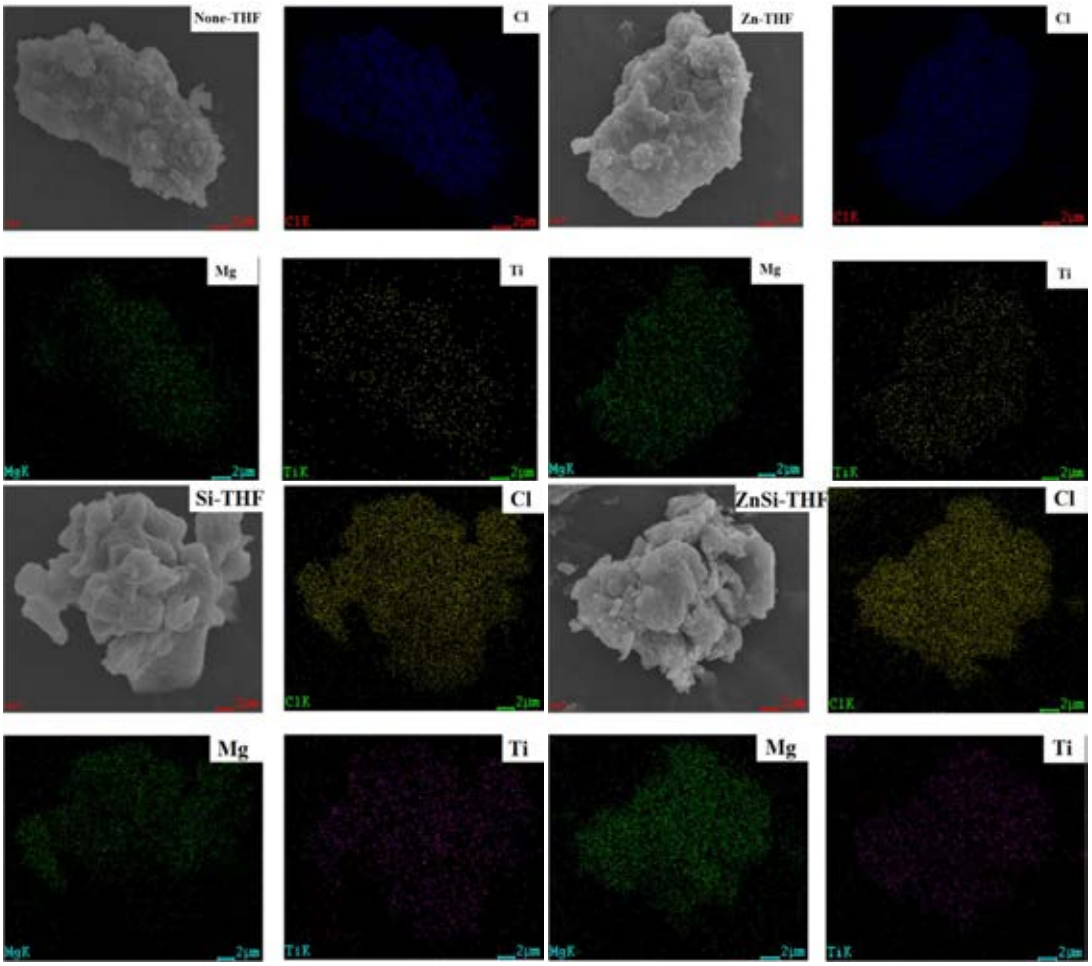

Figure 4.13 SEM/EDX mapping of None-THF, Zn-THF, Si-THF and ZnSi-THF catalysts.

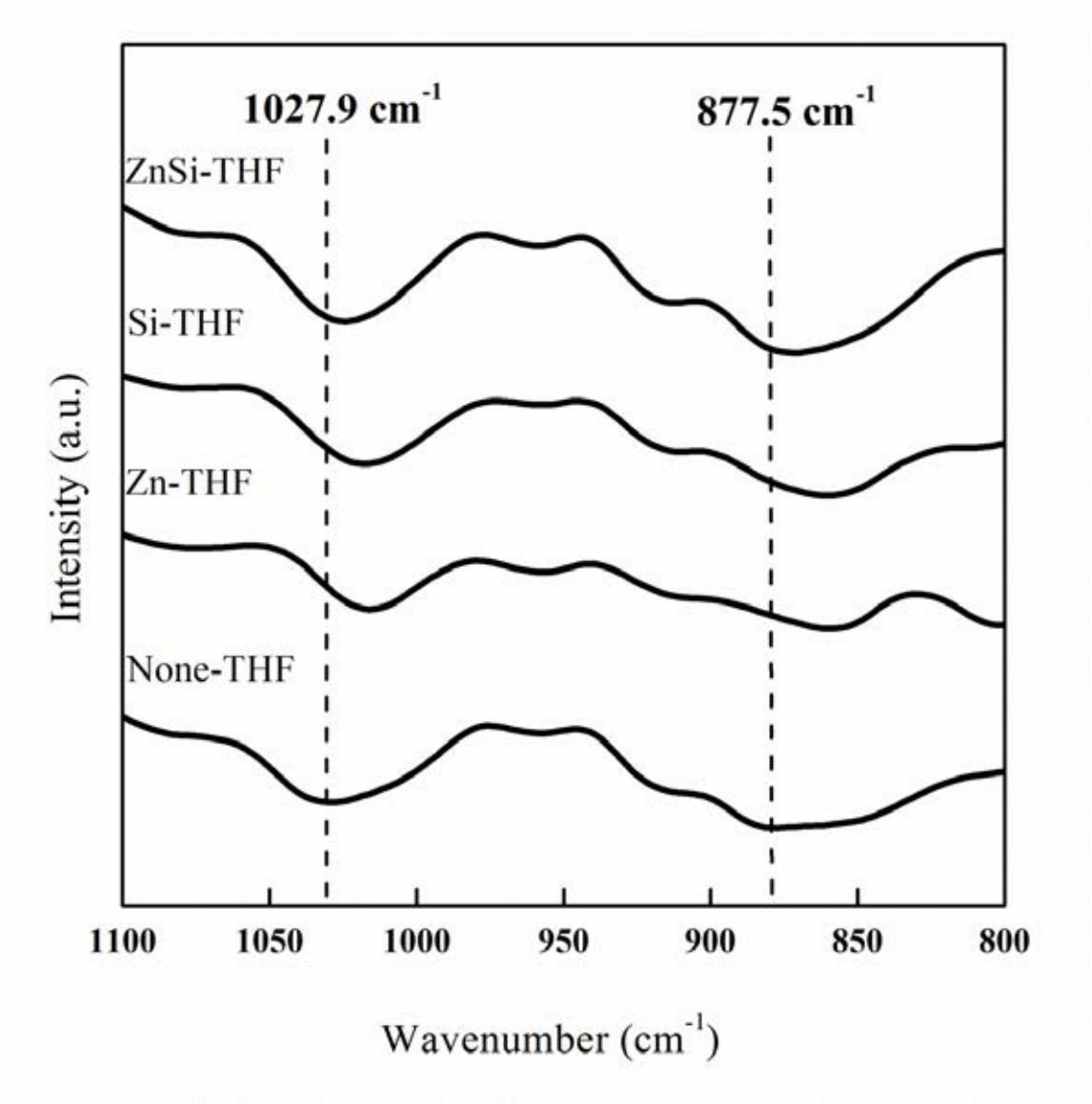

Figure 4.14 IR spectra of None-THF, Zn-THF, Si-THF and ZnSi-THF catalysts.

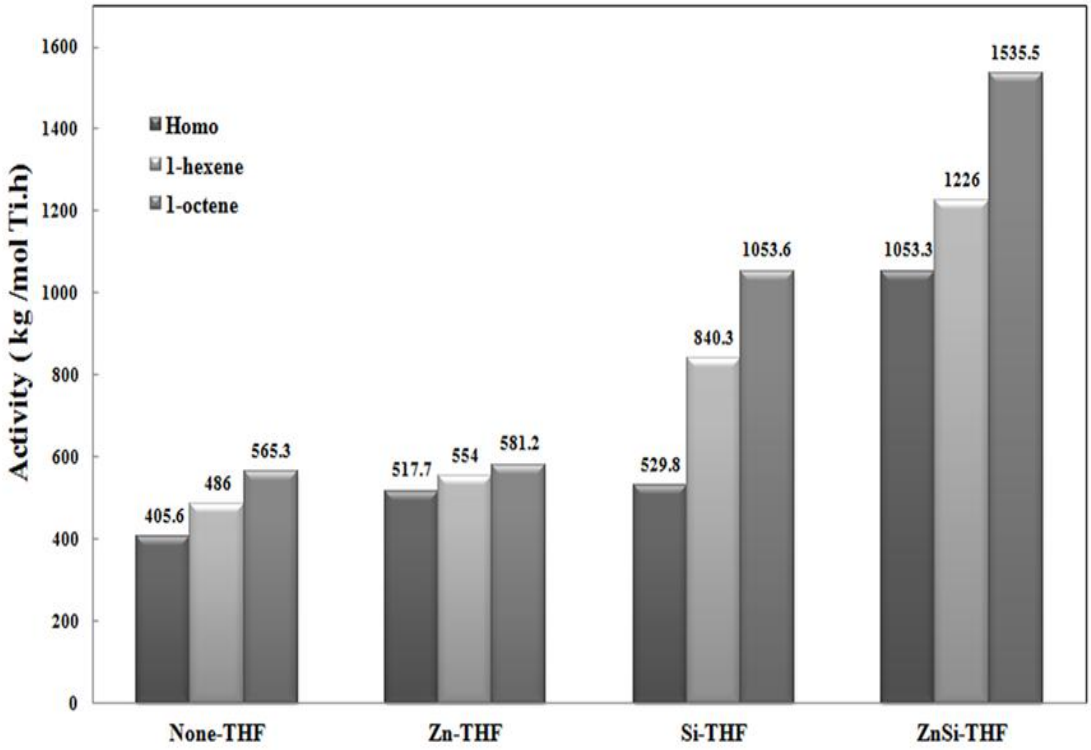

Figure 4.15 The activity of different catalysts in ethylene homo- and copolymerization with (1-hexene and 1-octene). Homopolymerization conditions: Weight of catalyst = 10 mg, a ratio of Al/Ti = 100, *n*-hexane = 30 ml, [ethylene] = 0.018 mol, *T* = 80 °C; Copolymerization conditions: Weight of catalyst = 10 mg, a ratio of Al/Ti = 100, total volume = 30 ml, [α-olefins] = 0.3 mol/l, *T* = 80 °C.

4.3.2 Effect of Lewis Acid on Catalytic Activity for Ethylene Homo- and Copolymerization

The ethylene homopolymerization was carried out in the presence of different additives ($ZnCl_2$, $SiCl_4$, and the combined $ZnCl_2$-$SiCl_4$) on $TiCl_4/MgCl_2$/THF catalysts for comparative study on catalytic activities influenced by different catalysts. The polymerization activities of $TiCl_4/MgCl_2$/THF catalysts modified with Lewis acid are summarized in Figure 4.15. The trend of catalytic activities was in the order of ZnSi-THF > Si-THF > Zn-THF > None-THF. The $ZnCl_2$-$SiCl_4$ was the most effective modifier for $TiCl_4/MgCl_2$/THF system because the Lewis acid compound probably increases the chain propagation rate constant [42, 78] owing to an increase in the Ti

concentration on catalyst surface. Moreover, the activity of catalysts increased with decreasing the intensity of XRD patterns of $MgCl_2$/THF complexes since the addition of Lewis acid compounds could remove the THF from the catalyst, especially for the $ZnCl_2$-$SiCl_4$ system as seen in the XRD results in Figure 4.12. This was in a good agreement with the result reported by Chang *et al.* [42] with the introduction of DEAC into the $MgCl_2$-THF complex. It was also found that the yields of ethylene polymerization were enhanced by adding DEAC into the catalysts due to some of THF removal.

In addition, Figure 4.15 shows also the activities of catalysts obtained from ethylene/1-hexene and ethylene/1-octene copolymerizations. Comparison in ethylene homopolymerization, it could be concluded that the enhancement of catalytic activities by introducing a small amount of 1-olefins, which was named as the "comonomer effect", can be found in both of metallocene and ZN catalyst system [28, 42, 94-96]. For the ethylene/1-hexene copolymerization, the catalytic activities were in the order of ZnSi-THF > Si-THF > Zn-THF > None-THF. This result revealed an increase in the activity when the metal halides were introduced in $TiCl_4$/$MgCl_2$/THF catalytic system during catalyst preparation step. This can be explained by an easier access of the comonomer to the active site, caused by an increase in acidic sites by the introduction of metal halides into $TiCl_4$/$MgCl_2$/THF catalytic system. Some authors proposed that Lewis acid modifications had a positive effect on ethylene copolymerization with 1-olefins in both metallocene and Ziegler-Natta catalysts [28, 140] . Kaivalchatchawal *et al*. [140] reported that the modified metallocene catalyst with BCl_3 enhanced the catalytic activity in ethylene/1-hexene copolymerization due to an increase of acidic sites by BCl_3. Moreover, Chen and Fan [28] proposed that the addition of $AlCl_3$ in ZN catalyst can alter the distribution of active centers due to Lewis acidity of $AlCl_3$ could lead to a remarkable increase in the catalytic activity in ethylene/1-hexene copolymerization as well. In this work, the introduction of $SiCl_4$ and $ZnCl_2$ (as Lewis acid) produced the acid sites of ZN catalyst (as confirmed by FT-IR measurement) compared to the unmodified catalyst. Furthermore, a higher degree of activity increase for the mixture of $ZnCl_2$ and $SiCl_4$ than the introduction of only $SiCl_4$ or $ZnCl_2$ was observed. It is possible that the synergistic effect of double

metal halides generated more active sites, which are suitable for ethylene copolymerization.

All catalysts were also studied for ethylene/1-octene copolymerization. Figure 4.15 represents the catalytic activity for this system. The trend of catalytic activities, which was similar to that for ethylene/1-hexene copolymerization, was in the order of ZnSi-THF > Si-THF > Zn-THF > None-THF. Considering all catalysts, the activities of ethylene/1-octene copolymer were slightly higher than ethylene/1-hexene copolymer (Figure 4.15). This result clearly indicated that there was no significant effect of the chain length of comonomer on the catalytic activity as reported in previous investigation [136, 143]. However, Taniike *et al*. [97] reported that the effect of comonomer depended on the physical factors such as fragmentation of catalyst particles and monomer diffusion resistance. In this case, we found that the comonomer effect was mainly attributed to the monomer diffusion leading to the reduction of crystallinity of the surrounding polymer layer [123]. This brings an increase in the number of active sites resulting in high activity for copolymerization of ethylene with longer α-olefins [97, 123]. In practice, bulkier 1-octene increased the propagation rate constant for ethylene more than that of 1-hexene. When 1-octene inserted in active center, it could reduce the crystallinity of polymers easier than 1-hexene due to its size. The incorporation of ethylene monomer more increased in polymer chain because of easier access to the active centers.

4.3.3 Effect of Lewis Acids on Polymer Properties

The resulting homopolymers were further characterized by DSC and the viscosity method. Table 4.17 shows the influence of Lewis acids on the properties of polyethylene synthesized by $TiCl_4/MgCl_2$/THF catalytic system. This result showed that T_m, density and crystallinity of all homopolymers were similar to the unmodified catalyst as proven by DSC analysis. In addition, the viscosity average molecular weight (M_v) of the synthesized polyethylene was measured by the viscosity method. It was found that the presence of the Lewis acid in catalyst showed a trend to give a

slight increase in the M_v of polyethylene, especially for the modification of mixed metal chlorides ($ZnCl_2$-$SiCl_4$). An increase in the molecular weights of polymers was similar to those obtained from the $TiCl_4/MgCl_2$ catalyst modified by $AlCl_3$ [11]. This indicated that Lewis acid modifications could inhibit the chain transfer reaction during polymerization.

Table 4.17 The influence of Lewis acids on the properties of ethylene homo-polymerization

Catalysts	Melting temp. (T_m) in °C[a]	Density (d)[a] in g/cm^3	Crystallinity (X_c) in %[a]	Viscosity average molecular weight (M_v) in g/mol[b]
None-THF	134.28	0.939	52.56	383,936
Zn-THF	133.84	0.941	54.30	392.555
Si-THF	133.81	0.936	49.88	372,199
ZnSi-THF	132.56	0.940	53.21	423,086

[a] Determined by DSC.

[b] Measured by the viscosity method.

Normally, ^{13}C NMR is a powerful technique for characterization of the triad distribution and the determination of the comonomer insertion into the polymeric chain. The results of properties of the obtained ethylene/1-hexene and ethylene/1-octene copolymers from the different catalysts are represented in Tables 4.18 and 4.19, respectively. The insertion of ethylene in all catalyst systems provided copolymers with similar triad distributions. No HHH or OOO sequences were detected. As seen in Tables 4.18 and 4.19, it was found that the presence of the Lewis acid compounds in catalysts had a tendency to form random copolymers which was similar to the None catalyst. The results showed higher values of inserted comonomer when Lewis acid halides were added, indicating that α-olefin insertion are controlled by the access of the comonomer to the active center. Due to the increase in Lewis

acidic sites by the addition of Lewis acid halides, a comonomer can insert more easily into the active center, and thus the activity increased.

Table 4.18 Properties of the obtained ethylene/1-hexene copolymers from the different catalysts

Catalyst	[EEE]	[HEE]	[HEH]	[EHH]	[EHE]	[HHH]	H (%mol)
None-THF	0.8950	0.0667	0.0020	0.0019	0.0344	0.0000	3.6
Zn-THF	0.8588	0.0903	0.0000	0.0072	0.0437	0.0000	5.1
Si-THF	0.8652	0.0871	0.0007	0.0053	0.0416	0.0000	4.7
ZnSi-THF	0.8614	0.1162	0.0000	0.0125	0.0545	0.0000	6.7

E: ethylene monomer and H: 1-hexene comonomer

Table 4.19 Properties of the obtained ethylene/1-octene copolymers from the different catalysts

Catalyst	[EEE]	[OEE]	[OEO]	[EOO]	[EOE]	[OOO]	O (%mol)
None-THF	0.8513	0.1063	0.0033	0.0025	0.0366	0.0000	3.9
Zn-THF	0.8557	0.0769	0.0181	0.0057	0.0436	0.0000	4.9
Si-THF	0.8178	0.0811	0.0499	0.0056	0.0455	0.0000	5.1
ZnSi-THF	0.8485	0.0846	0.0120	0.0070	0.0480	0.0000	5.5

E: ethylene monomer and O: 1-octene comonomer

Considering the copolymer properties, the DSC analysis is usually considered at the second melting of all samples [93, 113]. The results including melting temperature, crystallinity, and density for 1-hexene and 1-octene comonomers are presented in Tables 4.20 and 4.21, respectively. As observed in these Tables, the density of all obtained copolymers is approximately 0.90-0.91g/cm^3 indicating a typical LLDPE structure [93]. Whether Lewis acid in $TiCl_4/MgCl_2/THF$ system was presented or not, the melting point and crystallinity of LLDPEs decreased with an increase in the insertion of 1-olefin. Thus, it can be concluded that the crystallinity and other properties are only depended on the amount of insertion of the α-olefin, but not on the type of the modifier or comonomer types [143, 144]. In addition, Tables 4.20 and 4.21 are also represented the viscosity average molecular weight (M_v) of the synthesized copolymers that was measured by the viscosity method. It could be observed that Lewis acid modification apparently results in a slight increase in M_v of copolymer obtained, especially for the modification of mixed metal chlorides ($ZnCl_2$-$SiCl_4$). An increase in the molecular weights of copolymers was found as same as those obtained from the metallocene catalyst modified by boron [145]. This indicated that Lewis acid modifications could inhibit the chain transfer reaction during polymerization.

Table 4.20 Properties of ethylene/1-hexene copolymers measured by DSC and the viscosity methods

Catalysts	Melting temp. (T_m)[a] in °C	Crystallinity (χ_c)[b] in %	Density (d)[c] in g/cm^3	Viscosity average molecular weight (M_v)[d] in g/mol
None-THF	128.28	29.73	0.913	333,349
Zn-THF	126.37	22.04	0.904	362,159
Si-THF	126.76	21.71	0.903	353,869
ZnSi-THF	124.63	22.59	0.904	386,977

[a] Melting temperature was characterized by DSC analysis

[b] The percentage of crystallinity was determined by the following equation:

( ) × 100, where = 290 J/g

[c] The density of copolymer was calculated according to the semi-empirical equation:

d = (2195+)/2500;

[d] The viscosity average molecular weight was measured by the viscosity method

Table 4.21 Properties of ethylene/1-octene copolymers measured by DSC and the viscosity methods

Catalysts	Melting temp. (T_m)[a] in °C	Crystallinity (χ_c)[b] in %	Density (d)[c] in g/cm^3	Viscosity average molecular weight (M_v)[d] in g/mol
None-THF	127.96	26.62	0.909	324,264
Zn-THF	126.93	26.00	0.908	368,807
Si-THF	127.06	26.40	0.908	366,609
ZnSi-THF	125.68	25.16	0.907	375,520

[a] Melting temperature was characterized by DSC analysis

[b] The percentage of crystallinity was determined by the following equation:

( ) 100, where = 290 J/g

[c] The density of copolymer was calculated according to the semi-empirical equation:

d = (2195+)/2500

[d] The viscosity average molecular weight was measured by the viscosity method

The morphologies of the obtained polyethylene are shown in Figure 4.16. The morphology of all homopolymers generating from different additives were similar. As can be seen in Figure 4.16, it can be observed that the copolymers obtained from the different catalysts were similar in both 1-hexene and 1-octene comonomer systems. It indicates that the crystalline structure of the obtained polymers seemed to be lower with increasing the amount of comonomer insertion [9].

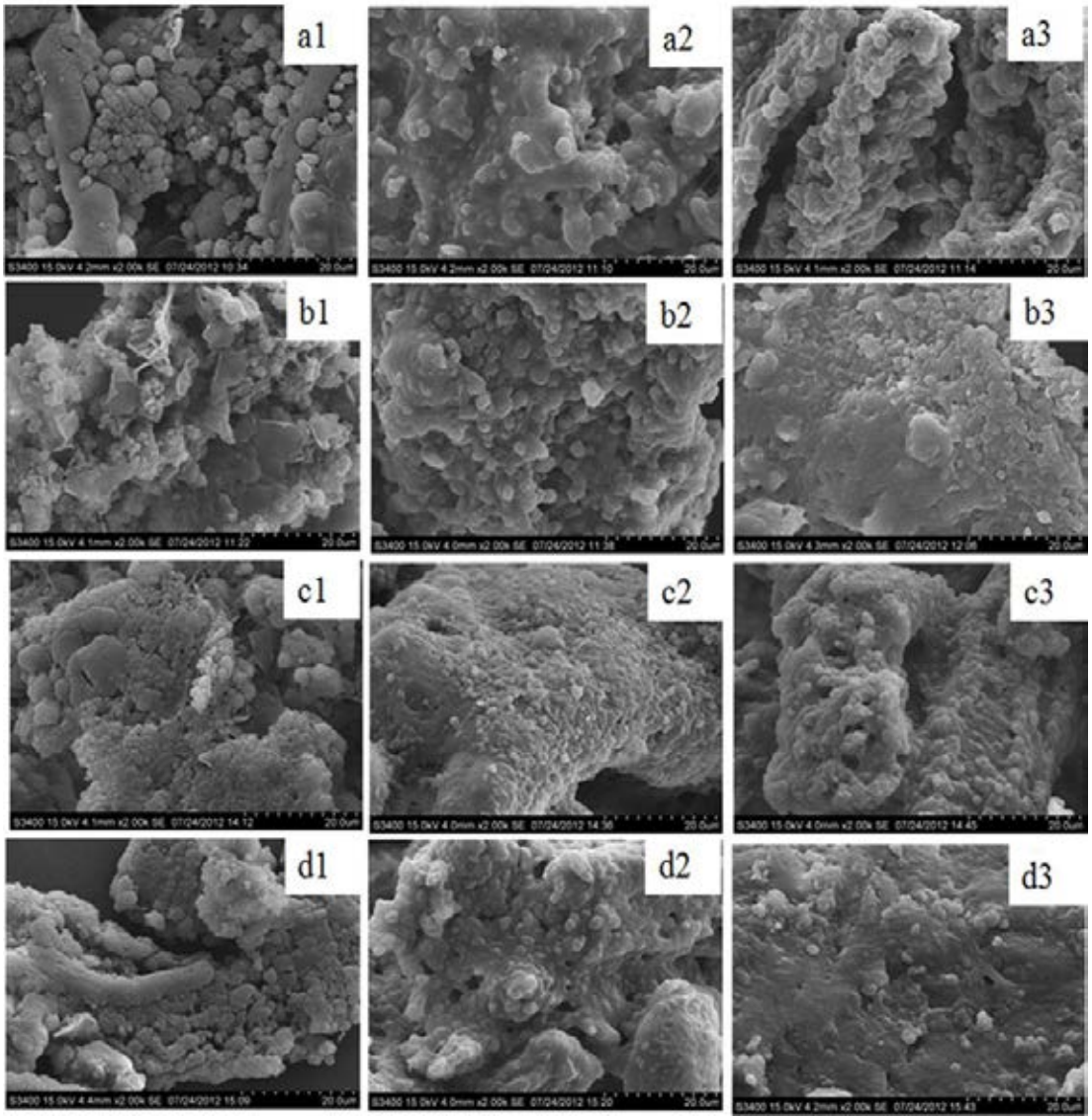

Figure 4.16 SEM images of ethylene homopolymer as well as ethylene/1-hexene and ethylene/1-octene copolymers at magnification 2000x: a) None-THF, b) Zn-THF, c) Si-THF, and d) ZnSi-THF, respectively.

CHAPTER V
CONCLUSIONS AND RECOMMENDATIONS

This chapter summarized the effects of Lewis acid compounds on the activities of Ziegler-Natta catalysts for ethylene polymerization. It could be concluded into three sections as seen in section 5.1. In addition, the recommendation for further study are further provided in section 5.2

5.1 Conclusions

This section provided the summary from the results and discussion section as follows.

5.1.1 Influence of Metal Chloride Compounds on Activity of $Mg(OEt)_2$-based Ziegler-Natta Catalyst for Ethylene Homo- and Copolymerization

Firstly, the influence of single metal chlorides on activity of $Mg(OEt)_2$-based Ziegler-Natta catalyst was tested in ethylene homo- and copolymerization. It was found that $SiCl_4$ exhibited the highest activity for both homo- and copolymerization of ethylene as a result of high efficiency of $SiCl_4$ to cleave poisoning OEt. According to the study of efficiency with various types of cocatalysts, it was found that the activity order is TEA > TIBA > TOA > DEAC, regardless of the catalyst type. This result could be explained that the catalytic activities decreased with increasing the bulkiness of the alkyl group and ligand of the aluminium. In addition, Lewis acid compounds could enhance the insertion of 1-hexene in case of ethylene copolymerization.

Lastly, influences of metal chlorides ($FeCl_2$, $MnCl_2$ and $ZnCl_2$) were examined on the chlorination of $Mg(OEt)_2$ precursor with $SiCl_4$ to form $MgCl_2$-supported Ziegler-Natta catalysts for ethylene polymerization. It was found that the addition of these metal chlorides during preparation markedly affected the chemical compositions and the ethylene polymerization performances obtained from the resultant catalysts without deviation of the particle morphologies. The ethylene homopolymerization activities of the catalysts were correlated with the surface Ti/Mg atomic ratio, which could be explained by the ease of monomer diffusion onto the catalyst surfaces. In addition, the $FeCl_2$-modified catalyst gave the best activity. For copolymerization, the 1-hexene incorporation was enhanced by the addition of any metal chlorides plausibly due to the enhanced coordination of 1-hexene at the Lewis acidic centers. Thus, it was concluded that the co-addition of another metal halide in the preparation of $Mg(OEt)_2$-based Ziegler-Natta catalysts for ethylene polymerization is one of the easiest approaches to improve the performances of the resultant catalysts. The modification with metal halide components still indicated good replication of spherical $Mg(OEt)_2$ particles as observed by SEM analysis.

5.1.2 Effects of $FeCl_2$ Doping on Characteristics and Catalytic Properties of Ziegler-Natta Catalyst Prepared by Different Catalyst Preparation Methods

In this section, $TiCl_4/MgCl_2$ catalyst systems modified with $FeCl_2$ was prepared by two different methods namely: $TiCl_4$-$MgCl_2$ complexes in THF soluble and recrystallization method with ethanol. These obtained catalysts were compared in terms of polymerization activities at similar condition of ethylene polymerization. It was found that $FeCl_2$ modification in both two catalyst preparation could help improving the activities, compared to the unmodified ones. As considered, the comparison between two types of catalyst preparation modified with $FeCl_2$, it is worth to note that Fe-THF catalyst showed higher activity than Fe-EtOH catalyst due to a suitable of interaction between $TiCl_4$ and $MgCl_2$ as proven by TGA and most Ti

atoms preferred to locate on the surface. However, the $FeCl_2$ modification for both in two methods did not affect the polyethylene properties such as the melting temperature (T_m), crystallinity (χ_c), and general morphologies.

5.1.3 Synergistic Effects of $ZnCl_2$-$SiCl_4$ Modified $TiCl_4/MgCl_2$/THF Catalytic System on Ethylene Homo- and Copolymerization

The $TiCl_4$ catalysts on $MgCl_2$/THF support modified with Lewis acid halides such as $ZnCl_2$, $SiCl_4$, and $ZnCl_2$-$SiCl_4$ mixtures were investigated for ethylene polymerization. The influence of Lewis acid halides caused the increase in the catalytic activity for ethylene polymerization in the sequence of ZnSi-THF > Si-THF > Zn-THF > None-THF. The addition of mixed metal chlorides ($ZnCl_2$-$SiCl_4$) remarkably enhanced polymerization activity (almost three times) because some THF removal from the catalyst leading to an increase in the amounts of titanium on the surface. However, the Lewis acid modifications did not affect the properties of resulting homopolymers. Moreover, ZnSi-THF catalyst could increase molecular weight of polyethylene. It was indicated that $ZnCl_2$-$SiCl_4$ modifications could inhibit the chain transfer reaction during polymerization.

The $TiCl_4$ catalysts on $MgCl_2$/THF supports modified by Lewis acid halides were investigated for ethylene copolymerizations with 1-hexene or 1-octene. It was found that ZN catalysts modified with Lewis acid halides could improve the polymerization activities, especially the mixtures of $ZnCl_2$-$SiCl_4$. The activity enhancement was achieved due to an increase in acidic sites from the Lewis acids modification as observed by FT-IR measurement. It was found that the characteristic C-O-C peaks of the modified catalysts were slightly shifted to lower wavenumber when compared to the unmodified catalyst. In addition, it was also disclosed that Zn-Si catalyst exhibited the highest 1-hexene and 1-octene insertions leading to the highest polymerization activities because $ZnCl_2$-$SiCl_4$ could rearrange the active center distribution, resulting in more generation of active centers with high

copolymerization ability. Practically, Lewis acid modification could enhance molecular weight of copolymers because of the inhibition of chain transfer reaction during polymerization. However, the properties of catalysts modified with $ZnCl_2$ and/or $SiCl_4$ such as melting temperature, crystallinity, and density were slightly decreased when compared to those obtained from the unmodified catalyst. These properties depended on the amount of α-olefins insertion, irrespective of types of the modifiers or the comonomer types.

5.2 Recommendations

In order to further improve the $TiCl_4/MgCl_2$ catalytic systems, some ideas derived from this research are suggested here for future research:

- To determine Lewis sites on the acidic modified $TiCl_4/MgCl_2$ catalyst, IR spectra of pyridine should be performed in cooperation with this investigation's technique.

- To confirm the amount Ti atom on the surface after modifying with $FeCl_2$ or Lewis acid compounds, X-ray photoelectron spectroscopy (XPS) should be employed in order to evaluate the Ti atom on catalyst surface.

- To understand the effects of Lewis acid compounds on polymer properties such as MWD, GPC analysis should be further investigated. However, the polymerization condition should perform with H_2 addition.

- According to Part III: Synergistic effects of $ZnCl_2$-$SiCl_4$ modified $TiCl_4/MgCl_2$/THF catalytic system on ethylene homo- and copolymerization, it was found that the catalysts modified with Lewis acid compounds indicated very high activities; however, the difference of trend of M_v for all polymers was not significant. Hence, number of active centers and catalytic behaviors, kinetic mechanism, and effects of Lewis acid on activity and M_v should be further studied.

REFERENCES

[1] Kashiwa, N. The discovery and progress of $MgCl_2$-supported $TiCl_4$ catalysts. Journal of Polymer Science Part A: Polymer Chemistry 42 (2004): 1-8.

[2] Böhm, L.L. The ethylene polymerization with Ziegler Catalysts: Fifty years after the discovery. Angewandte Chemie International Edition 42 (2003): 5010-5030.

[3] Chu, K.-J., Soares, J.B.P., Penlidis, A., and Ihm, S.-K. Effect of prepolymerization and hydrogen pressure on the microstructure of ethylene/1-hexene copolymers made with $MgCl_2$-supported $TiCl_3$ catalysts. European Polymer Journal 36 (2000): 3-11.

[4] Kissin, Y.V. Multicenter nature of titanium-based Ziegler–Natta catalysts: Comparison of ethylene and propylene polymerization reactions. Journal of Polymer Science Part A: Polymer Chemistry 41 (2003): 1745-1758.

[5] Ribour, D., Spitz, R., and Monteil, V. Modifications of the active sites distribution in the Ziegler-Natta polymerization of propylene using Lewis acids. Journal of Polymer Science Part A: Polymer Chemistry 48 (2010): 2631-2635.

[6] Nikolaeva, M.I., Mikenas, T.B., Matsko, M.A., Echevskaya, L.G., and Zakharov, V.A. Ethylene polymerization over supported titanium-magnesium catalysts: The effect of polymerization parameters on the molecular weight distribution of polyethylene. Journal of Applied Polymer Science 122 (2011): 3092-3101.

[7] Edward P. Moore, J., and S.p.A., M. The rebirth of polypropylene: Supported catalysts : How the people of the Montedison Laboratories revolutionized the PP industry. Hanser-Gardner Publications, 1998.

[8] Wu, L., Lynch, D.T., and Wanke, S.E. Kinetics of gas-phase ethylene polymerization with morphology-controlled $MgCl_2$-supported $TiCl_4$ catalyst. Macromolecules 32 (1999): 7990-7998.

[9] Liu, W., et al. Novel supported Ziegler-Natta catalyst for ethylene polymerization. Shiyou Huagong/Petrochemical Technology 42 (2013): 379-383.

[10] Huang, J.C.K., Lacombe, Y., Lynch, D.T., and Wanke, S.E. Effects of hydrogen and 1-butene concentrations on the molecular properties of polyethylene produced by catalytic gas-phase polymerization. Industrial & Engineering Chemistry Research 36 (1997): 1136-1143.

[11] Chen, Y.P., Fan, Z.Q., Liao, J.H., and Liao, S.Q. Molecular weight distribution of polyethylene catalyzed by Ziegler-Natta catalyst supported on $MgCl_2$ doped with $AlCl_3$. Journal of Applied Polymer Science 102 (2006): 1768-1772.

[12] Fukuda, K. Significant variation of molecular weight distribution (MWD) of polyethylene induced by different alkyl-Al co-catalysts using a novel surface functionalized SiO_2-supported Ziegler-Natta catalyst. Catalysis Communications 4 (2003): 657-662.

[13] Liu, B., et al. ^{27}Al MAS solid state NMR study on coordinative nature of alkyl-Al cocatalysts on a novel SiO_2-supported Ziegler–Natta catalyst for controlled multiplicity of molecular weight distribution. Journal of Molecular Catalysis A: Chemical 219 (2004): 363-370.

[14] Cho, H.S., Chung, J.S., and Lee, W.Y. Control of molecular weight distribution for polyethylene catalyzed over Ziegler-Natta/Metallocene hybrid and mixed catalysts. Journal of Molecular Catalysis A: Chemical 159 (2000): 203-213.

[15] Fukuda, K., et al. Significant variation of molecular weight distribution (MWD) of polyethylene induced by different alkyl-Al co-catalysts using a novel surface functionalized SiO_2-supported Ziegler-Natta catalyst. Catalysis Communications 4 (2003): 657-662.

[16] Cho, H.S., Choi, K.H., Choi, D.J., and Lee, W.Y. Control of molecular weight distribution (MWD) for polyethylene catalyzed over Ziegler-Natta/Metallocene hybrid catalysts. Korean Journal of Chemical Engineering 17 (2000): 205-209.

[17] Czaja, K., and BiaŁek, M. Effect of hydrogen on the ethylene polymerization process over Ziegler-Natta catalysts supported on $MgCl_2(THF)_2$. I. Studies of the chain-transfer reaction. Journal of Applied Polymer Science 79 (2001): 356-360.

[18] Chadwick, J.C., Garoff, T., and Severn, J.R. Traditional Heterogeneous Catalysts. Wiley-VCH Verlag GmbH & Co. KGaA, 2008.

[19] Ko, Y.S., and Jeon, J.-K. The effect of the compostion of heterogeneous polymerization catalyst on ethylene–1-butene copolymerization. Catalysis Today 132 (2008): 178-181.

[20] Tanase, S., et al. New synthesis method using magnesium alkoxides as carrier materials for Ziegler-Natta catalysts with spherical morphology. Macromolecular Reaction Engineering 2 (2008): 233-239.

[21] Kissin, Y. Alkene polymerization reactions with transition metal catalysts. Elsevier Science, 2008.

[22] Mülhaupt, R. Catalytic polymerization and post polymerization catalysis fifty years after the discovery of Ziegler's catalysts. Macromolecular Chemistry and Physics 204 (2003): 289-327.

[23] Ribour, D., Spitz, R., and Gromada, J. Controlled distribution of stereospecific sites in Ziegler-Natta catalyst systems. U.S. Patent 7851395, 2010.

[24] Chen, Y.-P., Fan, Z.-Q., Liao, J.-H., and Liao, S.-Q. Molecular weight distribution of polyethylene catalyzed by Ziegler–Natta catalyst supported on $MgCl_2$ doped with $AlCl_3$. Journal of Applied Polymer Science 102 (2006): 1768-1772.

[25] Garoff, T., and Leinonen, T. Mn doping of the Ziegler-Natta PP catalyst support material. Journal of Molecular Catalysis A: Chemical 104 (1996): 205-212.

[26] Fregonese, D., and Bresadola, S. Catalytic systems supported on $MgCl_2$ doped with $ZnCl_2$ for olefin polymerization. Journal of Molecular Catalysis A: Chemical 145 (1999): 265-271.

[27] Parada, A., Rajmankina, T., Chirinos, J.J., and Morillo, A. Influence of support recrystallization techniques on catalyst performance in olefin polymerization. European Polymer Journal 38 (2002): 2093-2099.

[28] Chen, Y.P., and Fan, Z.Q. Ethylene/1-hexene copolymerization with $TiCl_4/MgCl_2/AlCl_3$ catalyst in the presence of hydrogen. European Polymer Journal 42 (2006): 2441-2449.

[29] Malpass, D.B. Introduction to industrial polyethylene: Properties, catalysts, and processes Chichester: John Wiley and Sons Ltd, 2010.

[30] Andrew J. Peacock, and Calhoun, A. Polymer Chemistry: Properties and Applications. Munich: Hanser Gardner Publications, 2006.

[31] Xie, T., McAuley, K.B., Hsu, J.C.C., and Bacon, D.W. Gas phase ethylene polymerization: Production processes, polymer properties, and reactor modeling. Industrial & Engineering Chemistry Research 33 (1994): 449-479.

[32] Lu, Z., Zhang, Z., Li, Y., Wu, C., and Hu, Y. Synthesis of branched polyethylene by in situ polymerization of ethylene with combined iron catalyst ana Ziegler-Natta catalyst. Journal of Applied Polymer Science 99 (2006): 2898-2903.

[33] Kashiwa, N. Super active catalyst for olefin polymerization. Polymer Journal 12 (1980): 603-608.

[34] Soga, K., and Shiono, T. Ziegler-Natta catalysts for olefin polymerizations. Progress in Polymer Science (Oxford) 22 (1997): 1503-1546.

[35] Giannini, U. Polymerization of olefins with high activity catalysts. Die Makromolekulare Chemie 5 (1981): 216-229.

[36] Fink, G., Polymerization on molecular catalysts. In Handbook of Heterogeneous Catalysis, Ertl, G.; Knözinger, H.; Schüth, F.; Weitkamp, J., Eds. Wiley-VCH: Weinheim, 2008; Vol. 8.

[37] Barbé, P., Cecchin, G., and Noristi, L., The catalytic system Ti-complex/$MgCl_2$. In Catalytical and Radical Polymerization, Springer Berlin Heidelberg: 1986; Vol. 81, pp 1-81.

[38] Huang, R., Malizia, F., Pennini, G., Koning, C.E., and Chadwick, J.C. Effects of $MgCl_2$ crystallographic structure on active centre formation in immobilized single-centre and Ziegler–Natta catalysts for ethylene polymerization. Macromolecular Rapid Communications 29 (2008): 1732-1738.

[39] Di Noto, V., and Bresadola, S. New synthesis of a highly active δ-$MgCl_2$ for $MgCl_2/TiCl_4/AlEt_3$ catalytic systems. Macromolecular Chemistry and Physics 197 (1996): 3827-3835.

[40] Di Noto, V., Fregonese, D., Marigo, A., and Bresadola, S. High yield $MgCl_2$-supported catalysts for propene polymerization: Effects of ethyl propionate as internal donor on the activity and stereospecificity. Macromolecular Chemistry and Physics 199 (1998): 633-640.

[41] Auriemma, F., and Rosa, C.D. Formation of $(MgCl_2)_x$ polynuclear species during preparation of active $MgCl_2$ supported Ziegler–Natta catalysts from solid solvates with lewis bases. Chemistry of Materials 19 (2007): 5803-5805.

[42] Chang, H.-S., Song, W.-D., Chu, K.-J., and Ihm, S.-K. Effects of removing THF from the $TiCl_3(AA)/3MgCl_2/THF$ catalyst system on the ethylene-propylene copolymerization mechanism. Macromolecules 25 (1992): 2086-2092.

[43] Chu, K.-J., Chang, H.-S., and Ihm, S.-K. Effects of diethyl aluminum chloride (DEAC) addition to the catalysts prepared by reduction of $TiCl_4$ with EtMgCl on ethylene-propylene copolymerization. European Polymer Journal 30 (1994): 1467-1472.

[44] Karol, F., Cann, K., and Wagner, B., Developments with high-activity Titanium, Vanadium, and Chromium catalysts in ethylene polymerization. In Transition Metals and Organometallics as Catalysts for Olefin Polymerization, Kaminsky, W.; Sinn, H., Eds. Springer Berlin Heidelberg: 1988; pp 149-161.

[45] Kashiwa, N., Yoshitake, J., and Tsutsui, T., Olefin polymerizations with a highly active $MgCl_2$ supported $TiCl_4$ catalyst system: Comparison on the behaviors of propylene, butene-1 ethylene and styrene polymerizations. In Transition Metals and Organometallics as Catalysts for Olefin Polymerization, Kaminsky, W.; Sinn, H., Eds. Springer Berlin Heidelberg: 1988; pp 33-43.

[46] Luo, H. Studies on the formation of new, highly active silica-supported Ziegler–Natta catalyst for ethylene polymerization. Journal of Catalysis 210 (2002): 328-339.

[47] Yury, V.K., Chapter 4 Synthesis, Chemical composition, and Structure of transition metal components and cocatalysts in catalyst systems for alkene polymerization. In Studies in Surface Science and Catalysis, Yury, V. K., Ed. Elsevier: 2007; Vol. 173, pp 207-290.

[48] Forte, M.C., and Coutinho, F.M.B. Highly active magnesium chloride supported Ziegler-Natta catalysts with controlled morphology. European Polymer Journal 32 (1996): 223-231.

[49] Vasilenko, I.V., and Kostjuk, S.V. The influence of cocatalysts on 1-hexene polymerization with various supported magnesium – titanium catalysts. Polymer Bulletin 57 (2006): 129-138.

[50] Parada, A., Rajmankina, T., and Chirinos, J. Study of the $MgCl_2$ recrystallization conditions on Ziegler-Natta catalyst properties. Polymer Bulletin 43 (1999): 231-238.

[51] Parada, A., Rajmankina, T., Chirinos, J.J., Morillo, A., and Fernández, J.G. Catalytic systems based on $TiCl_4/MgCl_2/SiCl_{4-n}(OR)_n$ for olefin polymerization. Designed Monomers and Polymers 6 (2003): 1-10.

[5] Chirinos, J., Fernández, J., Pérez, D., Rajmankina, T., and Parada, A. Effect of alkoxysilanes formed in situ on the properties of Ziegler-Natta catalysts for olefin polymerisation. Journal of Molecular Catalysis A: Chemical 231 (2005): 123-127.

[53] Chung, J.S., Choi, J.H., Song, I.K., and Lee, W.Y. Effect of ethanol treatment in the preparation of $MgCl_2$ support for the propylene polymerization catalyst. Macromolecules 28 (1995): 1717-1718.

[54] Choi, J.H., Chung, J.S., Shin, H.W., Song, I.K., and Lee, W.Y. The Effect of alcohol treatment in the preparation of $MgCl_2$ support by a recrystallization method on the catalytic activity and isotactic index for propylene polymerization. European Polymer Journal 32 (1996): 405-410.

[55] Marques, M., Almeida, L., and Cruz, K. Influence of the preparation technigues of $MgCl_2/TiCl_4$ Ziegler-Natta catalyst on the performance in ethylene and propylene polymerization Chemstry and Chemical Technology 4 (2010): 291-296.

[56] Almeida, L.A., and Marques, M.d.F.V. Synthesis of a $TiCl_4$ Ziegler-Natta catalyst supported on spherical $MgCl_2 \cdot n$EtOH for the polymerization of ethylene and propylene. Macromolecular Reaction Engineering 6 (2012): 57-64.

[57] Thushara, K.S., et al. Toward an understanding of the molecular level properties of Ziegler-Natta catalyst support with and without the internal electron donor. Journal of Physical Chemistry C 115 (2011): 1952-1960.

[58] Gnanakumar, E.S., et al. $MgCl_2.6PhCH_2OH$ - A new molecular adduct as support material for Ziegler-Natta catalyst: Synthesis, Characterization and Catalytic activity. Dalton Transactions 40 (2011): 10936-10944.

[59] Gnanakumar, E.S., et al. $MgCl_2 \cdot 6C_6H_{11}OH$: A high mileage porous support for Ziegler-Natta catalyst. Journal of Physical Chemistry C 116 (2012): 24115-24122.

[60] Thushara, K.S., et al. $MgCl_24((CH_3)_2CHCH_2OH)$: A new molecular adduct for the preparation of $TiCl_x/MgCl_2$ catalyst for olefin polymerization. Dalton Transactions 41 (2012): 11311-11318

61] Gnanakumar, E.S., et al. $MgCl_2 \cdot 6CH_3OH$: A Simple molecular adduct and its influence as a porous support for olefin polymerization. ACS Catalysis 3 (2013): 303-311.

[62] Joseph, J., Singh, S.C., and Gupta, V.K. Morphology controlled magnesium ethoxide: Influence of reaction parameters and magnesium characteristics. Particulate Science and Technology 27 (2009): 528-541.

[63] Tanase, S., et al. Particle growth of magnesium alkoxide as a carrier material for polypropylene polymerization catalyst. Applied Catalysis A: General 350 (2008): 197-206.

[64] Dashti, A., et al. Kinetic and morphological study of a magnesium ethoxide-based Ziegler-Natta catalyst for propylene polymerization. Polymer International 58 (2009): 40-45.

[65] Dashti, A., et al. Kinetic and morphological investigation on the magnesium ethoxide-based Ziegler-Natta catalyst for propylene polymerization using typical external donors. Macromolecular Symposia 285 (2009): 52-57.

[66] Bell, C.F., and Lott, K.A.K. Modern Approach to Inorganic Chemistry. 3 ed. Tokyo: Tokyo Kagaku Dozin-Butterworth Co. Ltd., 1976.

[67] Shijing, X., Honglan, L., and Minghui, Z. Studies on $TiCl_4/Mg(OEt)_2$/EB supported catalysts propylene polymerization. Chinese Journal of Polymer Science (English Edition) 8 (1990): 253-260.

[68] Diedrich, B., and Keil, K.D. Process for the polymerization of olefins. U.S. Patent 3644318, 1972.

[69] Akimoto, S., and Kimura, A. Process for the production of polyethylene. U.S. Patent 4342855, 1982.

[70] Kimura, A., and Asahi, S. Process for polymerization of ethylene. U.S. Patent 4255544, 1981.

[71] Mizogami, S., Asahi, S., and Takeshita, Y. Titanium catalyst for the polymerization of olefins. U.S. Patent 4308170, 1981.

[72] E, B.D., and L, J.J. Olefin polymerization catalyst. U.S. Patent 4311612, 1982.

[73] Maruyama, K., Nomura, T., Ueno, H., and Inaba, N. Process for polymerization of olefins. U.S. Patent 4686265, 1987.

[74] Taftaf, M.I. Process for preparation of catalyst composition for ethylene polymerization. U.S. Patent 6992033, 2006.

[75] Derroitte, J.-L., and Delbouille, A. Process for the polymerization of olefins and catalysts therefore. U.S. Patent 4144390, 1979.

[76] Shamshoum, E.S., and Bauch, C.G. Polyolefin catalyst from metal alkoxides or dialkyls, production and use. U.S. Patent 5817591, 1998.

[77] Woo, S.I., and Kim, I. Highly active ziegler-natta catalyst for polymerizing HDPE and LLDPE and method for preparation thereof. U.S. Patent 5192729, 1993.

[78] Kryzhanovskii, A.V., and Pvanchev, S.S. Synthesis of linear polyethylene on supported ziegler-natta catalysts. Review. Polymer Science U.S.S.R. 32 (1990): 1312-1329.

[79] Wang, W., et al. Low isotactic polypropylene synthesized with a $MgCl_2/AlCl_3$-supported Ziegler catalyst. Journal of Molecular Catalysis A: Chemical 244 (2006): 146-150.

[80] Ribour, D., Monteil, V., and Spitz, R. Strong activation of $MgCl_2$-supported Ziegler-Natta catalysts by treatments with BCl_3: Evidence and application of the "Cluster" model of active sites. Journal of Polymer Science, Part A: Polymer Chemistry 47 (2009): 5784-5791.

[81] Kashiwa, N., and Yoshitake, J. The influence of the valence state of titanium in $MgCl_2$-supported titanium catalysts on olefin polymerization. Die Makromolekulare Chemie 185 (1984): 1133-1138.

[82] Nooijen, G.A.H. On the importance of diffusion ofcocatalyst molecules through heterogeneous Ziegler-Natta catalyst. European Polymer Journal 30 (1994): 11-15.

[83] Quoc, V.T. Application of stopped-flow technique to study particle morphology development at the initial stage of Ziegler-Natta propylene polymerization. Mater 's Thesis, School of Materials Science, Japan Advanced Institute of Science and Technology, 2009.

[84] Moore, E.P. Polypropylene Handbook: Polymerization, Characterization, Properties, Processing, Applications. Hanser-Gardner Publications, 1996.

[85] Zucchini, U., and Cecchin, G., Control of molecular-weight distribution in polyolefins synthesized with Ziegler-Natta catalytic systems. In Industrial Developments, Springer Berlin Heidelberg: 1983; Vol. 51, pp 101-153.

[86] Chen, Y.-p., and Fan, Z.-q. Ethylene/1-hexene copolymerization with $TiCl_4/MgCl_2/AlCl_3$ catalyst in the presence of hydrogen. European Polymer Journal 42 (2006): 2441-2449.

[87] Kong, Y., et al. With different structure ligands heterogeneous Ziegler–Natta catalysts for the preparation of copolymer of ethylene and 1-octene with high comonomer incorporation. Polymer 51 (2010): 3859-3866.

[88] Czaja, K., and Bialek, M. Microstructure of ethylene-1-hexene and ethylene-1-octene copolymers obtained over Ziegler - Natta catalysts supported on $MgCl_2(THF)_2$. Polymer 42 (2001): 2289-2297.

[89] Meng, W., Li, H., Li, J., and Chen, B. The effect of comonomer type and content on the properties of Ziegler-Natta bimodal high-density polyethylene. Journal of the Korean Chemical Society 55 (2011): 673-679.

[90] Białek, M., and Czaja, K. The effect of the comonomer on the copolymerization of ethylene with long chain α-olefins using Ziegler–Natta catalyst supported on $MgCl_2(THF)_2$. Polymer 41 (2000): 7899-7904.

[91] Quijada, R., Dupont, J., Miranda, M.S.L., Scipioni, R.B., and Galland, G.B. Copolymerization of ethylene with 1-hexene and 1-octene: Correlation between type of catalyst and comonomer incorporated. Macromolecular Chemistry and Physics 196 (1995): 3991-4000.

[92] Xia, S., Fu, Z., Huang, B., Xu, J., and Fan, Z. Ethylene/1-hexene copolymerization with $MgCl_2$-supported Ziegler–Natta catalysts containing aryloxy ligands. Part I: Catalysts prepared by Immobilizing $TiCl_3(OAr)$ onto $MgCl_2$ in batch reaction. Journal of Molecular Catalysis A: Chemical 355 (2012): 161-167.

[93] Mingkwan, W., Piyasan, P., and Bunjerd, J. Observation of different catalytic activity of various 1-olefins during ethylene/1-olefin copolymerization with homogeneous metallocene catalysts. Molecules 16 (2011): 373-383.

[94] Zhang, L., Fan, L., Fan, Z., and Fu, Z. Dependence of comonomer effect and hydrogen effect on internal donor in ethylene/1-hexene copolymerizations with $MgCl_2$-supported catalysts. E-Polymers 18 (2010): 1-9.

[95] Awudza, J.A.M., and Tait, P.J.T. The "Comonomer Effect" in ethylene/α-olefin copolymerization using homogeneous and silica-supported Cp_2ZrCl_2/MAO catalyst systems: Some insights from the kinetics of polymerization, active center studies, and polymerization temperature. Journal of Polymer Science Part A: Polymer Chemistry 46 (2008): 267-277.

[96] Kissin, Y.V., Mink, R.I., Nowlin, T.E., and Brandolini, A.J. Kinetics and mechanism of ethylene homopolymerization and copolymerization reactions with heterogeneous Ti-based Ziegler-Natta catalysts. Topics in Catalysis 7 (1999): 69-88.

[97] Taniike, T., et al. Kinetic elucidation of comonomer-induced chemical and physical cctivation in heterogeneous Ziegler-Natta propylene polymerization. Journal of Polymer Science, Part A: Polymer Chemistry 49 (2011): 4005-4012.

[98] Spitz, R., Masson, P., Bobichon, C., and Guyot, A. Propene polymerization with $MgCl_2$ supported Ziegler catalysts: Activation by hydrogen and ethylene. Die Makromolekulare Chemie 189 (1988): 1043-1050.

\[99] Pasquet, V., and Spitz, R. Irreversible activation effects in ethylene polymerization. Die Makromolekulare Chemie 194 (1993): 451-461.

[100] McKenna, T.F., and Soares, J.B.P. Single particle modelling for olefin polymerization on supported catalysts: A review and proposals for future developments. Chemical Engineering Science 56 (2001): 3931-3949.

[101] Hutchinson, R.A., Chen, C.M., and Ray, W.H. Polymerization of olefins through heterogeneous catalysis X: Modeling of particle growth and morphology. Journal of Applied Polymer Science 44 (1992): 1389-1414.

[102] Grof, Z., Kosek, J., and Marek, M. Modeling of morphogenesis of growing polyolefin particles. AIChE Journal 51 (2005): 2048-2067.

[103] Bukatov, V.I., et al. The morphology of polypropylene granules and its link with the titanium trichloride texture. Polymer Science U.S.S.R. 24 (1982): 599-606.

[104] Kakugo, M., Sadatoshi, H., and Sakai, J., Morphology of nascent polypropylene produced by $MgCl_2$ supported Ti catalyst. In Studies in Surface Science and Catalysis, Tominaga, K.; Kazuo, S., Eds. Elsevier: 1990; Vol. Volume 56, pp 345-354.

[105] Cecchin, G., Marchetti, E., and Baruzzi, G. on the mechanism of polypropene growth over $MgCl_2/TiCl_4$ catalyst systems. Macromolecular Chemistry and Physics 202 (2001): 1987-1994.

[106] Patthamasang, S., Jongsomjit, B., and Praserthdam, P. Effect of $EtOH/MgCl_2$ molar ratios on the catalytic pProperties of $MgCl_2$-$SiO_2/TiCl_4$ Ziegler-Natta catalyst for ethylene polymerization. Molecules 16 (2011): 8332-8342.

[107] Hiraoka, Y. Kinetic and morphological investigation of active sites for propylene polymerization with different $MgCl_2$ supported Ziegler-Natta catalysts. Doctoral dissertation, School of Materials Science, Japan Advanced Institute of Science and Technology, 2010.

[108] Taniike, T., Chammingkwan, P., Thang, V.Q., Funako, T., and Terano, M. Validation of BET specific surface area for heterogeneous Ziegler-Natta catalysts based on α s-plot. Applied Catalysis A: General 437-438 (2012): 24-27.

[109] Thang, V.Q., et al. New quenching procedure for preservation of Initial polymer/catalyst particle morphology in Ziegler-Natta olefin polymerization. Macromolecular Reaction Engineering 3 (2009): 467-472.

[110] Randall, J.C. Carbon-13 NMR of ethylene-1–olefin copolymers: Extension to the short-chain branch distribution in a low-density polyethylene. Journal of Polymer Science: Polymer Physics Edition 11 (1973): 275-287.

[111] Soga, K., Uozumi, T., and Park, J.R. Effect of catalyst isospecificity on olefin copolymerization. Die Makromolekulare Chemie 191 (1990): 2853-2864.

[112] Zhikang, X., Linxian, F., and Shiling, Y. ^{13}C-NMR study of ethylene-1-octene copolymers. Chinese Journal of Polymer Science (English Edition) 12 (1994): 193-200.

[113] Carlini, C., et al. Linear low-density polyethylenes by co-polymerization of ethylene with 1-hexene in the presence of titanium precursors and organoaluminium co-catalysts. Polymer 48 (2007): 1185-1192.

[114] Mori, H., Iguchi, H., Hasebe, K., and Terano, M. Kinetic Study of Isospecific active sites formed by various alkylaluminiums on $MgCl_2$-supported Ziegler catalyst at the initial stage of propene polymerization. Macromolecular Chemistry and Physics 198 (1997): 1249-1255.

[115] Rocha, T.C.J., Coutinho, F.M.B., and Soares, B.G. Effect of alkylaluminum structure on Ziegler-Natta catalyst systems based on Neodymium for producing high-cis polybutadiene. Polymer Bulletin 62 (2009): 1-10.

[116] Senso, N., Khaubunsongserm, S., Jongsomjit, B., and Praserthdam, P. The influence of mixed activators on ethylene polymerization and ethylene/1-hexene copolymerization with silica-supported Ziegler-Natta catalyst. Molecules 15 (2010): 9323-9339.

[117] Haward, R.N., Roper, A.N., and Fletcher, K.L. Highly active catalysts for ethylene polymerization by the reduction of $TiCl_4$ with organomagnesium compounds. Polymer 14 (1973): 365-372.

[118] Hsieh, E.T., and Randall, J.C. Monomer sequence distributions in ethylene-1-hexene copolymers. Macromolecules 15 (1982): 1402-1406.

[119] Da Silva Filho, A.A., Alves, M.D.C.M., and Dos Santos, J.H.Z. XPS and EXAFS characterization of Ziegler-Natta catalyst systems. Journal of Applied Polymer Science 109 (2008): 1675-1683.

[120] De Camargo Forte, M.M., Da Cunha, F.V., and Dos Santos, J.H.Z. Characterization and evaluation of the nature of chemical species generated in hybrid Ziegler-Natta/metallocene catalyst. Journal of Molecular Catalysis A: Chemical 175 (2001): 91-103.

[121] Fregonese, D., et al. $MgCl_2/TiCl_4/AlEt_3$ catalytic system for olefin polymerisation: A XPS study. Journal of Molecular Catalysis A: Chemical 178 (2002): 115-123.

[122] Kaushik, V.K., Gupta, V.K., and Naik, D.G. XPS characterization of supported Ziegler-Natta catalysts. Applied Surface Science 253 (2006): 753-756.

[123] Nejad, M.H., Ferrari, P., Pennini, G., and Cecchin, G. Ethylene homo- and copolymerization over $MgCl_2$-$TiCl_4$ catalysts: Polymerization kinetics and polymer particle morphology. Journal of Applied Polymer Science 108 (2008): 3388-3402.

[124] Ostrovskii, N.M., and Stoiljković, D. Evaluation of the effect of reaction and mass transfer on the growth of polymer particles in olefin polymerization. Theoretical Foundations of Chemical Engineering 45 (2011): 40-52.

[125] Kissin, Y.V. Active centers in Ziegler-Natta catalysts: Formation kinetics and structure. Journal of Catalysis 292 (2012): 188-200.

[126] Soga, K., and Shiono, T. Ziegler-Natta catalysts for olefin polymerizations. Progress in Polymer Science 22 (1997): 1503-1546.

[127] Fregonese, D., Mortara, S., and Bresadola, S. Ziegler-Natta $MgCl_2$-supported catalysts: Relationship between titanium oxidation states distribution and activity in olefin polymerization. Journal of Molecular Catalysis A: Chemical 172 (2001): 89-95.

[128] Chang, M., et al. Ziegler–Natta catalysts for propylene polymerization: Morphology and crystal structure of a fourth-generation catalyst. Journal of Catalysis 239 (2006): 347-353.

[129] Seth, M., and Ziegler, T. Polymerization properties of a heterogeneous Ziegler-Natta catalyst modified by a base: A theoretical study. Macromolecules 36 (2003): 6613-6623.

[130] Sobota, P. Ionization of $MgCl_2$ during the formation of α-olefin polymeryzation catalyst. Macromolecular Symposia 89 (1995): 63-71.

[131] Hakim, S., Nekoomanesh, M., and Nieat, M.A. Investigating the behaviour of a Bi-supported SiO_2/$TiCl_4$/THF/$MgCl_2$ catalyst in slurry ethylene polymerization: Activity and molecular weight. Iranian Polymer Journal (English Edition) 17 (2008): 208-216.

[132] Nejabat, G.R., Nekoomanesh, M., Arabi, H., Emami, M., and Aghaei-Nieat, M. Preparation of polyethylene nano-fibres using rod-like MCM-41/$TiCl_4$/$MgCl_2$/THF Bi-supported Ziegler-Natta catalytic system. Iranian Polymer Journal (English Edition) 19 (2010): 79-87.

[133] Ochedzan-Siodłak, W., and Nowakowska, M. Heterogeneous zirconocene catalyst on magnesium support $MgCl_2(THF)_2$ modified by $AlEt_2Cl$ for ethylene polymerisation. European Polymer Journal 41 (2005): 941-947.

[134] Chirinos, J., Fernández, J., Pérez, D., Rajmankina, T., and Parada, A. Effect of alkoxysilanes formed in situ on the properties of Ziegler–Natta catalysts for olefin polymerisation. Journal of Molecular Catalysis A: Chemical 231 (2005): 123-127.

[135] Seenivasan, K., Sommazzi, A., Bonino, F., Bordiga, S., and Groppo, E. Spectroscopic investigation of heterogeneous Ziegler-Natta catalysts: Ti and Mg chloride tetrahydrofuranates, their interaction compound, and the role of the activator. Chemistry - A European Journal 17 (2011): 8648-8656.

[136] Wannaborworn, M., and Jongsomjit, B. Ethylene/1-octene copolymerization over Ga-modified SiO_2-supported Zirconocene/MMAO catalyst using in situ and ex situ impregnation methods. Iranian Polymer Journal (English Edition) 18 (2009): 969-979.

[137] Kim, J.H., Han, T.K., Choi, H.K., Kim, I., and Woo, S.I. Copolymerization of ethylene and 1-butene with highly active TI/Mg bimetallic catalysts. Effect of partial activation by $AlEt_2Cl$. Macromolecular Rapid Communications 16 (1995): 113-118.

[138] Rönkkö, H.L., et al. Complex formation and characterization of $MgCl_2$/2-(2-ethylhexyloxy)ethanol adduct. Inorganica Chimica Acta 371 (2011): 124-129.

[139] Terano, M., Kataoka, T., and Keii, T. A study on the states of ethyl benzoate and $TiCl_4$ in $MgCl_2$-supported high-yield catalysts. Die Makromolekulare Chemie 188 (1987): 1477-1487.

[140] Kaivalchatchawal, P., Samingprai, S., Shiono, T., Praserthdam, P., and Jongsomjit, B. Effect of Ga- and BCl_3-modified silica-supported [t-BuNSiMe$_2$(2,7-t-Bu$_2$Flu)]TiMe$_2$/MAO catalyst on ethylene/1-hexene copolymerization. European Polymer Journal 48 (2012): 1304-1312.

[141] Bosowska, K., and Nowakowska, M. The roles for a Lewis base and $MgCl_2$ in third-generation Ziegler-Natta catalysts. Journal of Applied Polymer Science 69 (1998): 1005-1011.

[142] Kang, K.-S., Ok, M.-A., and Ihm, S.-K. Effect of internal lewis bases on recrystallized $MgCl_2$–$TiCl_4$ catalysts for polypropylene. Journal of Applied Polymer Science 40 (1990): 1303-1311.

[143] Bialek, M., and Czaja, K. The effect of the comonomer on the copolymerization of ethylene with long chain α-olefins using Ziegler-Natta catalysts supported on $MgCl_2(THF)_2$. Polymer 41 (2000): 7899-7904.

[144] Czaja, K., Białek, M., and Utrata, A. Copolymerization of ethylene with 1-hexene over metallocene catalyst supported on complex of magnesium chloride with tetrahydrofuran. Journal of Polymer Science Part A: Polymer Chemistry 42 (2004): 2512-2519.

[145] Jiamwijitkul, S., Jongsomjit, B., and Praserthdam, P. Effect of Boron-modified MCM-41-supported dMMAO/Zirconocene catalyst on copolymerization of ethylene/1-octene for LLDPE synthesis. Iranian Polymer Journal (English Edition) 16 (2007): 549-559.

APPENDICES

APPENDIX A
THE DATA OF SOLUTION VISCOSITY

Here, our polymerization was performed without H_2 addition, thus the molecular weight of polymers was very high. However, the molecular weights of the polymers were measured with a capillary viscometer to obtain the viscosity average molecular weight (M_v). For the calculation of M_v was shown below:

A.1 Polystyrene (PS) Standard-98,400

Initial concentration: 0.1g/100 ml

Solvent: 1,2,4 Trichlorobenzene

Temperature: 150 ºC $\eta_0 = 1.284$ cP

Table A.1 The experiment data of 98,400-polystyrene standard

Conc. (g/100ml)	Time (sec)			
	1	2	3	average
0.000	72.66	72.69	71.16	72.17
0.013	78.56	78.06	78.44	78.35
0.025	83.15	81.41	83.78	82.78
0.050	91.54	91.54	91.54	91.54
0.100	93.72	93.16	92.63	93.17

Conc. (g/100ml)	$\eta_r = t/t_0$	$\eta = \eta_0\eta_r$	$\eta_{sp} = (\eta-\eta_0)/\eta_0$	$\ln \eta_r$	$\ln (\eta_r)/c$	η_{sp}/c
0.000	1.000	1.284	0.000	0.000	-	-
0.013	1.086	1.394	0.086	0.082	6.323	6.59
0.025	1.147	1.473	0.147	0.137	5.486	5.88
0.050	1.268	1.629	0.268	0.238	4.755	5.37
0.100	1.291	1.658	0.291	0.255	2.554	2.91

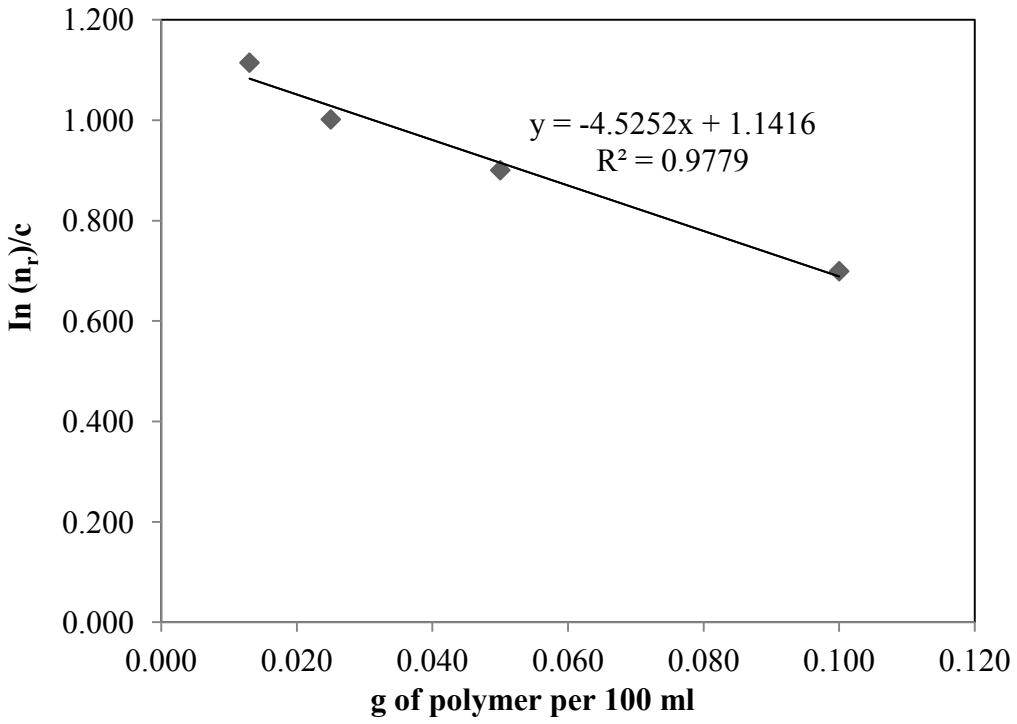

Figure A.1 Instrinsic viscosity of polystyrene-98,400

A.2 Polystyrene (PS) Standard-827,000

Table A.2 The experiment data of 827,000-polystyrene standard

Conc. (g/100ml)	Time (sec)			
	1	2	3	average
0.000	72.66	72.69	71.16	72.17
0.013	78.56	78.06	78.44	78.35
0.025	83.15	81.41	83.78	82.78
0.050	91.54	91.54	91.54	91.54
0.100	93.72	93.16	92.63	93.17

Table A.2 (Cont.) The experiment data of 827,000-polystyrene standard

Conc. (g/100ml)	$\eta_r = t/t_0$	$\eta = \eta_0\eta_r$	$\eta_{sp} = (\eta-\eta_0)/\eta_0$	ln η_r	ln $(\eta_r)/c$	η_{sp}/c
0.000	1.000	1.284	0.000	0.000	-	-
0.013	1.086	1.394	0.086	0.082	6.323	6.59
0.025	1.147	1.473	0.147	0.137	5.486	5.88
0.050	1.268	1.629	0.268	0.238	4.755	5.37
0.100	1.291	1.658	0.291	0.255	2.554	2.91

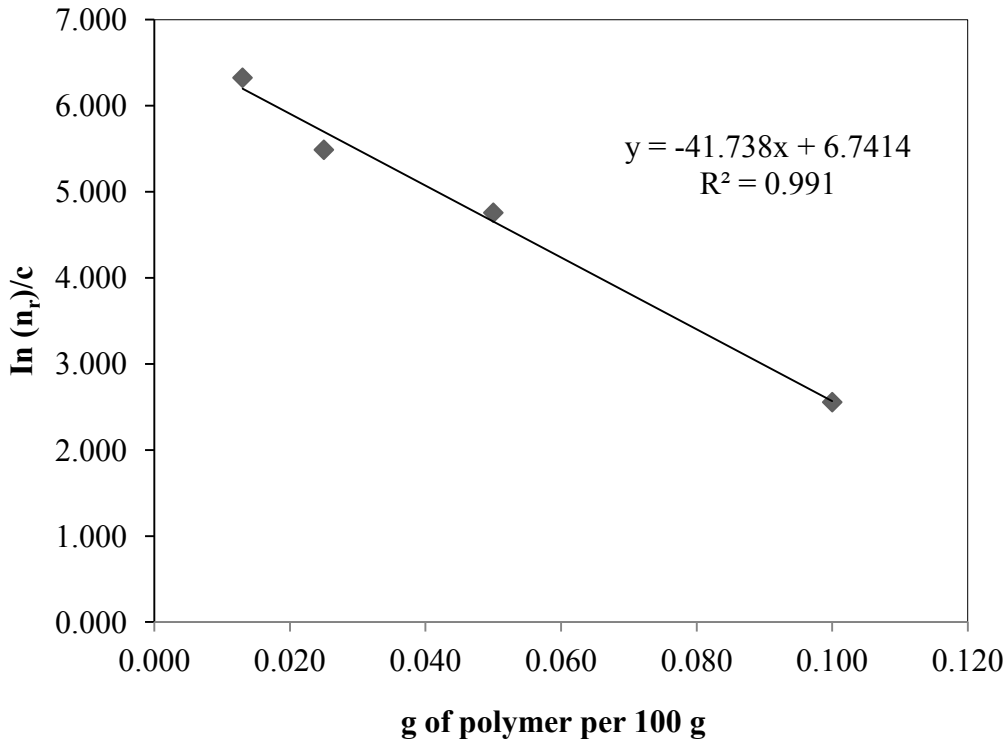

Figure A.2 Intrinsic viscosity of polystyrene-827,000

A.3 Calculation of Viscosity Average Molecular Weight (M_v) of Polyethylene

Intrinsic viscosity was determined from Kraemer Equation

$$(\ln \eta_r)/C = [\eta \quad + k'' [\eta]^2 c \qquad (A.1)$$

where k'' is constant

η_r is relative viscosity

c is concentration in g/dl and

$[\eta]$ is determined from the extrapolation of $[(\ln \eta_r)/c]_{c=0}$ at zero concentration. From plotting between $[(\ln \eta_r)/c]$ and c, the $[\eta]$ value was determined and shown below:

Table A.3 Intrinsic viscosity and viscosity average molecular weight of PS standard

Sample	**Intrinsic viscosity** $[\eta]$	**Viscosity average molecular weight (M_v)**
PS 98,400	1.1416	98,400
PS 827,000	6.7416	827,000

According to the Mark-Houwink-Sakurada relation, the correlation between intrinsic viscosity and molecular weight, the correlation of the value of intrinsic viscosity with the molecular weight of the polymer in a solvent can be represented as:

$$[\eta] = K' M_v^{\,a} \qquad (A.2)$$

We can determine the K' and a value from data of both PS-standard samples. Where K' = 7.8047 x 10^{-5} dl/g and a = 0.8343 are the constants for polyethylene and 1,2,4 trichlorobenzene at 150 ºC

Table A.4 Intrinsic viscosity and viscosity average molecular weight of obtained polyethylene

Catalysts	**Types of polyethylene**	**Intrinsic viscosity** $[\eta]$	**Viscosity average molecular weight** (M_v)
None-THF	Homopolymer	3.5588	383,936
Zn-THF	Homopolymer	3.6252	392,555
Si-THF	Homopolymer	3.4678	372,199
ZnSi-THF	Homopolymer	3.8591	423,086
None-THF	Ethylene/1-hexene copolymer	3.1634	333,349
Zn-THF	Ethylene/1-hexene copolymer	3.3894	362,159
Si-THF	Ethylene/1-hexene copolymer	3.3250	353,869
ZnSi-THF	Ethylene/1-hexene copolymer	3.5823	386,977
None-THF	Ethylene/1-octene copolymer	3.0911	324,264
Zn-THF	Ethylene/1-octene copolymer	3.4411	368,807
Si-THF	Ethylene/1-octene copolymer	3.4243	366,609
ZnSi-THF	Ethylene/1-octene copolymer	3.4936	375,520

APPENDIX B
XPS DATA OF $Mg(OEt)_2$-BASED ZIEGLER-NATTA CATALYST

Effects of various metal chloride components were examined on ethylene polymerization performances of $Mg(OEt)_2$-based Ziegler-Natta catalysts. Metal chlorides were added together with $SiCl_4$ in the chlorination stage of $Mg(OEt)_2$. In addition, these obtained catalysts were characterized by XPS measurement in order to better understand the influence of metal chloride components on the chemical environment of Ti atom on catalyst surface. The binding energy (BE) values of Ti 2p are represented in Table B.1.

Table B.1 The binding energy (BE) values relative to Ti 2p XPS peaks of the obtained catalysts[a]

Metal Chlorides	BE of Ti $2p_{1/2}$ (eV)	BE for Ti $2p_{3/2}$ (eV)
None-MGE	465.8	460.2
Si-MGE	464.6	459.0
Fe-MGE	464.7	458.9
Mn-MGE	464.0	458.2
Zn-MGE	464.9	459.0

[a] The BE was determined by referencing to Mg 2s (90.1 eV)

APPENDIX C
^{13}C NMR SPECTRA OF POLYPROPYLENE

The microstructure and also triad distribution of copolymers were characterized with ^{13}C NMR following each method reported by Randall [110], Soga et al. [111], and Zhikang *et al*. [112]. The detail of determination for ethylene/α-olefin copolymer was interpreted as follow:

C1. For Ethylene/1-hexene Copolymer

The integration areas of ^{13}C NMR in the specific ranges are listed.

I(A) = 39.5 – 42.0 ppm

I(B) = 38.1 ppm

I(C) = 33.0 – 36.0 ppm

I(D) = 28.5 – 31.0 ppm

I(E) = 26.5 – 27.5 ppm

I(F) = 24.0-25.0 ppm

I(G) = 23.4 ppm

I(H) = 14.1 ppm

Triad distribution was determined as the followed:

[EHE] = I(B)

[EHH] = 2[I(G) – I(B) – I(A)]

$$[HHH] = 2I(A) + I(B) - I(G)$$

$$[HEH] = I(F)$$

$$[HEE] = 2[I(G) - I(A) - I(F)]$$

$$[EEE] = (1/2)[I(A) + I(D) + I(F) - 2I(G)]$$

Then the fractions of ethylene and 1-hexene insertions were calculated:

$$\%E = [EEE] + [HEE] + [HEH]$$

$$\%H = [HHH] + [EHH] + [EHE]$$

C2. For Ethylene/1-octene Copolymer

Zhikang *et al*.[112] are divided the spectrum of ethylene/1-octene copolymer into ten regions, defined as A-I. Utilizing regions A, B, D, F, G, H, and some necessary relationships, one can readily derive the following Equations for the relative triad concentration:

$$[EOE] = I(B)$$

$$[OOE] = 2[I(A) - I(D)]$$

$$[OOO] = I(D)$$

$$[OEO] = I(H)$$

$$[EEO] = [I(G) + I(D) - I(B) - 2I(A)]$$

$$[EEE] = (1/4)[2I(F) + I(D) - I(G) - I(B)]$$

Where I(A) – I(H) stand for the total area of regions A – H respectively.

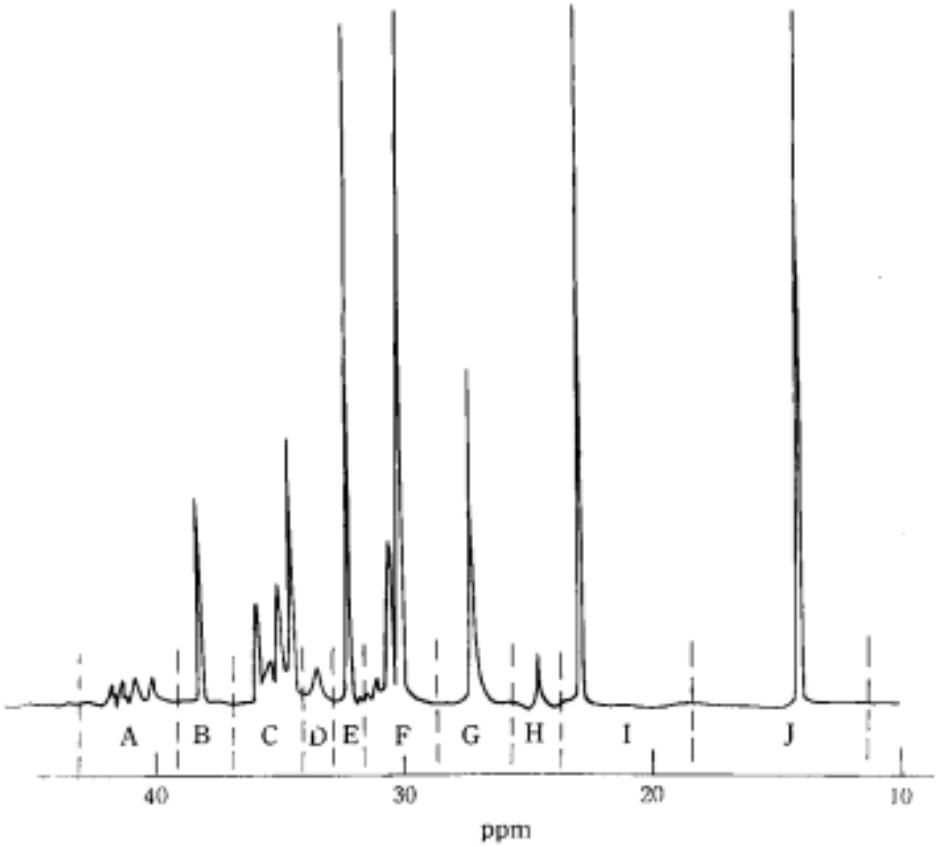

Figure C.1 Typical 13C NMR spectrum of ethylene/1-octene copolymer [112] .

The monomer composition can be calculated from the triad distributions by the Equations:

%E = [EEE] + [EEO] + [EOE]

%O = [OOO] + [OOE] + [EOE]

APPENDIX D
LIST OF PUBLICATION

D1. International Publications

1. Wanna Phiwkliang, Bunjerd Jongsomit, Piyasan Praserthdam, Effect of $ZnCl_2$- and $SiCl_4$-doped $TiCl_4/MgCl_2/THF$ catalysts for ethylene polymerization, Journal of Applied Polymer Science, Accepted 2013.

2. Wanna Phiwkliang, Bunjerd Jongsomit, Piyasan Praserthdam, Synergistic effects of the $ZnCl_2$-$SiCl_4$ modified $TiCl_4/MgCl_2/THF$ catalytic system on ethylene/1-hexene and ethylene/1-octene copolymerizations, Chinese Journal of Polymer Science, Accepted 2013.

3. Wanna Phiwkliang, Bunjerd Jongsomit, Piyasan Praserthdam, Influence of $FeCl_2$ in $TiCl_4/MgCl_2/THF$ catalyst for polymerization of ethylene, to be submitted to e-Polymers 2013.

4. Wanna Phiwkliang, Bunjerd Jongsomjit, Piyasan Praserthdam, Toshiaki Taniike, Minoru Terano, Effects of various mixed metal chlorides-$SiCl_4$ on activity of $Mg(OEt)_2$-based Ziegler-Natta catalyst for ethylene homo- and copolymerization, to be submitted to Research Trends 2013.

D2. International Conferences

1. Poster: Wanna Phiwkliang, Bunjerd Jongsomjit, Piyasan Praserthdam, Toshiaki Taniike, Minoru Terano, Effects of various metal chlorides on ethylene homo- and copolymerization using $Mg(OEt)_2$-based Ziegler-Natta catalyst, 8th International Colloquium on Heterogeneous Ziegler-Natta Catalysts, Kanazawa, Japan, March 27-30,2012.

VITA

Miss Wanna Phiwkliang was born on January 30, 1985 in Suphanburi, Thailand. She graduated high school from Sa-nguanying School, Suphanburi in 2004. She received Bachelor‘s Degree in Chemical Engineering From Silpakorn University in 2008. After the B.Eng graduation, she consequently continued studying Doctoral Degree of Chemical Engineering, Chulalongkorn University since May 2008 and received the Dusadeepipat Scholarship from Chlalongkorn University. During her research years, she spent one year for extending her research at Terano Laboratory, School of Materials Science, Japan Advanced Institute of Technology, Japan.